Tampere University

Petteri Kangasluoma

MEDIUM VOLTAGE NETWORK RESIDUAL EARTH FAULT CURRENT ESTIMATION METHODS

Faculty of Information Technology
and Communication Sciences
Master of Science Thesis
November 2019

ABSTRACT

Petteri Kangasluoma: Medium Voltage Network Residual Earth Fault Current Estimation Methods
Master of Science Thesis
Tampere University
Master's Degree Programme in Electrical Engineering
November 2019

Extensive cabling during 2010s has drastically changed the earth fault behaviour of the rural area distribution network. Against the assumptions of traditional earth fault analysis, cable network zero sequence series impedance is nonnegligible, thus zero sequence voltage applied over the zero sequence impedance during an earth fault generates a resistive component to the earth fault current in addition to the capacitive component. In the resonant earthed neutral system, capacitive earth fault current can be compensated with inductive Petersen coils, but the resistive current component cannot be compensated with Petersen coils. Increase of resistive earth fault current will increase the absolute value of the residual earth fault current flowing to ground during the earth fault and consequently cause dangerous touch voltages.

The reactive component of the residual earth fault current is mostly known but the resistive component is associated with multiple uncertainties. The harmonic component is out of the scope of this thesis and thus omitted. Due to the uncertainties, calculation of the resistive earth fault current has proven to be complicated, but if residual earth fault current is to be calculated accurately, the resistive component must be calculated or estimated first.

The SFS 6001: 2018 standard states that if the residual earth fault current in resonant earthed neutral system is unknown the value can be assumed 10% of the network capacitive earth fault current. However, as extensive cabling increases resistive earth fault current production of the network, the validity of this assumption has caused concern. Therefore, the aim of this thesis was to develop a practically oriented model for estimating residual earth fault current that can easily be applied to multiple locations in the network. Secondly, the validity of the 10% assumption specified by the standard was studied in Elenia's network.

The network information system used in Elenia is currently unable to take into account the cable network zero sequence impedance, thus a statistical examination was performed based on network data from 45 primary transformer areas. The measurements from centralized Petersen coil regulators were utilized in the examination, since the regulators provide real-time measurement of the network resistive earth fault current production.

In the statistical examination the dependency of resistive earth fault current from other network parameters was studied. The objective was to identify variables that correlate with resistive earth fault current, so that they could be used to estimate the resistive earth fault current. After the correlation analysis, correction factors were assigned to the variables and the results were compared to the measurements from the regulators. The conclusion was that the resistive earth fault current can be estimated to be 5% of the total capacitive earth fault current.

This result was applied to residual earth fault current calculation and the obtained values were again compared to the values calculated from the measurements. There was only a minor difference, which implies that the developed model yields accurate results. More importantly, the developed model proved to provide more accurate results than the estimation method specified in SFS 6001, that acted as a reference. In addition, there are two alternative interpretations of the method specified in the standard, so depending on the interpretation, the results were either too high or too low when applied to Elenia's network. However, the results of this thesis are heavily dependent on the properties of the network, thus results should only be applied to networks with similar configuration.

Keywords: residual earth fault current, resistive earth fault current, touch voltages

The originality of this thesis has been checked using the Turnitin OriginalityCheck service.

TIIVISTELMÄ

Petteri Kangasluoma: Keskijänniteverkon jäännösmaasulkuvirran arviointimenetelmät
Diplomityö
Tampereen yliopisto
Sähkötekniikan diplomi-insinöörin tutkinto-ohjelma
Marraskuu 2019

2010-luvulla toteutettu laajamittainen kaapelointi on merkittävästi muuttanut maaseudun keskijännitteisen jakeluverkon maasulkuilmiöitä. Vastoin perinteisen maasulkuanalyysin oletuksia, kaapeliverkon nollasekvenssin sarjaimpedanssia ei voida jättää huomiotta, sillä vaikuttaessaan kaapeliverkon nollaimpedanssin yli, maasulun aikainen nollajännite generoi maasulkuvirtaan kapasitiivisen komponentin lisäksi myös resistiivisen komponentin. Sammutetussa verkossa kapasitiivinen maasulkuvirta voidaan kompensoida Petersenin keloilla, mutta perinteiset laitteistot, jotka hyödyntävät ainoastaan Petersenin kelaa, eivät pysty kompensoimaan resistiivistä komponenttia. Resistiivisen maasulkuvirran kasvu suurentaa maasulun jäännösvirran itseisarvoa, joka vian aikana maahan virratessaan saattaa aiheuttaa vaarallisia kosketusjännitteitä.

Jäännösmaasulkuvirran komponenteista reaktiivinen komponentti on pääosin tunnettu, mutta resistiiviseen komponenttiin liittyy monia epävarmuustekijöitä. Harmoninen komponentti on rajattu tämän työn ulkopuolelle, joten sitä ei huomioida tässä yhteydessä. Epävarmuustekijöiden takia resistiivisen maasulkuvirran laskenta on osoittautunut hankalaksi, mutta mikäli jäännösmaasulkuvirtaa halutaan laskea tarkasti, on resistiivisen komponentin suuruus laskettava tai arvioita ensin.

SFS 6001: 2018 standardin mukaan, jos sammutetun verkon jäännösmaasulkuvirran arvoa ei tunneta, sen suuruudeksi voidaan olettaa 10% verkon kapasitiivisesta maasulkuvirrasta. Kuitenkin kaapeloidun verkon määrän kasvaessa, kasvaa myös jäännösmaasulkuvirran resistiivinen osuus, jolloin standardin 10% oletuksen soveltuvuudesta ei voida olla varmoja. Tämän työn tavoite onkin kehittää jäännösmaasulkuvirran arviointimenetelmä, joka tarjoaa käytännönläheisen tavan arvioida jäännösmaasulkuvirran suuruuttaa eri verkon osissa. Toisena tavoitteena on tarkastella standardin 10% oletuksen tarkkuuttaa Elenian verkossa.

Elenialla käytössä oleva verkkotietojärjestelmä ei toistaiseksi pysty huomioimaan kaapeliverkon nollasekvenssin sarjaimpedanssia, joten työssä suoritettiin tilastollinen tarkastelu, jossa pohjadatana oli verkkotiedot 45 päämuuntaja-alueelta. Tarkastelussa hyödynnettiin keskitettyjen Petersenin kelojen säätäjien mittauksia, jotka mittasivat verkon tuottaman resistiviisen maasulkuvirran reaaliaikaista arvoa.

Tilastollisessa tarkastelussa tutkittiin resistiivisen maasulkuvirran riippuvuutta eri verkkoparametreista. Tavoitteena oli tunnistaa muuttujia, jotka korreloivat resistiivisen virran kanssa, jotta näitä muuttujia voitaisiin käyttää reisistiivisen maasulkuvirran arviointiin. Korrelaatioanalyysin jälkeen muuttujille etsittiin sopiva korjauskerroin ja tuloksia verrattiin Petersenin kelojen säätäjiltä saatuihin mittaustuloksiin. Tarkastelussa havaittiin, että verkon tuottaman resistiivisen virran suuruudeksi voidaan arvioida 5% verkon kapasitiivisesta kokonaismaasulkuvirrasta.

Kun tätä tulosta sovellettiin jäännösmaasulkuvirran laskentaan, ja saatuja tuloksia verrattiin jälleen mittaustulosten perusteella laskettuihin jäännösmaasulkuvirran arvoihin, tulokset olivat verrattain tarkkoja. Huomattavaa on, että kehitetyn mallin tuottamat tulokset olivat tarkempia kuin verrokkina toimineen SFS 6001: 2018 mukaan lasketut arvot. Standardin määrittelemä arviointimenetelmä soveltuu huonosti Elenian verkkoon, sillä riippuen standardin tulkinnasta tulokset olivat joko merkittävästi liian suuria, tai vastaavasti merkittävästi liian pieniä. On kuitenkin syytä huomioida, että työssä saadut tulokset riippuvat olennaisesti tutkitun verkon ominaisuuksista, eikä tuloksia näin ollen tule soveltaa kuin rakenteeltaan samankaltaisiin verkkoihin.

Avainsanat: jäännösmaasulkuvirta, resistiivinen maasulkuvirta, kosketusjännitteet

Tämän julkaisun alkuperäisyys on tarkastettu Turnitin OriginalityCheck –ohjelmalla.

PREFACE

This Master's thesis was commissioned by Elenia Oy and it has been a privilege to work with such great colleagues, whom I want to thank for their generous help during this project. Most of all, I want to thank my teammates in Network Assets and Investments team, with special thanks to my instructor Jarkko Peltola for his great advice and support during this work. I would also like to thank my thesis supervisor Ari Nikander from Tampere University for his valuable comments.

This work has given me a great opportunity to apply different disciplines and skills I have learned during my studies. The student years have been better than I ever imagined, and I genuinely want to thank all those amazing people I have met during this time in Vaasa and Tampere. It has been a pleasure.

Above all, I want to thank my family and my beloved wife Jenni, for your love and support throughout these years has made this possible.

Tampere, 15th November 2019

Petteri Kangasluoma

TABLE OF CONTENTS

LIST OF SYMBOLS AND ABBREVIATIONS

AC	Alternating current
DSO	Distribution system operator
GMR	Geometric mean radius
HV	High voltage
LV	Low voltage
MSE	Mean square error
MV	Medium voltage
OHL	Overhead line
PAW	Power auxiliary winding
XLPE	Cross-linked polyethylene

$3\underline{I}_0$	Sum of zero sequence currents
$\underline{a}$	Phase shift operator
B_0	Shunt susceptance
$C1, C2$	Line shunt capacitances
d	Distance between cable conductors
d_0	Distance between cable conductor and earth wire
D_e	Equivalent penetration depth
$\underline{E}$	Pre-fault line-to-neutral voltage
e, b	Correction factors
f	System frequency
$\underline{I}_1, \underline{I}_2, \underline{I}_0$	Positive, negative and zero sequence currents
I_B	Body current
$\underline{I}_C$	Capacitive current
I_{Cc}	Capacitive earth fault current flowing to the substation
I_{Cd}	Capacitive earth fault current compensated by the distributes units
I_{Ctot}	Total capacitive earth fault current produced by the network
I_E	Current to earth
I_{ew}	Current in cable earth wire
$\underline{I}_f$	Earth fault current
$\underline{I}_H$	Harmonic current
$\underline{I}_L$	Inductive current
I_{Lc}	Inductive current of centralized Petersen coil
I_{Ld}	Sum of inductive currents of distributed Petersen coils
I_{Ltot}	Total inductive current of the compensation units
$\underline{I}_p$	Current of the background network
I_{pos}	Petersen coil current production in present coil position
$\underline{I}_R$	Receiving end current
I_R	Resistive earth fault current
$\underline{I}_R, \underline{I}_S, \underline{I}_T$	Phase currents
$\underline{I}_{re}$	Residual earth fault current
I_{res}	Current of the resonance point
I_{Rp}	Centralized Petersen coil parallel resistor current
$\underline{I}_S$	Sending end current
I_{sc}	Current in cable screen
j	imaginary unit
K	Compensation degree

l	Cable length
L	Inductance
n	Number of units
r	Reduction factor
R	Resistance
R, S, T	Phase indicators of the three-phase system
r'_c	Geometric mean radius of conductors
r'_{ew}	Geometric mean radius of the earth wire
r'_{sc}	Geometric mean radius of the screen
r_c	Cable conductor radius
R_c	Conductor resistance
R_E	Resistance to earth
r_{ew}	Cable earth wire radius
R_{ew}	Earth wire resistance
R_f	fault resistance
R_g	Ground resistance
R_N	Compensation coil parallel resistor
r_{sc}	Cable screen radius
R_{sc}	Screen resistance
$\underline{U}$	Voltage
$\underline{U}'_R$, $\underline{U}'_S$, $\underline{U}'_T$	Phase voltages during the fault
$\underline{U}_0$	Neutral point voltage, zero sequence voltage
U_{0end}	End of the line zero sequence voltage
U_{0n}	Neutral displacement voltage
$\underline{U}_1$, $\underline{U}_2$	Positive and negative sequence voltage
U_E	Earthing voltage
U_R	Receiving end voltage
U_r	Voltage with respect to reference earth
$\underline{U}_R$, $\underline{U}_S$, $\underline{U}_T$	Healthy state phase voltages
U_S	Sending end voltage
U_S	Step voltage
U_T	Touch voltage
U_{TP}	Permissible touch voltage
x	distance from earthing electrode
X	Reactance
X_{0M}	Primary transformer zero sequence reactance
X_N	Compensation coil reactance
$\underline{Y}$	Admittance
$\underline{Z}$	Impedance
$\underline{Z}_1$, $\underline{Z}_2$, $\underline{Z}_0$	Positive, negative and zero sequence impedance
$\underline{Z}_E$	Impedance to earth
$\underline{Z}_N$	Neutral point impedance
$\underline{Z}_T$	Body impedance
μ_0	Permeability of the free space
ρ	Ground resistivity
$\Sigma\underline{I}$	Sum current
φ	Phase displacement
φ_{RCA}	Characteristic angle
ω	System angular frequency

1. INTRODUCTION

Electricity is one of the key enablers of modern society as many of the applications and innovations that shape our contemporary way of life are heavily reliant on electricity. The consumption is all around us and thus, we are increasingly dependent on undisrupted distribution of electricity. In the Nordic countries, reliability of distribution caused concern after the disastrous storms at the beginning of 2010s. As a result, in 2013 the Finnish parliament ratified the new Electricity Market Act stating that by the end of the year 2028 storms or snow loads must not cause power outages that exceed 6 hours in urban areas or 36 hours in rural areas. (Electricity Market Act 588/2013)

To meet the legislative requirements, Distribution System Operators (DSO) are extensively renewing their networks. The fault frequency in overhead line (OHL) medium voltage (MV) network is high and, since the MV network faults caused by storms and snow loads affect large number of customers the conclusion has been to increasingly replace the OHLs with underground cables. This thesis was commissioned by Elenia Oy, the second largest DSO in Finland and a pioneer in rural area network cabling.

Even though underground cables withstand climatic disturbances better than OHLs, the electrical properties are remarkably different. Shunt capacitance of an underground cable is significantly larger than in OHL, and series inductance is smaller, respectively. This causes new challenges since the increase of network shunt capacitance proportionally increases the capacitive earth fault current and reactive power production in the network.

Capacitive earth fault current can be compensated with a neutral point resonant earthing coil, also known as Petersen coil, named after the inventor Waldemar Petersen. The share of the earth fault current that is not compensated is called residual current. It consists of the uncompensated reactive component, the resistive component and possible harmonics. The standard of high-voltage electrical installations SFS 6001, published by the Finnish Standards Association, states that in the resonant earthed MV network, if the total residual earth fault current is unknown, the value can be assumed to be 10% of the network capacitive earth fault current. (SFS 6001: 2018) During an earth fault the residual current can energize earthed network components and possibly cause

danger for human safety. DSO must ensure that this ground potential rise during the earth fault does not exceed the safety limitation specified in the SFS 6001 standard.

Underground cables and compensation devices both produce resistive earth fault current that cannot be compensated with Petersen coil. For hazard voltage examinations in networks consisting mainly of OHL, the 10% residual current assumption has been applicable. However, as the share of cabled MV network increases, the resistive component of the residual earth fault current increases, too. The danger is that the 10% assumption is too optimistic an estimation of the magnitude of the residual current, which leads to underestimated results in hazard voltage examinations. Hence, the feasibility of this 10% assumption in extensive cable networks must be investigated in detail.

The impact of the large-scale cabling has been a topic of intense research in recent years. For example, Guldbrand (2009), Pekkala (2010), Vehmasvaara (2013) and Nikander and Mäkinen (2017) have studied the earth fault behaviour of cabled MV network, and the problems arising from the increase of the residual earth fault current resistive component have been addressed. However, calculation of resistive earth fault current in the network is associated with multiple uncertainties and the parts of the network where problems might arise are difficult to identify. That is why the objective of this thesis is to gain better understanding of how the resistive component is produced. Secondly, the aim is to provide a method that enables to estimate the magnitude of the produced resistive current with the information available in the network information system. Better understanding of the source of the problem enables to focus the corrective safety actions properly.

In this thesis the theoretical concepts related to the MV network earth faults and resistive current production are presented in Chapters 2 and 3. Electrical safety and touch voltages related to earth faults as well as requirements from the SFS 6001 standard for high-voltage electrical installations are covered in Chapter 4, while research methods and results of this study are presented in Chapters 5 and 6.

2. EARTH FAULTS IN MV NETWORK

An earth fault occurs when a live network part is galvanically connected to ground potential. The connection can happen between one or two phases and the ground, but in this thesis only single-phase earth faults are considered. An earth fault is undesirable because conducting ground operates as a part of the circuit forming a return path for the fault current. While the fault is on, the current flow in the ground can energize earthed network parts and possibly cause danger for human safety. In network operation, safety is always a key factor, and it is also one of the main interests in this thesis. The safety aspects and touch voltages related to earth faults are treated more in detail in Chapter 4. In MV networks earth faults are caused by multiple different mechanisms, for example trees falling on to OHLs or incautious excavation performed nearby underground cables.

Under normal operating conditions, loading and line impedances in all three phases are close to equal and thus the system can be assumed symmetrical. Phase voltage magnitudes are also close to equal and the phasors are spaced 120° apart. Consequently, during an earth fault, voltage asymmetry occurs according to Figure 1 where fault is in phase *S*. The connection to ground usually happens via a fault resistance R_f, but if there is no resistance in between the conductor and the ground, the earth fault is called solid. During the fault, voltage of the faulted phase *S* is a product of the fault current $\underline{I}_f$ and the fault resistance R_f. This causes voltage of the faulted phase to decrease and the voltages of the healthy phases to increase.

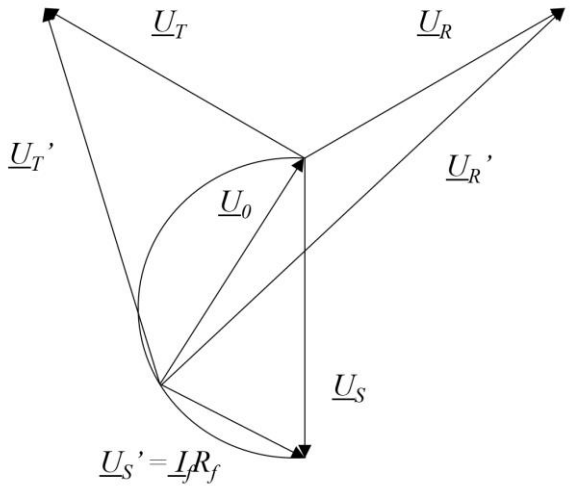

Figure 1. *Phase voltages in a healthy state ($\underline{U}_R$, $\underline{U}_S$, $\underline{U}_T$) and during a non-solid earth fault ($\underline{U}_R'$, $\underline{U}_S'$, $\underline{U}_T'$). (Edited from Lakervi and Partanen 2008)*

In Figure 1 $\underline{U_0}$ denotes neutral point voltage that is measured between the ground and the system neutral point. The magnitude of the neutral point voltage is dependent on the voltage asymmetry of the phase voltages. In the phasor diagram, neutral point voltage and the voltage of the faulted phase are depended on each other and the phasors move along the half circle drawn in the figure. If the earth fault is solid, the voltage of the faulted phase approaches zero and the magnitude of the neutral point voltage is of a size with the healthy state line-to-neutral voltage. Consequently, the voltage of the two healthy phases will increase almost to the level of the healthy state line-to-line voltage.

2.1 Representation of asymmetrical faults with symmetrical components

Symmetrical faults such as three-phase short circuit or component disconnection can be represented with single phase equivalent circuit since all phases are equal in magnitude. This approach simplifies the analysis but is only applicable in symmetrical condition. On the contrary, under the asymmetrical condition, such as earth fault, all phases should be analysed separately. This would be laborious and time consuming. Therefore, the method of the symmetrical components has been applied to asymmetrical fault analysis.

The method of symmetrical components is based on an idea that any asymmetrical set of three phase voltages or currents can be expressed with three separate systems of symmetrical phasors. These sequence networks are a purely mathematical representation and the component networks do not physically exist in the power system but as the asymmetrical condition can be replaced with three symmetrical sequence networks single phase equivalent circuits can again be applied to simplify the fault analysis. (Lakervi and Holmes 1995)

The symmetrical components consist of positive, negative and zero sequence networks that are illustrated in Figure 2. The positive system has three phasors with equal magnitude, 120˚ phase displacement and counterclockwise rotation. The positive sequence phasors are oriented R-S-T. The negative sequence phasors are also spaced 120˚ apart and rotate counterclockwise, but the orientation is reversed, being R-T-S. The zero sequence phasors all have equal magnitude and are rotating in the same direction as positive and negative sequence but are in phase with each other. The speed of rotation is determined by system angular frequency ω. (Lakervi and Holmes 1995)

Every phase value can be expressed as a sum of its sequence components as follows:

$$\begin{aligned} \underline{U}_R &= \underline{U}_{R1} + \underline{U}_{R2} + \underline{U}_{R0} \\ \underline{U}_S &= \underline{U}_{S1} + \underline{U}_{S2} + \underline{U}_{S0} \\ \underline{U}_T &= \underline{U}_{T1} + \underline{U}_{T2} + \underline{U}_{T0} \end{aligned} \tag{1}$$

where the index 1 denotes positive, 2 negative and 0 zero sequence components.

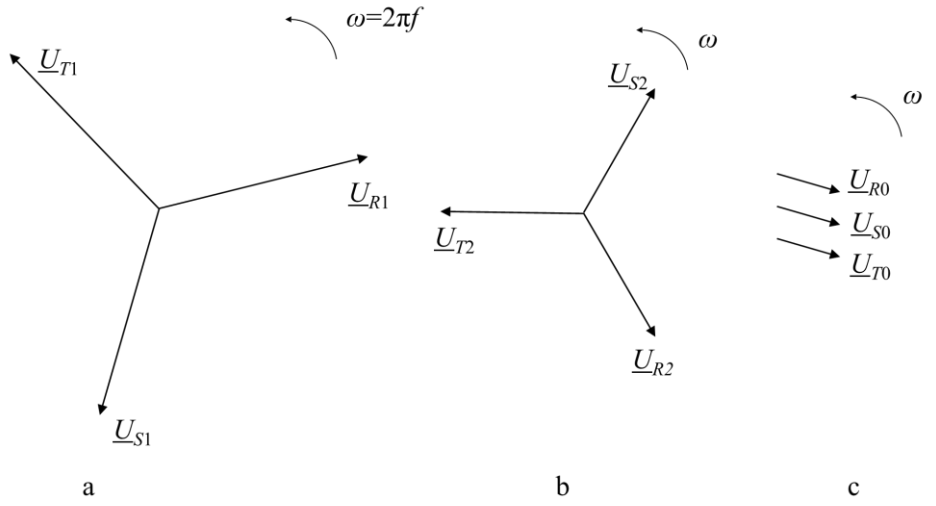

Figure 2. *The sequence networks: (a) positive sequence, (b) negative sequence and (c) zero sequence. (Edited from Lakervi and Holmes 1995)*

In healthy state, positive sequence equals to phase values of the system i.e. negative and zero sequence are only present while asymmetry occurs. Consequently, neutral point voltage $\underline{U}_0$ in Figure 1 can be considered as zero sequence voltage. By introducing phase shift operator $\underline{\mathrm{a}} = e^{\mathrm{j}120} = 1\angle 120^\circ$ phase values and symmetrical components in equation (1) can be presented in matrix form using only components of one phase. Hence, sequence components will be denoted without letter index as $\underline{U}_1, \underline{U}_2, \underline{U}_0$.

$$\begin{bmatrix} \underline{U}_R \\ \underline{U}_S \\ \underline{U}_T \end{bmatrix} = \begin{bmatrix} 1 & 1 & 1 \\ 1 & \underline{\mathrm{a}}^2 & \underline{\mathrm{a}} \\ 1 & \underline{\mathrm{a}} & \underline{\mathrm{a}}^2 \end{bmatrix} \begin{bmatrix} \underline{U}_0 \\ \underline{U}_1 \\ \underline{U}_2 \end{bmatrix} \tag{2}$$

Matrix equation can be formed for phase currents respectively.

$$\begin{bmatrix} \underline{I}_R \\ \underline{I}_S \\ \underline{I}_T \end{bmatrix} = \begin{bmatrix} 1 & 1 & 1 \\ 1 & \underline{\mathrm{a}}^2 & \underline{\mathrm{a}} \\ 1 & \underline{\mathrm{a}} & \underline{\mathrm{a}}^2 \end{bmatrix} \begin{bmatrix} \underline{I}_0 \\ \underline{I}_1 \\ \underline{I}_2 \end{bmatrix} \tag{3}$$

In the power system all the sequence currents face corresponding impedances. Partly the impedances are the same and partly different. The sequence impedances are illustrated in the simplified example of Figure 3

$$\begin{aligned} \underline{Z}_1 &= \underline{Z}_2 = \underline{Z} \\ \underline{Z}_0 &= \underline{Z} + 3\underline{Z}_N \end{aligned} \tag{4}$$

$\underline{Z}_N$ being neutral point impedance and $\underline{E}$ pre-fault line-to-neutral voltage of the faulted phase. (Elovaara and Haarla 2011)

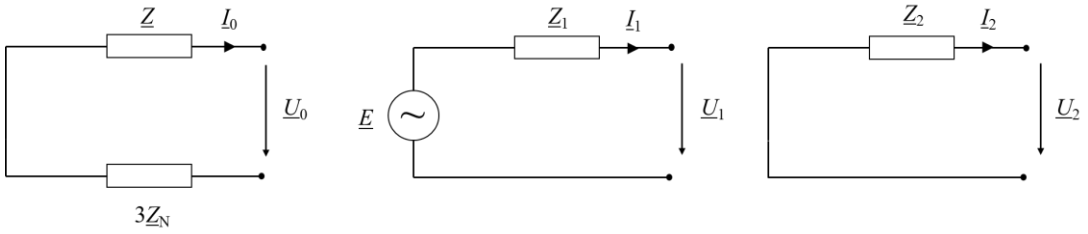

Figure 3. *Zero-, positive- and negative sequence systems. (Elovaara and Haarla 2011)*

In Figure 3 sequence networks are presented with Thevenin's equivalent circuit. Voltage source $\underline{E}$ is only connected to the positive sequence and all the sequence impedances are determined by the components connected to the physical network but are independent of each other.

During the single-phase earth fault, the sequence networks are coupled in series as illustrated in Figure 4. The derivation of the sequence network coupling in different fault scenarios is presented in detail by Elovaara and Haarla (2011). The neutral point impedance and fault resistance are represented threefold, because zero sequence currents of all three phases flow through them.

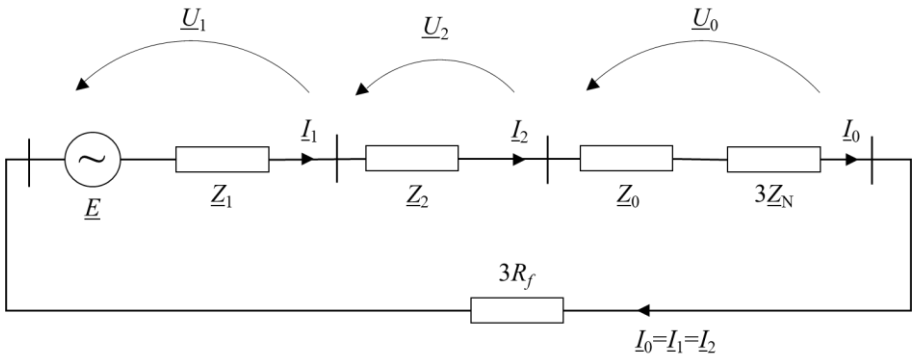

Figure 4. *Series coupling of sequence networks during a single-phase earth fault. (Elovaara and Haarla 2011)*

2.2 System neutral earthing

In asymmetric fault condition the neutral earthing method effects heavily on behaviour of the system. To illustrate this, following matrix equation for sequence currents can be derived from equation (3)

$$\begin{bmatrix} \underline{I}_0 \\ \underline{I}_1 \\ \underline{I}_2 \end{bmatrix} = \frac{1}{3}\begin{bmatrix} 1 & 1 & 1 \\ 1 & \underline{a} & \underline{a}^2 \\ 1 & \underline{a}^2 & \underline{a} \end{bmatrix}\begin{bmatrix} \underline{I}_R \\ \underline{I}_S \\ \underline{I}_T \end{bmatrix} \tag{5}$$

from which can be seen

$$\underline{I}_0 = \frac{1}{3}(\underline{I}_R + \underline{I}_S + \underline{I}_T)\,. \tag{6}$$

Now, there is zero sequence current $\underline{I}_0$ only if the sum of the phase currents is non-zero. This means that only if phase voltages are asymmetric, in which case sum of phase currents is non-zero, there exist zero sequence current in the network. This implies that in asymmetric fault conditions neutral point earthing has a significant role, since zero sequence current flows through the neutral point. (Bastman 2018)

In the following sections two of the most common neutral earthing methods in Finnish distribution systems, isolated neutral and resonant earthed system are presented. Both methods of are widely applied but the latter has been increasingly deployed due to the increase of capacitive earth fault current produced by underground cabling.

2.2.1 Isolated neutral system

In isolated neutral system there is no connection in between ground and system neutral. This makes zero sequence impedance of the transformer neutral point appear as infinite and thereby, during the earth fault the only way to close the circuit is via the line shunt capacitances. The magnitude of the network total shunt capacitance is determined by the length of the interconnected lines and the total zero sequence impedance formed by the capacitances is large. (Lakervi and Holmes 1995)

Single phase earth fault in isolated neutral system is illustrated in Figure 5. In the simplified circuit, lines are represented only as shunt capacitances C_1 and C_2. This is justified by an assumption that the line series impedance is insignificantly small compared to the shunt capacitance and thereby can be ignored. (Lakervi and Holmes 1995) This assumption is applied in traditional earth fault analysis but feasibility of this assumption in extensive cable networks is better discussed in Section 2.5.

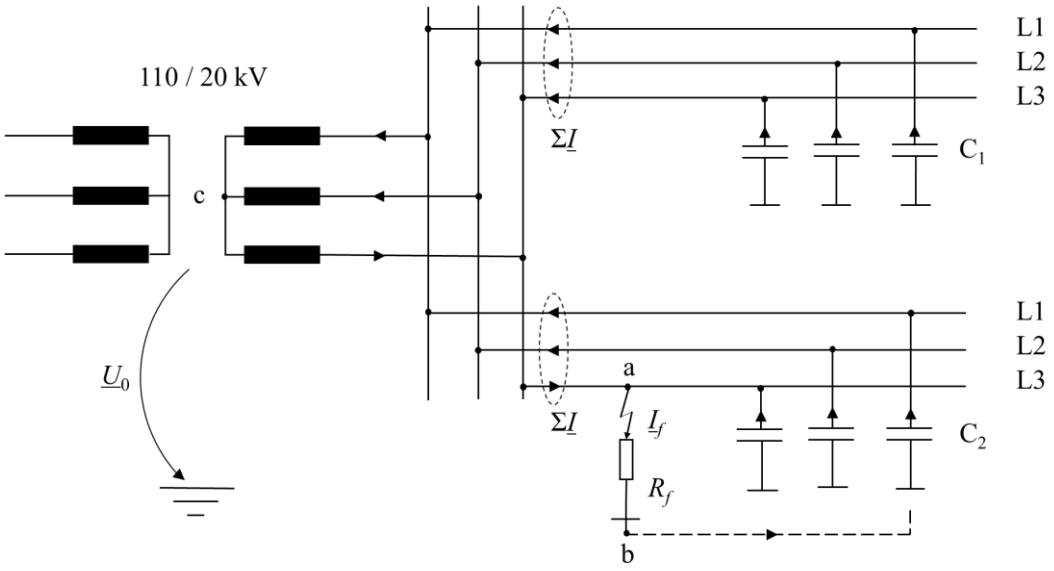

Figure 5. *Single-phase earth fault on an isolated neutral system. (Edited from Lakervi and Holmes 1995)*

In Figure 5 the connection to ground in point a happens via the fault resistance R_f from where the fault current returns to the network via ground and shunt capacitances. The current flows from the healthy feeders to the neutral point of the transformer and from there back to the fault point. $\Sigma\underline{I}$ is the sum current seen by the protective relays in the beginning of each feeder. In the healthy feeders the direction of the current is towards the bus bar, but in the faulted feeder the direction of the sum current is towards the network.

The isolated neutral system presented in Figure 5 can be simplified into equivalent circuit of Figure 6 where total shunt capacitance of the network is denoted with 3*C.*

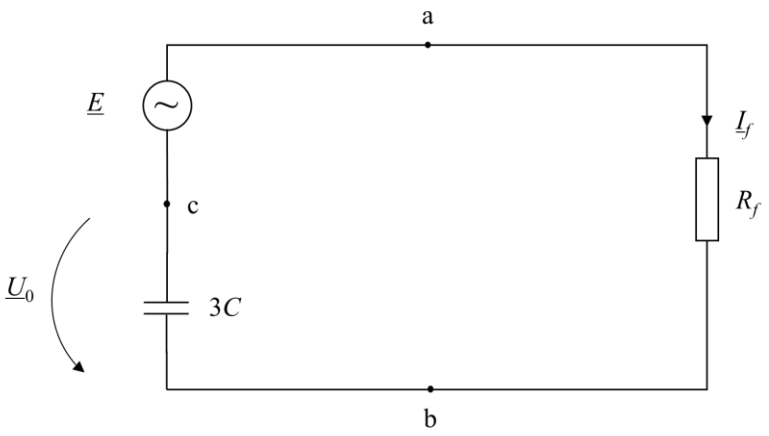

Figure 6. *Equivalent circuit of earth fault in isolated neutral system. (Edited from Lakervi and Holmes 1995)*

According to Lakervi and Holmes (1995) from Figure 6 equations for fault current and neutral point voltage in isolated neutral system can be defined with respect to pre-fault line-to-neutral voltage $\underline{E}$ as follows

$$\underline{I}_f = \frac{\underline{E}}{R_f + \frac{1}{\mathrm{j}3\omega C}} = \frac{\mathrm{j}3\omega C}{1 + \mathrm{j}3\omega C R_f} \tag{7}$$

$$\underline{U}_0 = \frac{1}{\mathrm{j}3\omega \mathrm{C}}(-\underline{I}_f) = \frac{-1}{1 + \mathrm{j}3\omega \mathrm{C}}\underline{E} \tag{8}$$

2.2.2 Resonant earthed neutral system

If transmission lines are considered as shunt capacitances is the produced earth fault current purely capacitive and so it can be compensated with inductive arc suppression coil also known as Petersen coil. By inserting the inductive coil into the neutral point of the system and dimensioning it so that the absolute value of the coil inductance equals to line capacitance, capacitive earth fault current can theoretically be totally compensated. Figure 7 presents a system with resonant earthed neutral where L denotes Petersen coil inductance and R resistive losses of the coil and a parallel resistor.

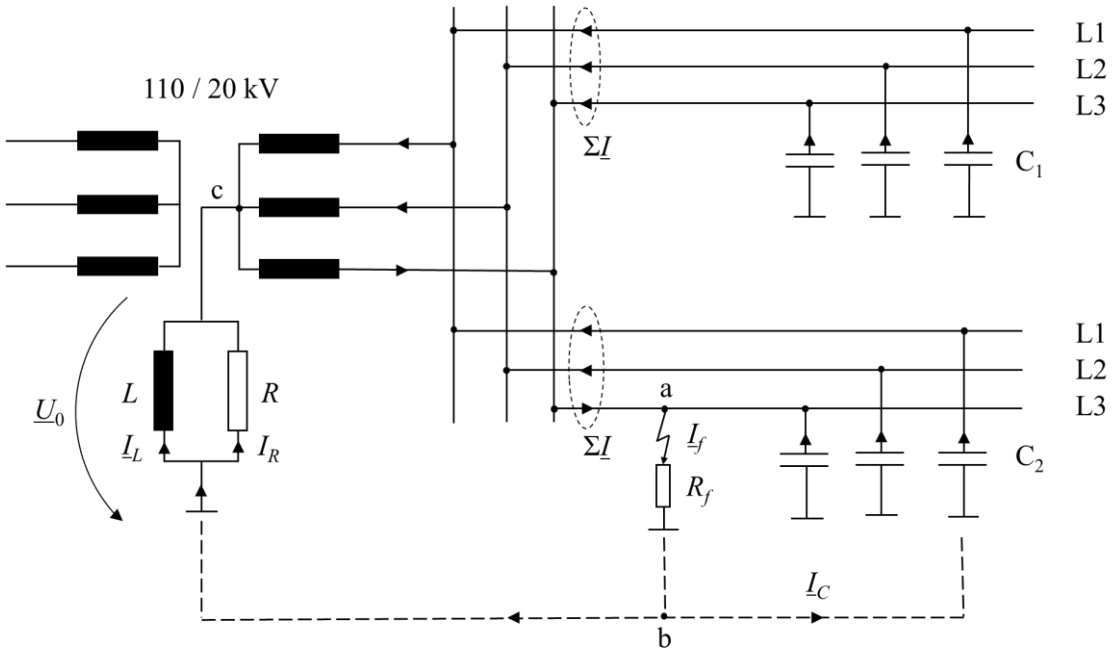

Figure 7. *Single-phase earth fault on a resonant earthed neutral system. (Edited from Lakervi and Holmes 1995)*

Now, the fault current has a return path also via system neutral point in addition to line capacitances but the zero sequence voltage applied over Petersen coil produces

inductive current component $\underline{I}_L$ that is summed to the capacitive fault current so that the current at the fault location is compensated to the desired degree. I_R denotes the resistive current component that is in this example considered significantly smaller than $\underline{I}_L$ but the properties of resistive earth fault current are discussed in detail in Section 2.5.2 and Chapter 3.

Figure 8 presents an equivalent circuit of resonant earthed system of Figure 7. Neutral point devices and the capacitances of healthy feeders C_1 are connected in parallel and the resulting current is denoted as $\underline{I}_p$. If the system would contain multiple healthy feeders, they would be connected in parallel with C_1. The fault current generated by the faulted feeder capacitances C_2 is denoted with $\underline{I}_f$-$\underline{I}_p$ which is summed to $\underline{I}_p$ at the neutral point of the transformer and from there the total fault current $\underline{I}_f$ flows to the fault point.

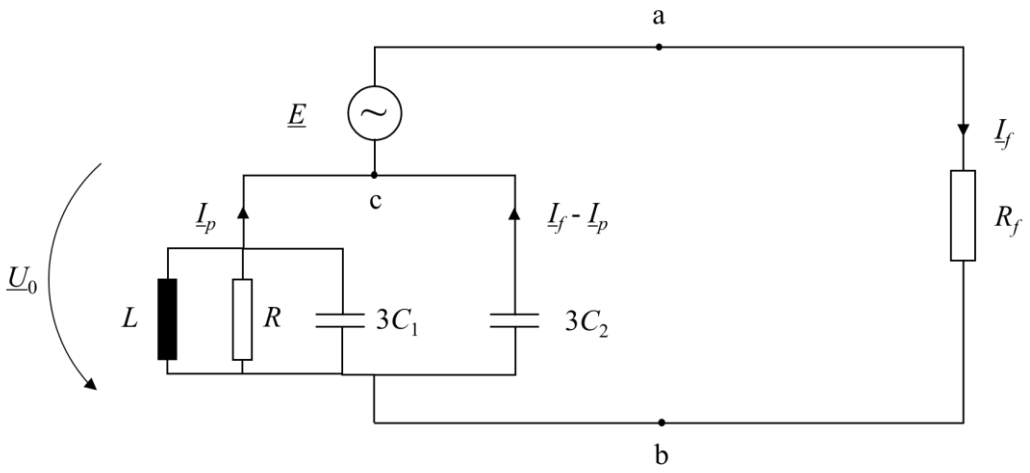

Figure 8. *Equivalent circuit for resonant earthed system of Figure 7. (Edited from Lakervi and Holmes 1995)*

According to Lakervi and Holmes (1995) equations for total earth fault current and neutral point voltage with respect to total line capacitance and pre-fault voltage can be derived from equivalent circuit of Figure 8 as

$$\underline{I}_f = \frac{\underline{E}}{R_f + \dfrac{R}{1+\mathrm{j}R\left(3\omega C - \dfrac{1}{\omega L}\right)}} \tag{9}$$

$$\underline{U}_0 = \frac{-R}{R_f + R + \mathrm{j}RR_f\left(3\omega C - \dfrac{1}{\omega L}\right)}\underline{E} \tag{10}$$

2.3 Earth fault current compensation

Changes in legislative requirements have contributed to the increase of network cabling as many of the Finnish DSOs have decided to renew parts of their OHL networks with underground cables. In turn the cabled networks produce greater earth fault current as the cable shunt capacitance can be 30-40 times higher than shunt capacitance of the corresponding OHL. Earth fault current can energize earthed network parts and possibly cause danger for human safety. The system requirements and safety aspects related to hazards voltages and earth faults are better discussed in Chapter 4 but to prevent the problems arising from the increase of earth fault current the network earth fault current production should be controlled. One control option is compensation devices since capacitive earth fault current and inductive current generated by the Petersen coil have 180˚ phase displacement and therefor cancel each other. According to Elovaara and Haarla (2011) for complete compensation should

$$\omega L = \frac{1}{3\omega C} \tag{11}$$

The degree of compensation can be determined by dimensioning of the Petersen coil inductance. On the other hand, changes in network topology affect the total shunt capacitance and capacitive earth fault current so to keep the compensation degree constant coil inductance should be adjustable. The compensation degree is defined as:

$$K = \frac{\underline{I}_L}{\underline{I}_C} \tag{12}$$

where K is compensation degree, $\underline{I}_L$ is inductive current of the Petersen coil and $\underline{I}_C$ is the capacitive component of the earth fault current. If $K > 1$ system is overcompensated so the residual current is inductive and if $K < 1$ system is undercompensated and residual current is capacitive. If $K = 1$ system is efficiently compensated but this is an undesired condition because now equation (11) holds and system is in resonance. The fault current is efficiently compensated but it oscillates between capacitances and inductances and can cause harmonics and over-voltages that can lead to component breakdowns. So, network should be operated near the resonance point $K \approx 1 \pm 5\%$ but not directly at resonance. It is a matter of choice and tradition if system is operated undercompensated or overcompensated. In Sweden MV networks are typically operated overcompensated but in Finland undercompensated. (Elovaara and Haarla 2011)

Earth fault current at the fault location $\underline{I}_f$ is the resulting current after compensation, so it can be denoted also as residual earth fault current that is defined as a sum of inductive,

capacitive and resistive components and possible harmonics. In SFS 6001: 2018 standard residual current is defined as

$$|\underline{I}_f| = |\underline{I}_{re}| = \sqrt{|\underline{I}_C + \underline{I}_L|^2 + |I_R|^2 + |\underline{I}_H|^2} \quad (13)$$

Where $\underline{I}_H$ is the harmonic component that includes all the frequencies of the earth fault current that are outside the nominal frequency. Harmonics do affect the earth fault behaviour of the system but are out of the scope of this thesis and are thus omitted in the following study. For more information about earth fault related harmonics see Nikander and Mäkinen (2017). Reactive components of the equations (13) can be compensated but active component i.e. the resistive component cannot be compensated with Petersen coil. Phasor diagram of residual current composition is presented in Figure 9 where inductive current is smaller than capacitive current so system is undercompensated and residual current is slightly capacitive but contains also the resistive component.

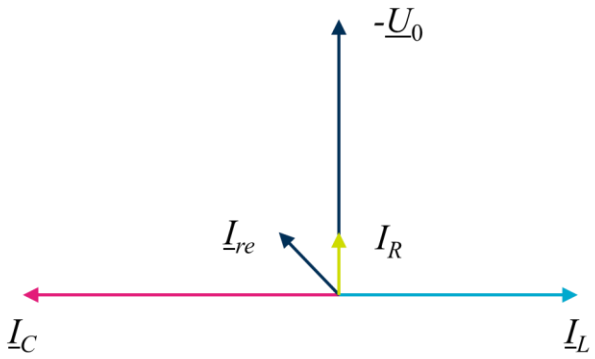

Figure 9. *Phasor diagram of an earth fault in an undercompensated system.*

Petersen coils are connected to the neutral point of the system but earth fault compensation in general can be implemented in multiple ways, mainly instead of just single coil there can be multiple Petersen coils located along the feeders of the network. Coil that is connected to the substation is called centralized coil and the ones that are located along the feeders are called distributed coils. Centralized and distributed compensation methods and their characteristics are presented in the following section.

2.3.1 Centralized compensation

Centralized compensation coils are connected to the substation. If neutral point is provided at secondary winding of the 110/20 kV primary transformer Petersen coil is connected there as illustrated in Figure 7. This requires transformer secondary winding to be star-coupled and neutral point connection to be provided. In Finland some DSOs,

including Elenia, have YNd coupled primary transformers so the secondary side of the transformer is delta-coupled and neutral point does not exist naturally. In a substation with delta-coupled primary transformer neutral point must be created artificially with separate ZN coupled earthing transformer that is connected to the substation bus bar. Compensation coil is then connected between ground and earthing transformer neutral point. With YNd primary transformer additional earthing transformer causes extra costs but also brings benefits.

Pekkala (2010) notes that if YNyn transformer primary winding has an unearthed neutral, during an earth fault the zero sequence current from the MV network causes magnetic unbalance because the zero sequence current has no return path in the primary side. Thus, the zero sequence current creates zero sequence flux in the core of the transformer. The zero sequence flux will find its path from yoke to yoke through the tank of the transformer and cause heating and resistive losses. The resistive losses in turn generate resistive component to the earth fault current.

Because of the zero sequence flux in the core, the zero sequence impedance of the YNyn transformer can be remarkably higher compared to a corresponding transformer with a delta-winding. The problem can be avoided with delta-connected tertiary winding that is not intended for loading. The delta-connected stabilising winding provides ampere-turn balance for the zero sequence current. Thus, the zero sequence flux is not generated to the core, which gives a reasonable zero sequence impedance. (ABB ltd 2004)

YNyn transformers are used by some DSOs and even though Petersen coil connection is seemingly easier, the zero sequence properties presented above favour the implementation of the delta secondary winding. Another factor that supports YNd transformers is that, in case the primary transformer is disconnected, and backup supply is provided from another substation also the compensation capacity is disconnected. If Petersen coil is connected to the bus bar via the earthing transformer compensation capacity remains even if the primary transformer is disconnected.

Changes in network topology affect total earth fault current and centralized coil must be adjusted accordingly to keep compensation degree constant. Centralized coil inductance is tuned with a regulator that measures zero sequence voltage since in network resonance point zero sequence voltage reaches its maximum value and compensation degree can be adjusted accordingly. In Figure 10 a simulated Petersen coil tuning curve during a bus bar fault is presented. When coil inductance is 205 mH the inductive

reactance equals capacitive reactance, hence system is in resonance and zero sequence voltage reaches its maximum value. (Guldbrand 2009)

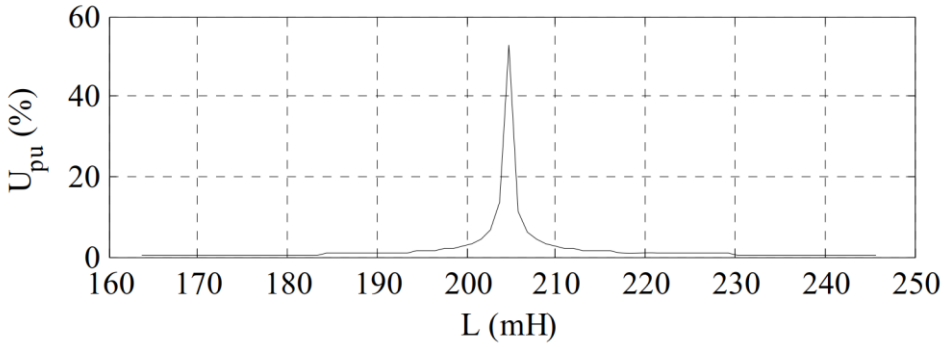

Figure 10. *Petersen coil tuning curve. (Guldbrand 2009)*

2.3.2 Distributed compensation

Centralized coils typically have compensation capacity of 100 – 250 A but especially when long rural area OHL feeders are replaced with cable the earth fault current produced by the network can exceed the capacity of the centralized coil. If smaller distributed coils can be placed along the cabled feeders the produced earth fault current can be compensated locally. Secondary substations provide practical facilities for coil placement, but again neutral point connection is needed in the 20 kV side. ZNzn or ZN(d)yn coupled distribution transformers have the neutral point in MV side so compensation units are typically connected there, so that the compensation unit and distribution transformer are both inside the same tank. Distributed coils are typically smaller than centralized coils having average compensation capacity of 5 – 15 A that is only adjustable with a no-load-tap-changer so that the amount of compensation is fixed when the compensation coil is energized.

Centralized and distributed compensation methods do not exclude each other but are many times implemented simultaneously. This approach is called mixed compensation where centralized coil is used to adjust the compensation degree, whereas distributed coils are intended to compensate most of the capacitive fault current produced by the feeders. Consequently, the degree of distributed compensation is strongly related to the location and the size of the galvanically interconnected network, therefore universal values for dimensioning of the distributed compensation degree cannot be given. A simplified example of mixed compensation is illustrated in Figure 11.

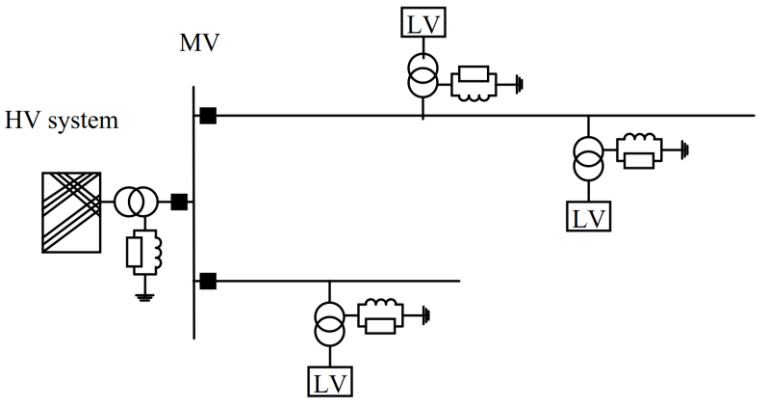

Figure 11. *An example of mixed compensation where Petersen coils are placed centrally at the substation and distributed in secondary substations. (Guldbrand and Samuelsson 2007)*

Guldbrand and Samuelsson (2007) suggest that a practical way to place the distributed coils is to consider the location of network disconnectors so that when a part of the network is disconnected also a corresponding amount of compensation is disconnected. This maintains the compensation degree of the rest of the network. Guldbrand and Samuelsson (2007) and Jaakkola and Kauhaniemi (2013) have studied how the distance in between distributed compensation units effects the behaviour of the system in different fault scenarios. In these researches another factor that effects coil placement is cost since more frequent the coils are more investment costs and maintenance costs they generate. Both studies propose 10 – 20 km distance to be cost-efficient and technically adequate in mixed compensation but according to Guldbrand and Samuelsson (2007) practical aspects such as already mentioned disconnector locations and ratings of the distribution transformers also influence the coil placement.

2.3.3 Compensation principles in Elenia's network

Since 2009 Elenia has built all new MV network with cable. This resulted in a need for large-scale compensation so most of the MV network is operated resonant earthed and these substations are equipped with at least one centralized coil. Compensation degree measured in percents can result significantly different magnitude of earth fault reactive component in different locations as the increase of earth fault current is unequal throughout the network. Therefore, in Elenia's network absolute value compensation is applied so that all the compensated substations are always 5 A undercompensated. To reinforce the compensation capacity distributed compensation is widely applied. Placement of the coils is determined mostly by the location of the disconnectors so that the concerned section contains corresponding amount of compensation. Degree of distributed compensation can vary depending the need of compensation. Generally, if

the earth fault current produced by the network is high the degree of distributed compensation is also high because centralized coils can compensate only 100 – 250 A depending on the rating, so the compensation must be reinforced with distributed units. Histogram of the distribution of degree of distributed compensation in Elenia's network is presented in Figure 12.

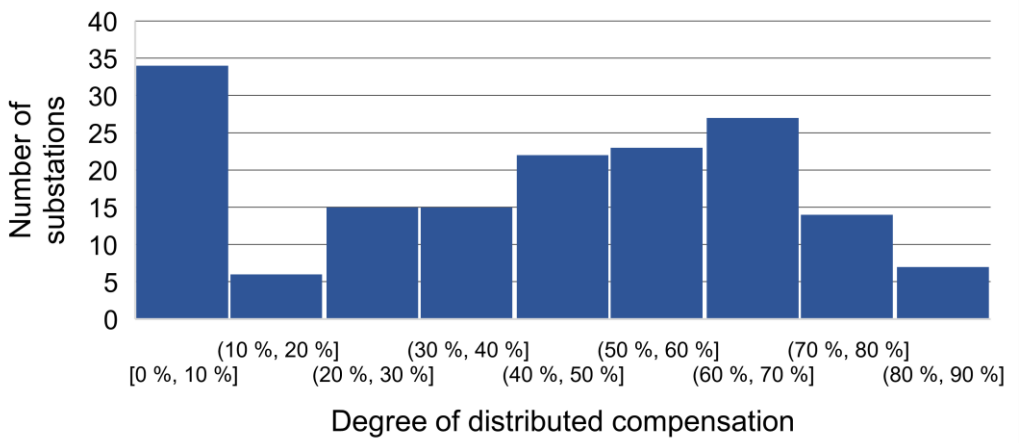

Figure 12. *Distribution of distributed compensation degree in Elenia's network in 2019. Isolated neutral substations excluded.*

Only substations with resonant earthed neutral are included in Figure 12 so that 0% distributed compensation indicates that the corresponding substation has only centralized coil. On the other hand, if the degree of distributed compensation is for example 60% this means that 60% of the total earth fault current is compensated distributedly and the remaining 40% centrally.

2.4 Earth fault protection in resonant earthed neutral system

In distribution networks single-phase earth faults are the most common fault type and thus fault detection and clearance are essential for safe network operation. Neutral earthing method and system requirements determine the adequate earth fault protection method and as the interest of this thesis is in resistive earth fault production in a resonant earthed MV network only protection methods relevant for that purpose are discussed more closely. For detailed treatment of network relay protection see Mörsky (1993).

In isolated neutral system fault current is purely capacitive, thus the phase displacement φ between $-\underline{U}_0$ and $\underline{I}_f$ is 90˚. This information can be exploited when arranging earth fault protection. Selectivity can be achieved with directional earth fault protection as the direction of the fault current is towards the network and current of the healthy phases is towards the substation. This is illustrated in Figure 5 in Section 2.2.1. When a protection

relay detects fault current flowing towards the network relay sends a tripping command to the corresponding circuit breaker that disconnects the faulted feeder.

In resonant earthed system capacitive fault current is compensated and therefore the phase displacement between $-\underline{U}_0$ and $\underline{I}_f$ is not constant as it is in isolated neutral system. The current measurement for protection is physically implemented as sum current measurement located at the substation in the beginning of each feeder. In the faulted feeder, this measurement does not equal to the fault current experienced at the fault location as the fault current produced by the faulted feeder capacitance is not seen by the sum current measurement in the beginning of the feeder, because now the fault current passes through the measurement in both directions and is therefore cancelled. Therefore, the sum current seen by the faulted feeder relay equals to the current produced by the healthy feeders and neutral point devices. (Lakervi and Partanen 2008)

This can be seen from Figure 7 and Figure 8 in Section 2.2.2 where earth fault current at the fault location is a sum of $\underline{I}_p$ and fault current produced by the faulted feeder $\underline{I}_f - \underline{I}_p$. The sum current measurement $\Sigma\underline{I}$ seen by the faulted feeder protection relay equals to $\underline{I}_p$ which is the current produced by the healthy feeders and neutral point devices.

The angle and amplitude of the sum current measurement of the faulted feeder are not constant, because the construction of the faulted feeder determines if the measurement is capacitive or inductive. For example, if the faulted feeder is a long cabled feeder it produces considerably capacitive fault current. Now, the sum current is inductive as the measurement does not see the capacitive current of the faulted feeder but it sees the sum of the current of the healthy feeders and the neutral point devices, which in this case is inductive. On the other hand, if the faulted feeder is short and consist mainly OHL the sum current is capacitive, because now the capacitive current production of the faulted feeder is minimal, and the fault current is mostly produced by the healthy feeders.

Non-constant nature of the angle and amplitude of the sum current makes it difficult to arrange selective protection that is only based on the absolute value and angle of the sum current. To avoid this problem, reactive component can be omitted, and the directional earth fault protection of resonant earthed systems can be based on the resistive component of the fault current. The resistive component is calculated as a product of $\Sigma\underline{I}$ and cosine of φ. This is illustrated in Figure 13 where sum current $\Sigma\underline{I}$ is denoted with I_0 and φ_{RCA} denotes characteristic angle that is chosen according the neutral earthing method, being 0° in case of resonant earthed system. In the characteristics diagram operating zone indicates that if the $I_0\cos(\varphi)$ phasor reaches that area protection relay will operate and disconnect the corresponding feeder.

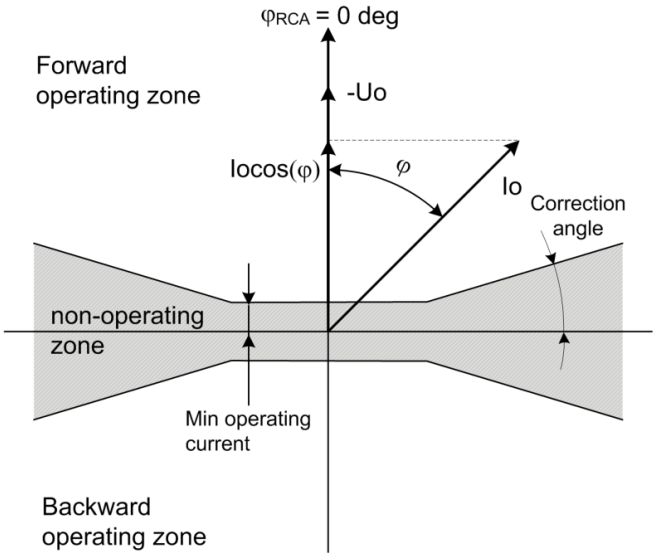

Figure 13. *Operating characteristic of directional earth fault protection based on resistive component. (ABB 2018)*

To ensure a reliable earth fault detection the magnitude of the resistive component must be large enough so that the relay is able to detect it. Resistive fault component is produced mostly by the losses of the Petersen coil and cable zero sequence series impedances but to ensure selective tripping resistive current can be magnified with a resistor that is connected in parallel with the centralized Petersen coil. The parallel resistor is illustrated in Figure 7 where it is denoted with R. During a fault voltage asymmetry occurs and zero sequence voltage over the resistor produces resistive current that flows towards the faulted feeder and can thus be detected by the relay.

Directional earth fault protection can be supplemented with $\underline{U_0}$ based protection function. The operating principle is rather simple, if the zero sequence voltage reaches certain threshold value, this indicates that an earth fault occurred somewhere in the system and the relay will trip. However, this method cannot detect the faulted feeder, thus it is not selective. $\underline{U_0}$ protection usually disconnects the entire substation and therefore relay operating time must be set so that directional fault current relay has enough time to operate first and $\underline{U_0}$ relay serves as a backup method. (Mörsky 1993)

2.5 Effects of extensive cabling

In typical three-phase MV cable the phase conductors have separate insulation but the phase wires are circulated around each other so that the distance between conductors is relatively small. On the contrary, OHL conductors have air gap insulation so they are installed on a pole with spacing between the conductors. Inductance is proportional to the conductor spacing; therefore, cable inductance is smaller than corresponding OHL.

Conductor capacitance on the other hand, is inversely proportional to the conductor spacing which yields a high capacitance for cables and low capacitance for OHLs.

Majority of rural area MV networks in Finland were built and maintained with OHLs before the legislation in Electricity Market Act (2013) redefined the requirements of reliability of distribution. Consequently, several Finnish DSOs are planning to partly replace their OHL networks with weather-proof underground cables. This transition has drastically changed the structure and electrical properties of MV network. Among the many features that will change along this makeover is the increase of capacitance that increases reactive power production and earth fault current production in the network. The design and operating principles that have been applied on OHL network do not necessarily resettle well in cable network. Especially the simplifications and assumption that have been used in traditional OHL earth fault analysis must be reconsidered. The different approaches in earth fault analysis can also be noticed by comparing sources from different ages. See for example Lakervi and Holmes (1995) and comparably Guldbrand (2009).

2.5.1 Assumptions of traditional earth fault analysis

Cables and OHLs can be mathematically modelled with a π-section equivalent circuit where admittance $\underline{Y}$ is divided in two parts that are connected in both ends of the section and impedance $\underline{Z} = R+\mathrm{j}X$ in between the admittances. In π-section cable parameters are centralized so that values can be given in per kilometre format. A π-section is illustrated in Figure 14 where $\underline{U}_S$ and $\underline{I}_S$ are sending end voltage and current and $\underline{U}_R$ and $\underline{I}_R$ are receiving end voltage and current.

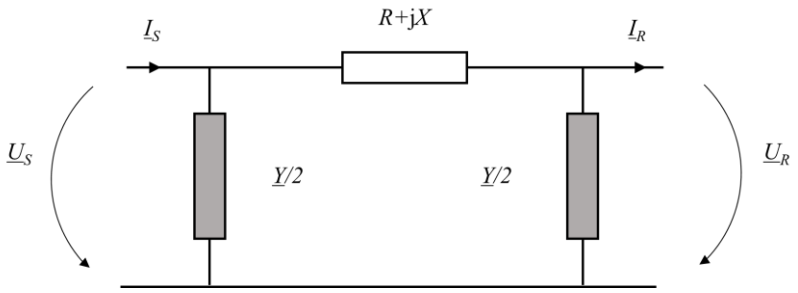

Figure 14. *Cable π-section equivalent circuit.*

In traditional nominal frequency earth fault analysis, most of the feeder length is assumed to be either OHL or urban area cable. In these cases, line series impedance $\underline{Z} = R+\mathrm{j}X$ is considered insignificantly small compared to the shunt admittance that consist mostly of capacitance. Urban area cable networks are composed of multiple short parallel feeders with large conductor cross-section. These feeders can be represented with

parallel connected π-sections so that the ratio of shunt capacitance and series impedance does not significantly change. Therefore, the shunt capacitance dominates the earth fault current production also in urban area cable network. (Lakervi and Partanen 2008) According to Nikander and Mäkinen (2017) this justifies the following assumptions in OHL network and urban area cable network:

- Length of each line type and total shunt capacitance are the dominant factors in earth fault analysis.
    - The number of feeders and length of distinct feeders are insignificant.
- The resulting earth fault current is almost completely capacitive and proportional to total feeder length and shunt capacitance of the line segments.
    - Earth fault current can be compensated with Petersen coil.
- Earth fault current and zero sequence voltage can be determined by network shunt capacitance, compensation coil reactance, parallel resistor resistance and fault resistance.
- Guldbrand (2009) also states that in traditional earth fault analysis location of the fault does not influence the earth fault behavior of the system.

The above mentioned assumptions are applied in Section 2.2 Figure 5 and Figure 7 where single-phase earth fault in isolated neutral system and resonant earthed system is presented. In these examples and corresponding equations (7-10) lines are represented only with capacitances C_1 and C_2 and series impedances are omitted.

In rural areas there are less feeders, but the length of individual feeder can be remarkably longer than in urban area. Therefore, the equivalent circuit representation is formed with series connection of multiple π-sections because single π-section only represents a short section of the feeder. Now, the effect of series impedance increases and is not necessarily negligible. (Nikander and Mäkinen 2017)

Cable zero sequence impedance decreases as a function of cable length but more importantly the resistive part of the impedance increases proportionally to the cable length. Guldbrand (2009) has simulated the cable zero sequence impedance as a function of cable length and compared the behaviour of a cable that is modelled only with shunt capacitance and a cable that is modelled with π-sections. The modelled cables have XLPE insulation and circular 95 mm^2 conductors. The simulation results are shown in Figure 15.

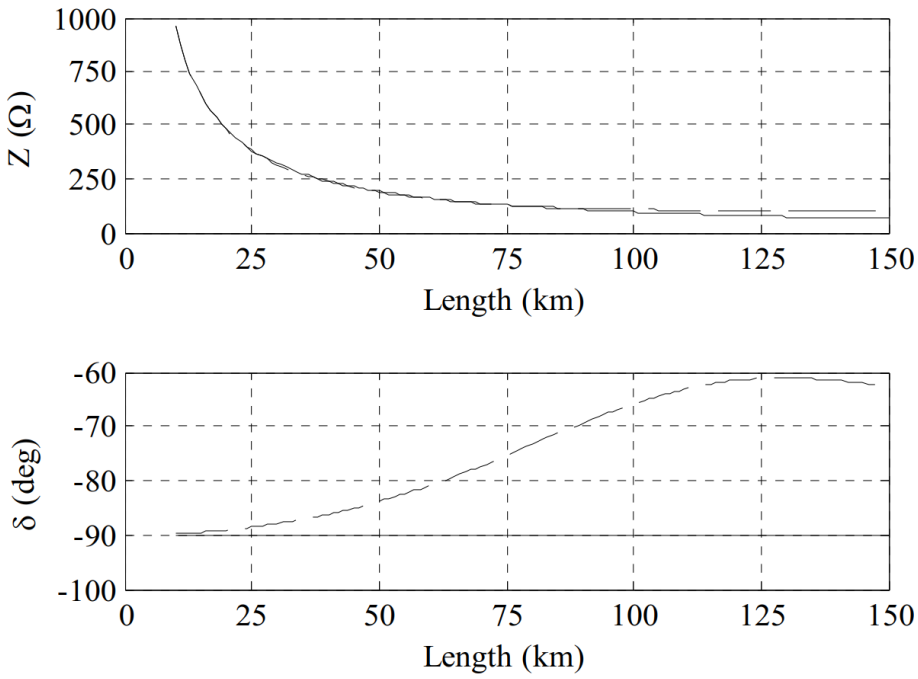

Figure 15. *Cable zero sequence impedance magnitude and argument modelled with π-section (dashed) and capacitance only (solid) as a function of cable length. (Guldbrand 2009)*

In Figure 15 the amplitude of the cable zero sequence impedance presented in the upper graph does not significantly change whether the cable is modelled with pure capacitance or π-section. In the lower graph when argument δ = -90˚ the impedance is completely capacitive, as expected in traditional earth fault analysis. However, π-section model shows that as cable length increases the argument decreases indicating an increase in the resistive component of the zero sequence impedance. This resistive component affects the earth fault analysis and therefore, as the cable length increases the assumption that series impedance is negligible is no longer valid. This also implies that the traditional earth fault analysis is not accurate in networks consisting of long cable feeders. (Guldbrand 2009)

2.5.2 Earth fault current resistive component

Capacitive impedance component is proportional to the cable length but as seen in Figure 15, when cable length exceeded 25 km the resistive component of the cable zero sequence impedance becomes non-negligible. According to Nikander and Mäkinen (2017) in long cable feeders also a resistive current component is generated to the fault current in addition to the capacitive current. Resistive fault current is produced with respect to the zero sequence voltage as illustrated in Figure 16 where U_0 is applied over the π-section. Cable is modelled with a single equivalent π-section, X_{0m} denotes primary

transformer zero sequence reactance, R_N is parallel resistor and X_N is compensation coil reactance. Cable shunt susceptance is B_0 and $R_0 + jX_0$ is zero sequence impedance.

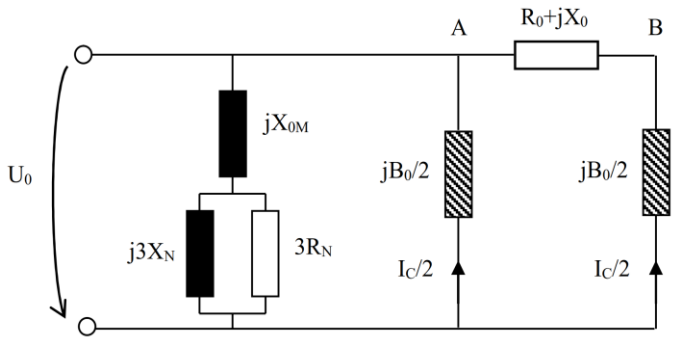

Figure 16. *Simplified equivalent circuit of zero sequence network in cable network. (Nikander and Mäkinen 2017)*

In Figure 16 zero sequence voltage is applied over primary transformer and neutral point devices and point A that indicates the first half of the cable susceptance. However, the voltage applied over point B is not equal to the voltage over point A. This is caused by capacitive charging current that flows through the series impedance causing voltage losses which in turn generates the resistive current component. (Nikander and Mäkinen 2017)

Long cable feeders in rural area network oppose a new challenge to earth fault control and safety aspects. Before the extensive cabling during 2010s the resistive current produced by the network was mostly disregarded or at least the effect on residual fault current was estimated to be minor. The problems arising from the increase of the resistive component has been addressed in several researches such as Guldbrand (2009), Pekkala (2010), Vehmasvaara (2013) and Nikander and Mäkinen (2017). Because the resistive current component cannot be compensated with Petersen coils its increase can compromise safe network operation. In resonant earthed network equipped with adjustable Petersen coil the capacitive fault current component is always nearly constant. However, as cable length increases, resistive component can increase even beyond the level of compensated capacitive current and possibly increase the absolute value of the residual current to an unaccepted level.

Guldbrand (2009) has simulated the behavior of earth fault current components with respect to cable length when cable is modelled with parallel connected π-sections, as in urban area and series connected π-sections, as in rural area. The results are illustrated in Figure 17 where resistive component is in upper graph and capacitive component is in lower graph. The simulation in conducted with the same 95 mm^2 XLPE cable as in Figure 15.

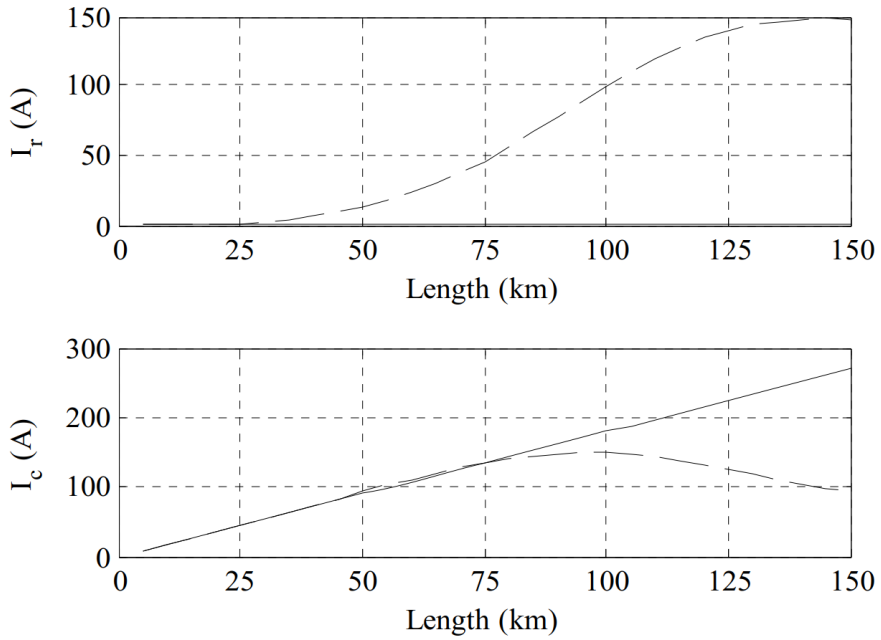

Figure 17. *Resistive and reactive components of earth fault current in urban system with several short cables (solid) and rural system with one long cable (dashed). Guldbrand (2009)*

Simulation verifies the intuitive result that when cable is modelled as parallel connected urban area network, cable can be considered as pure capacitance and capacitive component increases linearly and solid line of the resistive component in the upper graph is zero regardless of the cable length. When series connected model representing long rural area network is applied the results are different. Now, as cable length reaches certain threshold value the resistive component starts to increase. In this simulation approximately 25 km. This is in accordance with the theory presented earlier that the series impedance and resistive earth fault current of long cable feeders are non-negligible. The capacitive current behaves similarly in both simulation cases until after 75 km the lines separate because the series connected rural system reaches the fundamental frequency resonance peak at 100 km cable length. (Guldbrand 2009)

3. RESISTIVE EARTH FAULT CURRENT PRODUCTION IN MV NETWORK

Cable network zero sequence series impedance produces resistive earth fault current with respect to zero sequence voltage but there are also other sources such as resistive losses of the compensation devices and centralized Petersen coil parallel resistor that produces resistive current to ensure selective protection. The sum of these resistive current sources enlarges the absolute value of the residual earth fault current because unlike the capacitive component, resistive component cannot be compensated with Petersen coils.

The challenge is that cable zero sequence impedance is associated with multiple uncertainties and hence the parameters that affect resistive earth fault current production are not given as data sheet values. This is partly because of external factors, such as cable installation and grounding connections along the cable feeder, which can vary significantly in different locations. Therefore, calculating resistive current is difficult and requires certain assumptions that lead to inaccuracies. This in turn creates uncertainties in earth fault hazard voltage examinations because if resistive current is inaccurate also the absolute value of the residual current is inaccurate. Residual current is the fault current experienced at the fault location and if the magnitude exceeds safety limitations the ground potential rise near earthed network parts can cause danger for human safety. Because of the uncertainties in zero sequence impedance it is hard to identify the parts of the network where the resistive current might increase so that it can cause problems.

Section 2.5.2 demonstrates that network resistive current production is relevant only in the case of long cable feeders. During the current decade, cabling of rural area MV network has been one of the key factors shaping the electricity distribution industry in Finland. Elenia has set a goal of 75% of the entire network to be cabled by 2028. This ensures that the reliability of distribution required by legislation will be reached. On the other hand, extensive cabling means that long cabled feeders are no longer rarity and thus means to estimate resistive current production are needed. This Chapter presents the general aspects and properties of different sources of resistive earth fault current.

3.1 Cable zero sequence impedance

Cable zero sequence impedance is not known as cable type specific line constant. According to Nikander and Mäkinen (2017) zero sequence series impedance is influenced by:

- conductor cross-section
- cable screen(s) and corresponding impedance
- geometric dimensions of the cable
- possible earth wire and corresponding impedance
- ground resistivity
- cable grounding and grounding impedances.

Therefore, cable zero sequence impedance is dependent not only on the electrical properties of the cable but also the installation and surrounding circumstances such as ground properties which in addition might not be constant over the length of the cable. That is why there is no universal values for cable zero sequence series impedance.

When an earth fault occurs and phase conductor is simultaneously connected to earthed screen and ground potential the fault current has three return paths: cable screen, conducting earth wire or other nearby conductors and ground. This is illustrated in Figure 18 where $\underline{I}_{sc}$ is the current flowing in cable screen, $\underline{I}_{ew}$ is the current in earth wire, $\underline{I}_{\mathrm{E}}$ is the current in ground and R_{E} is the resistance to earth potential. Voltage $\underline{U}$ is applied over all three phases.

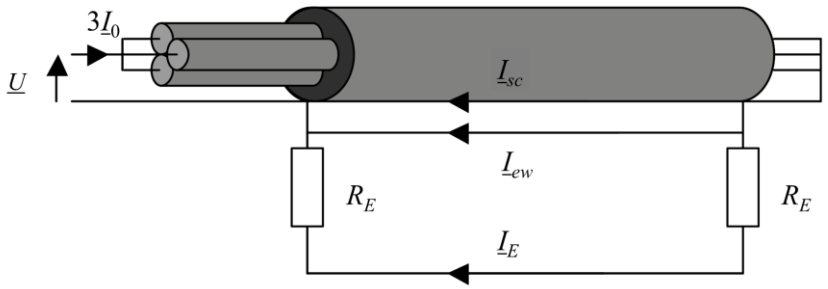

Figure 18. *Earth fault current return paths in three phase cable with common screen. (Edited from Guldbrand 2009)*

The phase conductors and return path conductors form three circuits. The cable in Figure 18 has a common screen but some cable types such as AHXAMK-W have separate screens for all conductors. Zero sequence impedance depends on self and mutual impedances of the three current paths in Figure 18, impedances are defined by the cable structure, dimensions and return path properties. (Nikander and Mäkinen 2017)

According to Guldbrand (2009) from the current paths zero sequence impedance can be formed as

$$\underline{Z}_0 = \frac{\underline{U}}{\underline{I}_0} = \frac{3\underline{U}}{\underline{I}_{sc} + \underline{I}_{ew} + \underline{I}_E} \tag{14}$$

3.1.1 Calculation methods

The zero sequence impedance in equation (14) can be calculated with matrix equation that are based on general flux equations derived for the three circuits of Figure 18. The matrix equations are formed from the self and mutual impedances of the conductors and return paths. The model is based on the equations by Carson (1926) and detailed derivation of the model is presented by Da Silva and Bak (2013) and Guldbrand (2006).

In the following example calculation model and cable model are based on the work by Guldbrand (2009) where cable with common screen is used. The properties of a such cable are presented in Figure 19 where cable screen radius is r_{sc} and the distance between conductors is denoted with d and conductor radius with r_c. Installation includes an earth wire with radius r_{ew} and distance d_0 from the cable.

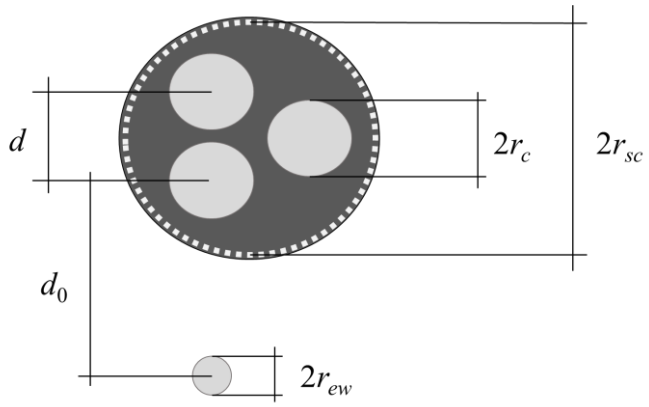

Figure 19. *Cable dimensions with additional earth wire. (Edited from Guldbrand 2009)*

This configuration forms the three circuits that create the mutual and self impedances between conductor and screen, conductor and earth wire and conductor and earth. Based on these connections resistance and reactance matrixes that compose the impedance matrix can be formed. For detailed derivation of the impedance matrix see Da Silva and Bak (2013). Matrix equations are as follows:

$$\underline{Z} = R_{matrix} + \mathrm{j}X_{matrix} \tag{15}$$

$$R_{matrix} = \begin{bmatrix} R_{sc} + R_c & R_c & R_c \\ R_c & R_{ew} + R_c & R_c \\ R_c & R_c & 2R_E + R_c \end{bmatrix} \tag{16}$$

$$X_{matrix} = \frac{\omega \mu_0}{2\pi} l \cdot \begin{bmatrix} \ln \frac{r_{sc}^2}{r_{sc}^{'} r_c^{'}} & \ln \frac{d_0 r_{sc}}{d_0 r_c^{'}} & \ln \frac{D_e r_{sc}}{D_e r_c^{'}} \\ \ln \frac{d_0 r_{sc}}{d_0 r_c^{'}} & \ln \frac{d_0^2}{r_{ew} r_c^{'}} & \ln \frac{D_e d_0}{D_e r_c^{'}} \\ \ln \frac{D_e r_{sc}}{D_e r_c^{'}} & \ln \frac{D_e d_0}{D_e r_c^{'}} & \ln \frac{D_e^2}{r_e^{'} r_c^{'}} \end{bmatrix} \tag{17}$$

In the resistance matrix R_{matrix}

R_c is conductor resistance,

R_{sc} screen resistance,

R_{ew} earth wire resistance and

R_{E} is the earthing resistance.

In the reactance matrix X_{matrix}

μ_0 is the permeability of the free space,

l is the cable length, [m]

D_{e} is the equivalent penetration depth [m] (see eq. 18) and

r'_{c} denotes geometric mean radius (GMR) of the conductors (see eq. 19),

r'_{sc} GMR of the screen, and

r'_{ew} GMR of the earth wire.

Based on Carson (1926) equivalent penetration depth is defined as

$$D_e = 659\sqrt{\frac{\rho}{f}} \tag{18}$$

Where ρ is the ground resistivity [Ωm] and f is system frequency [Hz].

According to Elovaara and Haarla (2011) in case of three conductors GMR is defined as

$$a' = \sqrt[3]{a_{12} a_{23} a_{31}} \tag{19}$$

where distance a_{ij} is the distance between centers of conductors i and j.

Zero sequence impedance equation (14) can be defined with the impedance matrix (15) as inverse of the sum of all inverse matrix elements:

$$\underline{Z}_0 = \frac{\underline{U}}{\underline{I}_0} = \frac{3\underline{U}}{\underline{I}_{sc} + \underline{I}_{ew} + \underline{I}_E} = \frac{3}{\sum_{i=1}^{3}\sum_{j=1}^{3}\underline{Z}_{ij}^{-1}} \quad (20)$$

Intuitively all the parameters have an influence on the zero sequence impedance but the length of the cable is especially interesting because the resistive current production increases as cable length increases. Also, the influence of the additional earth wire is interesting because Pekkala (2010) and Malm et al. (2015) state that the additional earth wire can remarkably decrease the zero sequence impedance. The influence of the earth wire is also related to the uncertainties in resistive current calculations because some cable types, such as AHXAMK-W include an earth wire but if other cable types are used external earth wires can be installed next to the cable as in Figure 19. The problem related to external earth wires is that they are not always properly documented in DSOs network information system or there can be other conducting materials nearby the cable that have similar effect on the zero sequence impedance as intentionally installed earth wires. So, if existence of an earth wire or related conductor is unknown it is nearly impossible to account the impact on the impedance value.

The zero sequence impedance matrix equations (15-20) were calculated with respect to cable length with and without the additional earth wire. The parameters used in the simulation were analogous to Guldbrand (2009) and hence the results are also in accordance. Cable properties and parameters are presented in Table 1 and Table 2. Conductor and earth wire material is copper.

Table 1. *Cable properties.*

Conductor area	Screen area	Earth wire distance	Resistance to earth, R_e	Earth wire area
95 mm^2	25 mm^2	0.1 m	10 Ω	35 mm^2

Table 2. *Cable dimensions used in zero sequence impedance simulation.*

Cable	r_c [m]	r_{sc} [m]	d [m]	r_{ew} [m]	d_0 [m]	R_c [mΩ/m]	R_{sc} [mΩ/m]	R_{ew} [mΩ/m]
3x95/25	0.0058	0.024	0.02	0.0033	0.1	0.107	0.8	0.52

The simulation results are illustrated in Figure 20. Results are in Ω/km format, so the values represent the line constant at the corresponding cable length. This also illustrates the nonlinear nature of the zero sequence impedance with respect to cable length.

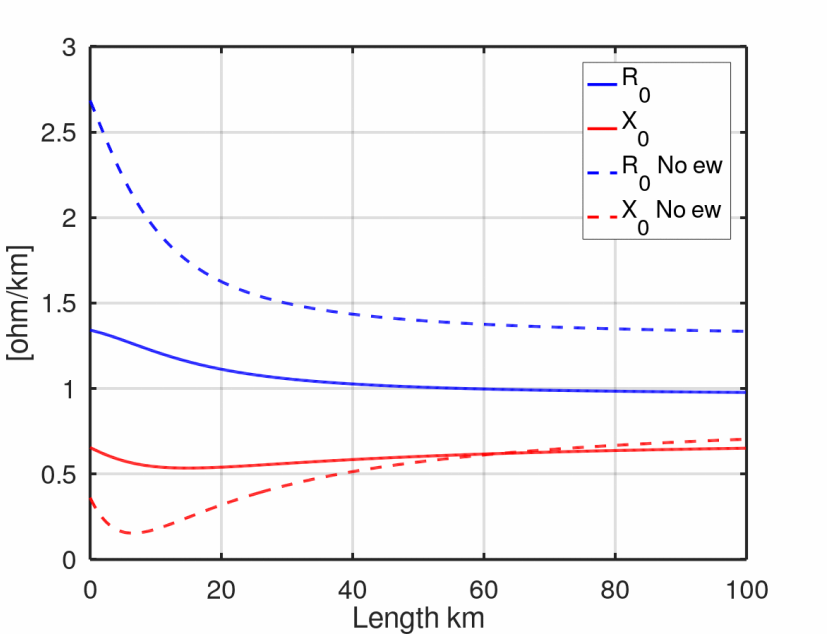

Figure 20. *Cable zero sequence resistance and reactance with earth wire (solid) and without earth wire (dashed) as a function of cable length. Calculated with equations (15-20).*

In this simulation the resistance to earth R_E is constant at all cable lengths and therefore its effect is accentuated at short lengths. According to Guldbrand (2009) when cable length exceeds 60 km the impedance of the cable screen and earth wire increases so that a large proportion of the current flows through the ground and hence zero sequence resistance is close to constant for the rest of the cable length.

The impact of the additional earth wire is clearly seen in Figure 20. The dashed line representing cable installation with no earth wire has notably larger zero sequence resistance than the solid line representing cable with earth wire. On the other hand, earth wire decreases zero sequence inductance when considering short cables. This indicates that installing earth wire into cable assembly has significant effect on the resistive earth fault current production of the cable network. Likewise, this result verifies the assumption that earth wires increase the uncertainties related to zero sequence impedance and resistive earth fault current calculation. Any conducting material with earth connection nearby the cable can electrically act in the same way as the earth wire. Together with the intentional earth wires they can affect the zero sequence resistance notably and the problem is that the presence of these grounded conductors is in many cases unknown for the DSO.

The study and simulations conducted by Guldbrand (2009) show that also cable dimensions and installation effect the behaviour of the zero sequence impedance.

Additionally, resistance to earth has an influence and is also highly dependent on the condition of the ground, which in turn increase the uncertainties.

Zero sequence impedance calculation method used by Pekkala (2010) and Vehmasvaara (2013) is originally composed by G. Henning from ABB. The model is presented in equation (21) and it assumes earth fault current to return through the cable screen and earth, hence the effect of an external earth wire is not included in the model.

$$\underline{Z}_0 = l\left(R_c + 3\frac{\mathrm{j}\omega\mu_0}{2\pi}\ln\frac{r_s}{\sqrt[3]{r_c' d^2}}\right) + \frac{3lR_{sc}\left[2R_E + l\left(R_g + \frac{\mathrm{j}\omega\mu_0}{2\pi}\ln\frac{D_e}{r_{sc}'}\right)\right]}{2R_E + l\left(R_{sc} + R_g + \frac{\mathrm{j}\omega\mu_0}{2\pi}\ln\frac{D_e}{r_{sc}'}\right)} \tag{21}$$

Where R_g is the ground resistance [Ω/m], defined as

$$R_g = \frac{\omega\mu_0}{8} \tag{22}$$

To compare the results given by the two presented approaches also equation (21) was calculated with respect to cable length and the results are given in Ω/km format. The cable dimensions and properties are according to Table 1 and Table 2 and the results are illustrated in Figure 21.

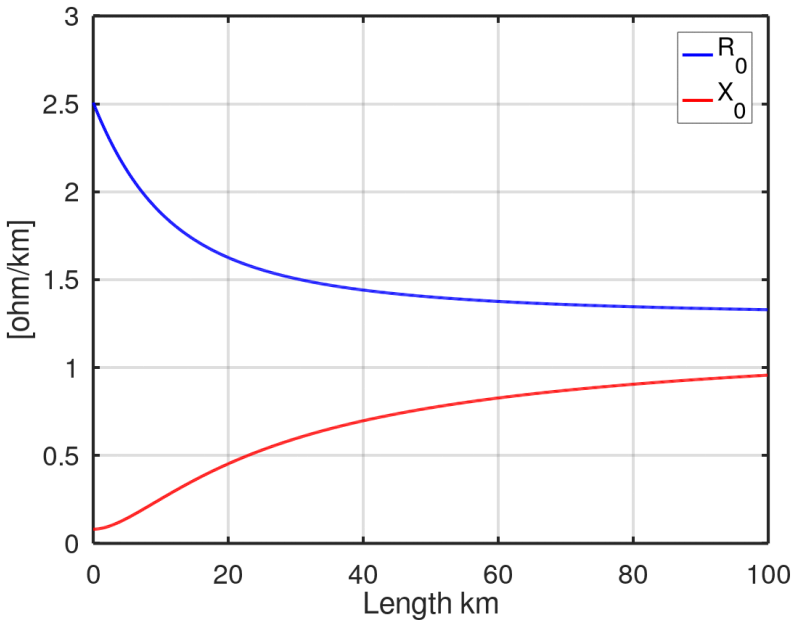

Figure 21. *Cable zero sequence resistance and reactance with respect to cable length calculated with equation (21).*

The results of equation (21) are similar to the results obtained with matrix equations (15-20) if the effect of the earth wire is ignored. The behaviour is close to equal, impedance

decreases when cable length increases. Also, the values obtained with the two models are close to each other which implies that both models are adequate if there are no earth wires or related conductors nearby the cable.

3.1.2 Discussion

In traditional earth fault analysis, the effect of zero sequence impedance was mostly ignored and there was no need for detailed calculation models. Now, alongside increased cabling the need for reliable calculation model has emerged, but the change does not happen over-night. According to Malm et al. (2015) there is only limited experience in implementing different calculation methods, in addition these models contain several uncertainties that are related to properties of the cable and the installation location.

The results and references presented in this Chapter also highlight the nonlinear nature of cable zero sequence impedance which is in accordance with the study by Malm et al. (2015). Their research regarding cable zero sequence impedance calculation methods and measurements concluded that calculation models can be derived but the models need to be examined case-by-case. This means that generalizations that would simplify the analysis are difficult to make without compromising accuracy.

Cable parameters are mostly fed to calculation softwares in Ω/km format and then multiplied with the corresponding cable length. The results in this Chapter show that the series impedance values do not increase linearly with respect to cable length. This means that case-specific analysis would be needed but considering the uncertainties high precision calculation would not be reasonable. Another finding during this work was that some network information systems no not support zero sequence impedance values in radial network computation. This means that even if sensible series impedance values could be obtained it would be impossible to apply them in everyday network design and planning operations. Therefore, if DSO wants to include the resistive current component to earth fault analysis, different means to estimate resistive current production in the network are needed.

3.2 Compensation devices

Compensation devices in this context consider central and distributed Petersen coils. The capacitive earth fault current produced by the long cable feeders causes voltage drops along the cable series impedance, which in turn generates the resistive component to earth fault current. Capacitive fault current production at the end of the long feeders

can be decreased with distributed compensation. In case of long feeder if compensation is located near the cable capacitance the fault current flowing through the cable series impedance will be smaller and so the resistive current production can also be decreased. (Guldbrand and Samuelsson 2007)

Jaakkola and Kauhaniemi (2013) as well as Nikander and Mäkinen (2017) have reached similar results. In their simulations distributed compensation decreased the network resistive current production. If only central compensation was applied the capacitive current was efficiently compensated but the current flow in the cable series impedance produced resistive current component that in turn increased the absolute value of the residual current at the fault location.

The conclusion in the above-mentioned theoretical examinations and simulations is that with properly located and dimensioned distributed compensation coils the network resistive current production can be decreased. However, the coils are not ideal, so resistive losses are present which means that also the coils themselves produce minor resistive current during an earth fault. Yet, the purpose of the coils is to produce inductive current with respect to zero sequence voltage so the parameters and materials should be designed so that resistive losses are minimal. The central and distributed coils both generate losses and thus produce resistive earth fault current, but the size of the coil affect the losses so that the current production of the central coil is more than one individual distributed coil. However, as the number of distributed units increase so does the amount of losses. In case of the central coil resistive losses and resistive current production of are proportional to the coil inductance, more precisely the air gap of the core. The control of the compensation level is done by adjusting coil inductance by changing the air gap of the core. Structure, materials and size of the coil all affect the resistive losses so the values must not be generalized, but an example of resistive current production of a 250 A centralized Petersen coil used in Elenia's network is presented as a function of coil position I_{pos} in Figure 22. The nominal voltage is $20/\sqrt{3}$ kV.

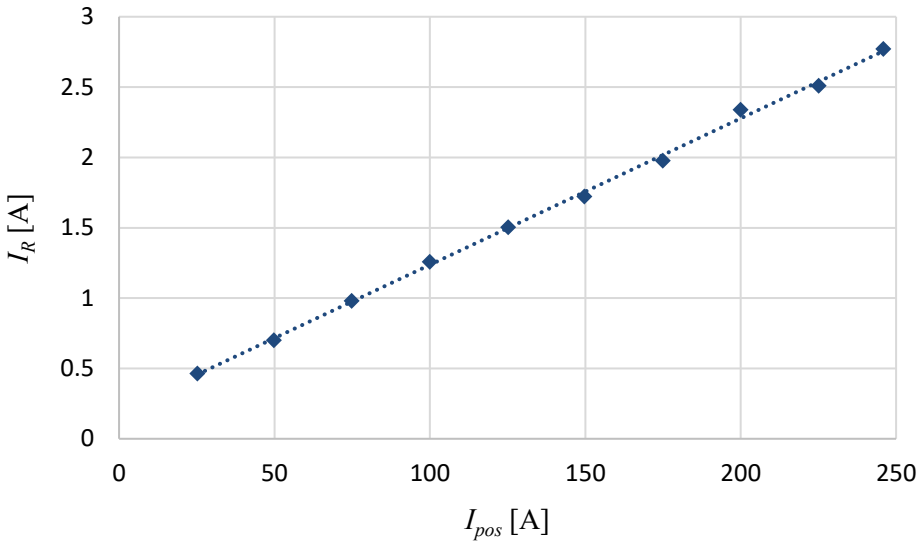

Figure 22. *Resistive current production of a 250 A centralized Petersen coil as a function of coil position.*

The compensation capacity, or position of the Petersen coil is often presented in terms of inductive current production. This makes it easier to quantify the compensation level because even though inductance and Henrys are the actual variable measures, current and Amperes are easier to compare with the fault current that is needed to compensate. Figure 22 illustrates that resistive current production is proportional to coil position but even in maximum loading the current generated by the coil losses is less than 3 A.

3.3 Central coil parallel resistor

For protection purposes a resistor is connected in parallel with the centralized Petersen coil. Healthy state zero sequence voltage is caused by natural voltage asymmetry due to asymmetry of the phase capacitances. High zero sequence voltage can cause unintentional tripping of the $\underline{U}_0$ protection relay so the zero sequence voltage is reduced with the parallel resistor. In OHL network voltage asymmetry is a result of difference in line length of the three phases but as the network is renewed with cable the length difference and thus voltage asymmetry and zero sequence voltage are reduced naturally.

On the other hand, earth fault protection of compensated MV network is based on measuring the resistive component of the earth fault current. So even though in cabled network zero sequence voltage reduction is not necessary to achieve selective tripping it is needed to increase the earth fault current resistive component with the parallel resistor. (Mörsky 1993) Depending the need, there are different principles to operate the parallel resistor. In Elenia's network parallel resistor is always connected but as

presented by Mörsky (1993) depending the network configuration there are also different approaches.

- The resistor is always connected (used in Elenia)
- the resistor is disconnected in healthy state but connected after a short delay when a fault occurs
- the resistor is connected in heathy state but disconnected when a fault occurs and after a short delay connected back on.

Study on system behaviour and advantages of the different parallel resistor operation principles is given by Isomäki (2010).

Parallel resistor is connected to a power auxiliary winding (PAW) of the centralized Petersen coil. Resistor connection and schematic diagram are illustrated in Figure 23.

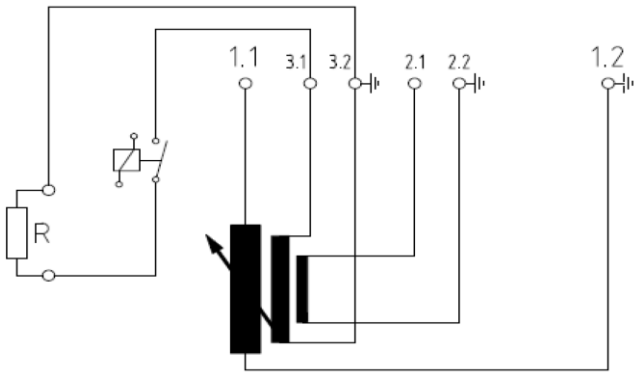

Figure 23. *Schematic diagram of the Petersen coil and the parallel resistor connection. 1.1-1.2 primary winding, 2.1-2.2 measurement winding, 3.1-3.2 PAW. (Isomäki 2010)*

Commonly PAW nominal voltage is 500 V and the resistor value can vary for example from 2 – 10 Ω. By Ohm's law and transformer turns ratio equation, primary winding side current produced by the resistor can be calculated as:

$$I_1 = \frac{U_2^2}{U_1 R} \tag{23}$$

where primary side is indicated with the index 1 and secondary side (500 V) with the index 2. The nominal voltage in the primary winding during a solid earth fault equals to healthy state line-to-neutral voltage $20/\sqrt{3}$ kV. Therefore, a 2.5 Ω resistor connected to PWA will induce approximately 8 A resistive current in the primary side. The primary winding side value is the current seen by the protection relay.

3.4 Network topology and fault location

A long cable feeder should be modelled as a series connection of multiple π-sections. In urban systems with short cables the π-sections are parallel coupled and cable impedance is purely capacitive. Thus, fault location does not affect the fault current magnitude. This can be seen in Figure 24 where coupling of sequence networks during an end of the line earth fault in urban system is illustrated. (Guldbrand 2009)

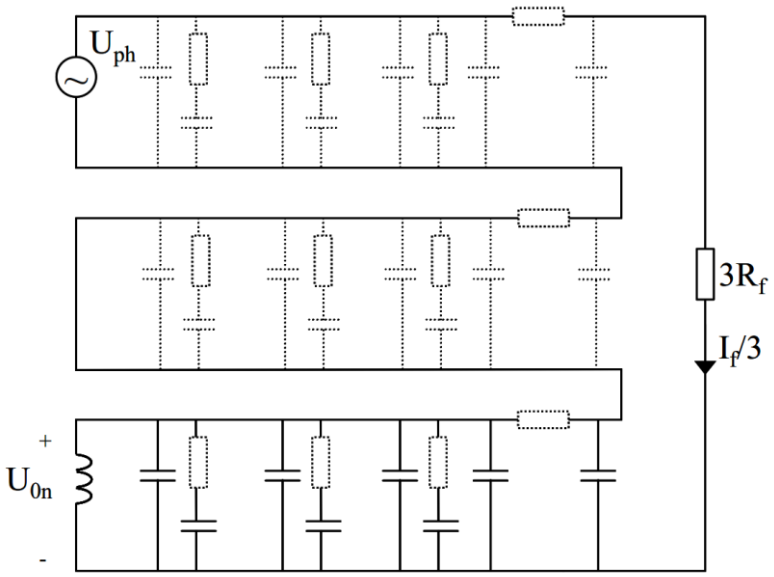

Figure 24. *Coupling of the sequence networks during an end of the line earth fault in an urban system. (Guldbrand 2009)*

On the contrary, in Figure 25 the sequence networks coupling during the end of the line earth fault is illustrated in rural system. Now series impedance is non-negligible and positive and negative sequence also influence the earth fault behaviour. The equivalent impedance is proportional to cable length and thus the fault location does affect the fault current magnitude. (Guldbrand 2009)

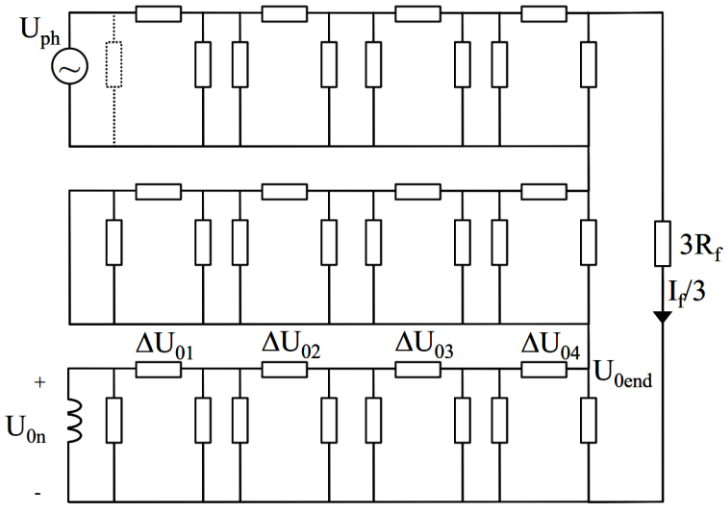

Figure 25. *Coupling of the sequence networks during an end of the line earth fault in a rural system. (Guldbrand 2009)*

According to Guldbrand (2009) the voltage in rural system is distributed over multiple series impedances which causes zero sequence voltage (U_{0end}) over the end of the line to be smaller than the neutral point displacement voltage (U_{0n}). Resistive as well as capacitive current is produced with respect to zero sequence voltage thus voltage reduction will decrease the fault current production. In traditional earth fault analysis the fault current is assumed to be independent of the fault location but as long cable feeders become more common the assumption might not be valid anymore.

The resistive properties of cable zero sequence series impedance are also called damping. Wahlroos and Altonen (2014) present measurements which indicate that increased damping due to long cables has impacts on the earth fault behaviour of the system. In Figure 26 the difference of earth fault transient damping in an earth fault near the substation and far-away from the substation is presented.

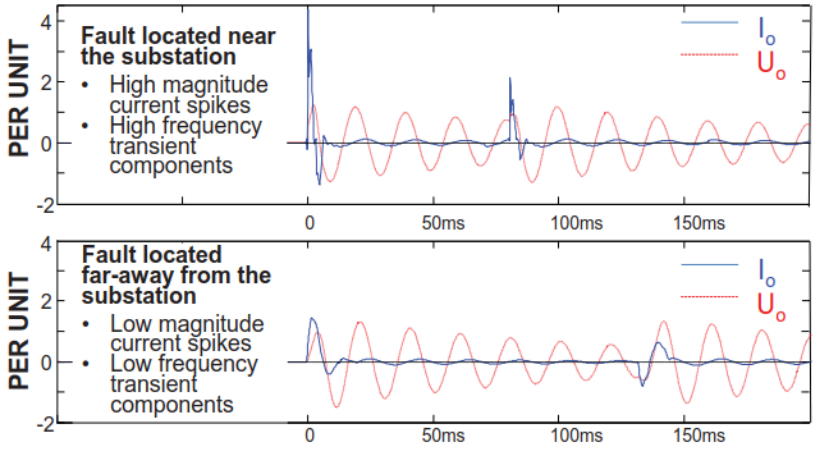

Figure 26. *Damping of earth fault transient due to fault location. (Wahlroos and Altonen 2014)*

In the upper graph fault is located close to the substation and in the lower graph approximately 30 km from the substation. The damping caused by cable series impedances is clearly visible as high transient peaks are cut form the lower graph. This indicates that in case of long cable feeders fault location affects the system damping and thus impacts the earth fault behaviour. The transient damping can make difficult to apply transient based earth fault protection methods. (Wahlroos and Altonen 2014)

The simulations by Nikander and Mäkinen (2017) support the theory that fault location affects capacitive as well as resistive current production in case of long cable feeders. In their study when the fault was at the end of the 50 km long cable the zero sequence voltage was reduced by 13% compared to the busbar fault and therefore resistive current at the fault location was reduced by approximately 20% compared to the busbar fault.

Another important result obtained by Nikander and Mäkinen (2017) is that also feeder configuration affects the resistive current production. In the simulation 50 km uniform cable was changed to 25 km cable with 2 km branches located 2 km apart so that the total cable length remained equal. The topology of the healthy feeders was similar in both simulation cases. During a busbar fault the current produced by the healthy feeders was not changed but the topology modification reduced the resistive current production of the faulted feeder by almost 40%. The zero sequence voltage was not significantly affected by the topology modification. This indicates that resistive current produced by the cable network is related to the location of the fault as well as the network topology. It is an important observation because in real networks feeders are mostly branched multiple times.

3.5 Measurement possibilities

Calculation of resistive earth fault current is associated with multiple uncertainties, but it is possible to measure the resistive current production in the healthy state of the network. Centralized Petersen coils are equipped with a regulator that analyses the network and adjusts the coil inductance to compensate feeder capacitances. The basic operating principle of the regulator was explained in Section 2.3.1. In addition to resonance point measurement and tuning of the Petersen coil, the regulator provides network parameters such as zero sequence voltage, inductive current produced by the coil in the present position, compensation degree, current of the resonance point and resistive current produced by the network during a solid earth fault. A screen view of one regulator is seen in Figure 27 where I_w (w stands for watt-metric) denotes the resistive current.

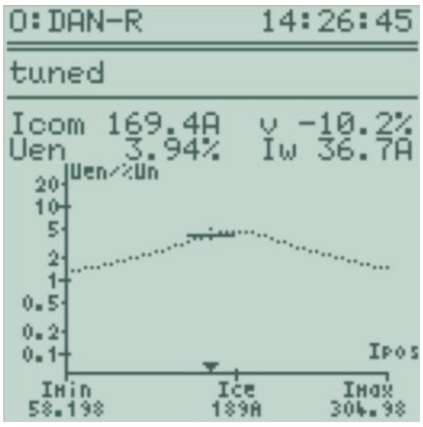

Figure 27. *Screen view of one Petersen coil regulator. (A-eberle GmbH 2017)*

The measurement is provided real time, so the parameters correspond the current switching state of the network. A more detailed description of how the regulator measures the resistive current is provided by A-eberle GmbH (2017).

4. HAZARD VOLTAGES AND SYSTEM REQUIREMENTS

If only continuity of distribution is considered operating the network during an earth fault would be beneficial and even technically possible because in ZNyn and Dyn coupled distribution transformers, the delta primary winding will balance the voltage asymmetry caused by the earth fault and the fault would not affect the customers. However, the current flowing from phase to ground can energize earthed network equipment and if there are energized components exposed to touch, safety might be endangered. In network operation safety is always a fundamental factor and that is why managing earth fault related hazard voltages is essential parts of reliability of distribution.

As illustrated in Figure 18 if the fault is in a cable the residual earth fault current has multiple return paths, so only a certain share of the current flows in the ground. Current flow in the ground, also called current to earth I_E, creates the ground potential rise that causes hazard voltages, thus current to ground is the main interest when considering electrical safety related to earth faults. The SFS 6001:2018 standard defines two ways to calculate I_E. If there are no compensation coils at the proximity of the earthing system, I_E is calculated

$$I_E = rI_{re} \tag{24}$$

where I_{re} is the absolute value of the residual earth fault current, see equation (13), r is the reduction factor that describes the ratio of I_E and $3I_0$ that is the sum of zero sequence currents of the phase conductors. Reduction factor depends on the cable properties, earthing system of the network and earthing conditions, so the value is case-specific. For detailed derivation of cable network reduction factor and effect of the earthing system, see Fickert et al. (2018). For three-phase MV cable, SFS 6001:2018 defines the reduction factor as

$$r = \frac{I_E}{3I_0} = \frac{3I_0 - I_{sc} - I_{ew}}{3I_0}. \tag{25}$$

In equation (25) current in screen I_{sc} and current in earth wire I_{ew} are reduced from $3I_0$ to obtain the share of the earth fault current that flows to ground. If r = 0 all the current flows in the screen or earth wire and no current flows in the ground. On the contrary, there are no ground wires in OHLs typically used in MV network, so the earth fault current

has no other return path except the ground and therefore r = 1 which means that all the residual current flows to ground from the fault point.

SFS 6001:2018 states that the second way of calculating I_E should be applied if there are compensation coils at the proximity of the fault, because the coils feed inductive current to the earthing system and thus the effect must be considered. The current to earth is then calculated as

$$I_E = r\sqrt{I_L^2 + I_{re}^2} \tag{26}$$

where I_L is the sum of the nominal currents of the parallel connected compensation coils and both I_L and I_{re} are absolute values.

The current to earth I_E encounters resistance to earth R_E that means the resistance seen from the fault point with respect to reference earth that is assumed to be so far away that the potential there is zero. (Saarijärvi et al. 2014) Besides the resistive component, ground connection has also reactive component and thus impedance to earth $\underline{Z}_E$ could also be used. However, according to IEEE 81-2012 standard, the reactive component is insignificant in 50 Hz frequency if only constricted earthing systems are considered but on the other hand, in global earthing system, especially in low ground resistivity areas the reactive component can reach major values and then the effect must be accounted. Consequently, earthing voltage U_E is caused by the earthing current I_E flowing through the resistance to earth R_E. U_E can be calculated

$$U_E = R_E I_E \tag{27}$$

U_E is the voltage applied between the earthing electrode and the reference earth, but the ground potential rise is depended on the distance from the fault point. According to Saarijärvi et al. (2014) when current to earth is fed from a single earthing electrode in homogenous ground the ground potential rise with respect to reference earth can be expressed with voltage U_r that is depended on the distance x from the electrode.

$$U_r(x) = \frac{\rho I}{2\pi x} \tag{28}$$

Where,

U_r is the voltage with respect to reference earth [V]
ρ is the ground resistivity [Ωm]
x is the distance to earthing electrode [m]
I is current [A]

Current flows to earth from the interface of the electrode and ground. If the electrode is hemispherical and the ground is homogenous, then also the current diverges from the electrode as hemispherical front as illustrated in Figure 28. Now, the resistance of each hemispherical and differentially thick section on the current path is depended on the ground resistivity, area of the hemisphere and thickness of the section. Therefore, the voltage over each differentially thick section is inversely proportional to the distance from the center of the electrode. (Saarijärvi et al. 2014)

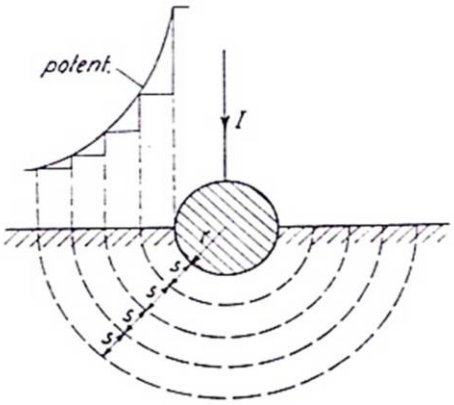

Figure 28. *Ground potential rise and current divergence around a hemispherical electrode during and earth fault. (Suuronen 2006)*

The equation (28) describes the ground potential rise around the electrode that feeds the current to ground. From the equation (28) can be seen that increase of the ground resistivity ρ increases the voltage, respectively. Nikander and Järventausta (2005) state that on the average the ground resistivity in the Nordic countries is higher than for example in Central Europe. This yields a higher risk of hazard voltages during an earth fault. Some approximate ground resistivity values are presented in Table 3. SFS 6001:2018 notes that changes in the moisture of the ground can temporarily affect the resistivity value on the top layers of the soil. Furthermore, the standard says that ground resistivity can vary remarkably in different depths, as soil is usually composed of multiple layers with diverse properties.

Table 3. *Ground, concrete and water resistivities. (SFS 6001: 2018)*

Substance	Average Ωm	Conventional range Ωm
Clay	40	25 …70
Clay mixed with sand	100	40 … 300
Mud, peat	150	50 … 250
Sand	2000	1000 … 3000
Moraine gravel	3000	1000 … 10000
Gravel	15000	3000 … 30000
Granite rock	20000	10000 … 50000
Concrete, wet or in the ground	100	50 … 500
Concrete, dry	10000	2000 … 100000
Lake or river water	250	100 … 400
Groundwater	50	10 … 150
Seawater	2.5	1 … 5

4.1 Effects of electricity on human body

Alternating current (AC) can cause severe damage when flowing through human body. Even minor current magnitude can result in muscle contractions, but larger currents also cause burns of different degree. Electrical injuries might have only minor effects on the outside of the skin but despite the seemingly small marks, tissue and organ damages on the inside can be large and serious. Rapid temperature rise of only 10 degrees Celsius from normal body temperature is enough to damage muscles, nerves and blood vessels. Inner electrical burns are especially complicated because the damages might show symptoms with a delay, even years after the accident. (Lahti 2017)

In fatal low voltage electrical injuries, the most common cause of death is ventricular fibrillation where electrical timing of the heart does not function normally and the ventricles contract in dyssynchrony so that the heart is unable to circulate blood through the body. (Tiainen 2017) According to Saarijärvi et al. (2014) ventricular fibrillation is caused by current density in the vicinity of the heart. When current density exceeds certain frequency dependent threshold, the risk of ventricular fibrillation increases rapidly. Current density can be estimated from total current flowing through human body I_{B}. Figure 29 illustrates the thresholds of effects of AC current on human body with respect to body current I_{B} and duration of the current flow, when current is flowing from left hand to feet.

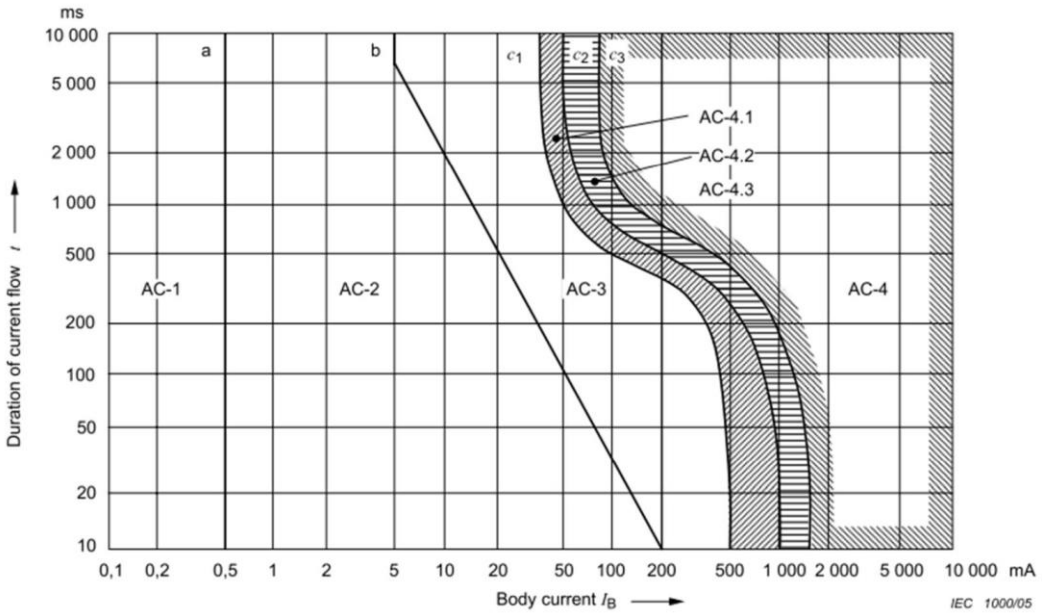

Figure 29. *Conventional time/current zones of effects of AC currents (15 – 100 Hz) on persons for a current path corresponding to left hand to feet. (IEC/TS 60479-1: 2005)*

In IEC/TS 60479-1 standard the effects of AC current are categorized in zones according to the current magnitude and duration of the current flow. The zones can be interpreted as:

- AC-1: imperceptible
- AC-2: perceptibility threshold, no muscle reactions
- AC-3: muscle contractions threshold, reversible effects
- AC-4: possible irreversible effects
- AC-4.1: up to 5% probability of ventricular fibrillation
- AC-4.2: 5-50% probability of ventricular fibrillation
- AC-4.3: over 50% probability of ventricular fibrillation.

The impedance of human body is not insignificant because the current flowing through body is restricted by the body impedance. The total impedance of human body is composed of skin impedance at the touchpoint and internal body impedance. The impedance is nonlinear and dependent on touch voltage U_{T} as illustrated in Figure 30. In low voltages skin impedance dominates the total impedance, resulting impedance values of multiple $\mathrm{k\Omega s}$. In low voltage values, also the area of the touchpoint affects the total impedance. When touch voltage exceeds 50 V skin impedance is partly shorted and as voltage exceeds 200 V, total impedance is mostly influenced by the internal body impedance. (Tiainen 2017)

Body impedance is not constant for all humans. That is why the impedance values in Figure 30 are given with confidence intervals so that the 95% line indicates the values that 95% of the population will not exceed and 5% line indicates values that that are lower with only 5% of the population.

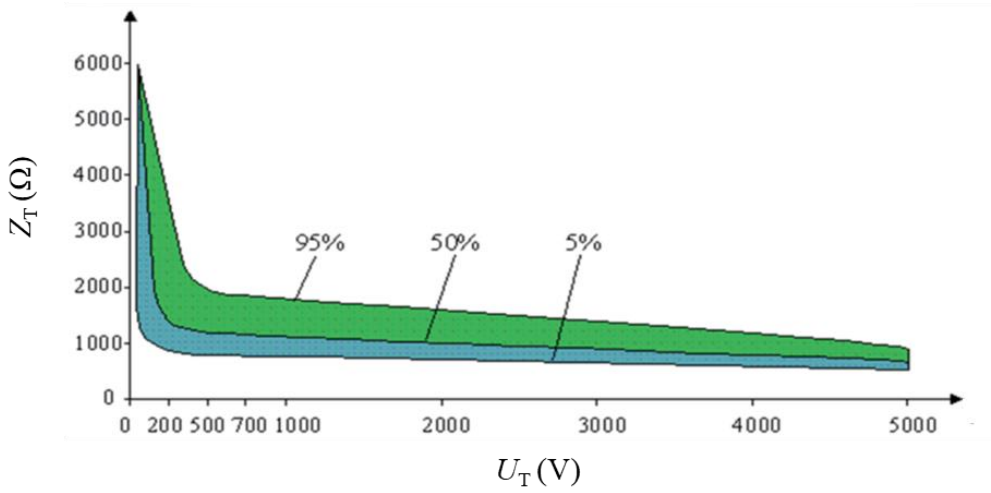

Figure 30. *Confidence intervals of human body impedance as a function of touch voltage. (Edited from Tiainen 2017)*

Considering the voltage dependency of body impedance, it is worth noticing that LV network line-to-ground voltage 230 V is generally enough to produce 100 mA current through human body. If the duration of the current flow is 1s, 100 mA current causes ventricular fibrillation with over 50% probability. (Lahti 2017)

4.2 Touch voltage requirements

Earth faults cause ground potential rise according to equation (28) so that the full potential is applied at the fault location and the potential is then decreased with respect to the distance from the fault. Ground potential rise causes potential difference in the ground that can result touch or step voltages. In Figure 31 b the potential distribution is illustrated with the curved lines starting from the top of the pole, also different step and touch voltages are illustrated. In scenario a, the person is in contact with the metallic frame and ground potential, thus the earthing voltage U_E is applied over the person. The full earthing voltage U_E is rarely applied over a person, but in the scenario b of Figure 31 a steel pole is energized by a live conductor so that the pole acts as an earthing electrode. Now, a person leaning to the pole has his/her hand and feet in different potential, thus touch voltage U_T is applied over the person. In addition, step voltage U_S is applied over the two feet of the person standing nearby the fault point. Step voltage is decreased as the distance from the fault increases. (Lakervi and Holmes 1995)

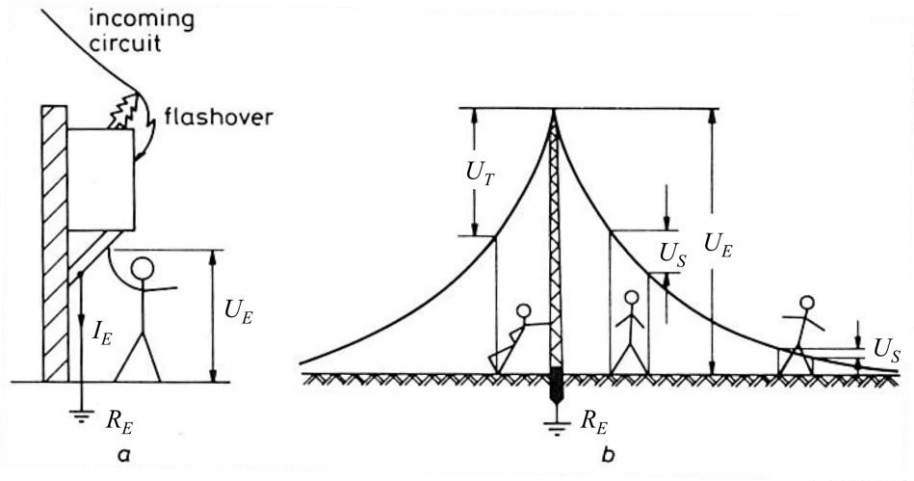

Figure 31. *Hazard voltages caused by an earth fault (Edited from Lakervi and Holmes 1995)*

Current flowing through body I_B is dependent on the voltage and on the other hand body impedance Z_T so when the threshold of hazardous body current is known (Figure 29) limits for permissible touch voltages U_{TP} can be derived with certain margin of certainty. SFS 6001:2018 standard defines the U_{TP} values according to Figure 32.

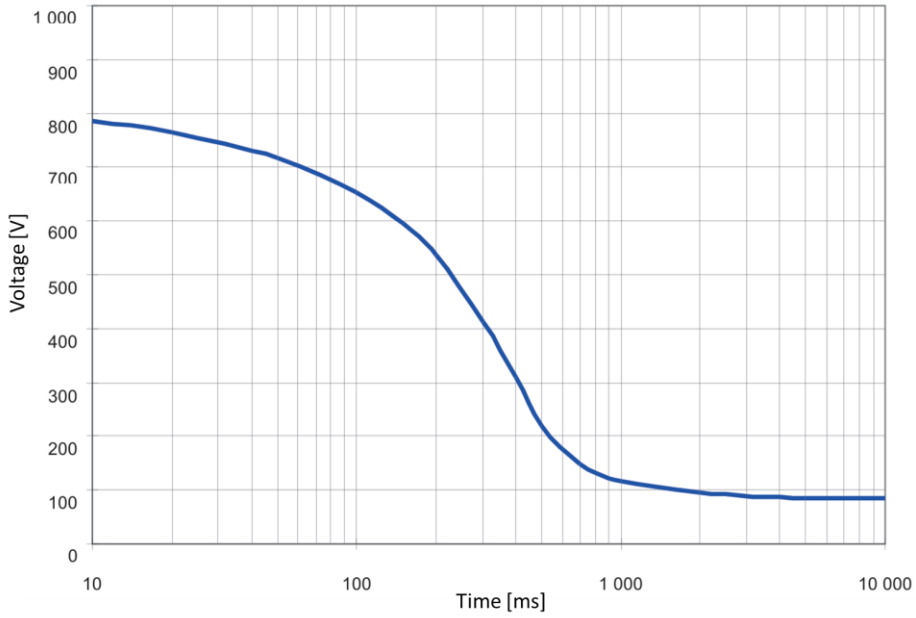

Figure 32. *Permissible touch voltages U_{TP} as a function of current flow duration. (SFS 6001:2018)*

SFS 6001: 2018 states that in high-voltage system, touch voltages are in permissible level, if:

1. System is part of global earthing system, introduced in Section 4.4, or
2. certain touch voltage and earthing requirements are fulfilled.

Option 2 requires that in the corresponding earthing system that is not considered global, earthing voltage U_{E} levels must be in permissible range, so that

$$U_E = I_E Z_E \leq 2U_{TP} \tag{29}$$

With certain prerequisites (SFS 6001:2018 Appendix E) also $U_{\mathrm{E}} \leq 4U_{\mathrm{TP}}$ level is accepted. Another way to fulfil option 2 is to prove by measurements that the U_{TP} levels in Figure 32 are not exceeded in the corresponding earthing system.

4.3 Residual earth fault current in SFS 6001

In resonant earthed neutral system the fault current at the fault location is called residual current. As presented in Section 2.3 equation (13) residual current is composed of

- Reactive component $\underline{I}_C + \underline{I}_L$
    - In an undercompensated system reactive component consists of the uncompensated capacitive fault current, due to the detuning of the centralized Petersen coil.
- Resistive component I_R
    - Resistive current produced by the network zero sequence impedances.
    - Centralized Petersen coil parallel resistor.
    - Losses of the Petersen coils.
- Harmonic component $\underline{I}_H$
    - Omitted in this thesis

Out of the components of the residual current, reactive component is known, since it can be calculated with the compensation degree K and the capacitive fault current produced by the network, which are both relatively easy to obtain. Resistive component, on the other hand, is associated with multiple uncertainties, mostly because of the non-trivial resistive current produced by the network zero sequence series impedances. The other sources of resistive current, centralized Petersen coil parallel resistor and losses of the centralized and distributed compensation coils are both assumed to be minimal.

SFS 6001:2018 states that if the value of the residual current in the resonant earthed neutral system is unknown the value can be assumed to be

$$I_{re}^{'} = 10\% I_C \tag{30}$$

So presumably residual current is approximately 10% of the network capacitive earth fault current $\underline{I}_C$. The assumption does simplify the earth fault analysis but as network

cabling continues and resistive current production increases respectively, feasibility of this assumption must be considered.

4.4 Earthing systems

An earthing system comprises of all interconnected earthing facilities in a specific area, but the extent of the interconnected facilities determines if the earthing system is considered local or global. The earth electrodes must have a galvanic connection so that the physically separate earthing facilities are electrically interconnected. Traditionally rural areas had only local earthing systems, because OHLs had no earth wires and thus the separate earth electrodes were not linked. Cables on the other hand, have earth wires and screens that are connected to system earthings at the substation and at the distribution transformers, hence these earth electrodes are galvanically connected. Cabling drastically changes the earthing connections of MV network.

Mäkinen (2016) has studied the MV network earthing systems and states that interconnected radial or meshed earthing systems contribute each other so that it rapidly impacts the common earthing impedance as the earthing system expands. The resulting earthing impedance is decreased as the number of connected distribution transformers increases, first connections having the biggest influence. This is illustrated in Figure 33 where resulting impedance to earth is presented as distribution transformers that individually have 20 Ω impedance to earth, are radially interconnect.

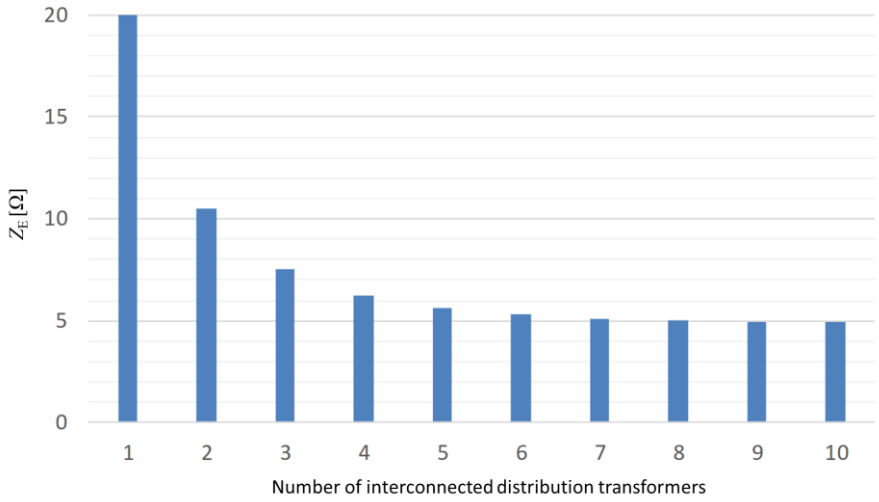

Figure 33. *Resulting impedance to earth as a function of number of radially interconnected distribution transformers spaced 1 km apart. Location of examination is at the beginning of the earthing system. (Mäkinen 2016)*

According to SFS 6001: 2018 a global earthing system has uniform earth connections by interconnected local earthing systems. The vicinity of interconnected earthing facilities ensures that dangerous touch voltages do not occur. The global earthing system enables earth fault current to diverge so that the ground potential rise at the local earthing system is limited. The standard also states that the existence of a global earthing system must be proven either by measurements or in typical cases by calculations. The typical examples of a global earthing system comprise of city centres or urban and industrial areas whit extensive HV and LV earthing.

5. PROBLEM DESCRIPTION AND RESEARCH METHODS

Since 2009 Elenia has built all new MV network with underground cable and the rapid increase of network capacitance and its multiplicative effects have already resulted several researches. The increase of resistive earth fault current is already noted in some of the commissioned studies such as Pekkala (2010) and Vehmasvaara (2013) but as the increase of resistive earth fault current has realized in some parts of the network more specific and practically oriented study was needed.

5.1 Touch voltage examinations and increase of resistive current

During an earth fault, the residual current flows to the fault point and results ground potential rise as presented in Chapter 4. Specifically, it is the current to ground I_{E} that causes the ground potential rise and equations (24-26) define the methods for calculating I_{E} based on SFS 6001:2018. However, equations (24-26) are case-specific because the value of the reduction factor depends on the type of conductor and quality of the earth connection, so in order to define a generalized scenario that provides a safe estimate of the current to ground, the effect of the reduction factor can be omitted, so that r = 1. This is in fact a generalization that produces results that might be worse than the situation actually is, but it is true if the fault is located at OHL section of the network. Therefore, residual current in total is assumed to flow to ground and touch voltage examinations are conducted so that the voltage to ground $U_E \leq 2U_{\mathrm{TP}}$, as specified in equation (29).

Now, $I_E = |\underline{I}_{re}|$, Z_E is the highest impedance value of the considered earthing system and U_{TP} value is based on Figure 32 where current flow duration time is the earth fault protection tripping delay. The examination is then conducted for all components in the system that contain an earth connection. These are for example substations and distribution transformers. Touch voltage examinations in Elenia are conducted in above mentioned manner.

Because of the assumption r = 1, it is particularly important to know the value of the residual earth fault current. The total value of the resistive component of the residual earth fault current is associated with uncertainties as presented in Chapter 3. Therefore, the residual current applied in touch voltage examinations is based on the definition of

SFS 6001 that says: if the value of residual current in resonant earthed neutral system is unknown the value can be assumed to be 10% of network capacitive earth fault current.

As MV network cabling has increased the share of cabled rural area network, there is a concern on the validity of the 10% estimation, thus there is a need for more accurate model. Resistive component cannot be compensated with the conventional Petersen coil systems and therefore if the resistive component increases remarkably the absolute value of the residual current increases, respectively. If the residual current estimation method is inaccurate, so are touch voltage calculations where the residual current values are applied.

5.2 Objective of the study

The objective of this study is to develop a model to estimate residual earth fault current in extensively cabled medium voltage network. Out of the components of the residual current, reactive component is known but the resistive component contains uncertainties, that are related to the cable network zero sequence series impedance, network topology and installation of the cable. Thus, the resistive earth fault component must be calculated or estimated more closely to gain more accurate values of the residual earth fault current. The harmonic component is also part of the residual current, but it is out of the scope of this thesis.

Theoretical models that could be applied in calculation of the resistive component are already presented for example by Guldbrand (2009) and Nikander and Mäkinen (2017) but there is a need for a more generalized approach. The mentioned researches provide models that can be used for accurate modelling of the resistive current in a specific location, but it would be difficult to apply the models to large number of distinct locations with various network topologies. Therefore, the goal of this thesis was to develop a model that allows resistive current component estimation with the information that is available in the network information system. The resistive current values can then be used in calculation of residual earth fault current, which in turn is used in touch voltage examinations. Because the model should adapt according to the changes in the network, the model can be used in protection design, to see how the residual earth fault current magnitude is changed if more cable is connected to the system, or alternatively if some parts of the network are disconnected. This enables agile estimation of the touch voltages in different locations and in different switching states of the network.

The second objective was to examine if SFS 6001 10% assumption is applicable in Elenia's network. Besides, if the assumption in the standard is inaccurate, a more precise model would enable to identify the locations in the network, where resistive earth fault current might increase the residual current, so that the touch voltage requirements are possibly exceeded.

Another factor that should be considered, is that as SFS 6001: 2018 states that 10 % is taken from network *capacitive earth fault current,* it does not specify the interpretation in detail. If the distributed compensation devices are used, the amount the distributed units compensate is fixed and the corresponding share of the earth fault current is compensated as the fault occurs. That is why the network capacitive earth fault current can also be interpreted as the share of the fault current that flows to the substation and is compensated by the centralized coil. These currents are illustrated in Figure 34.

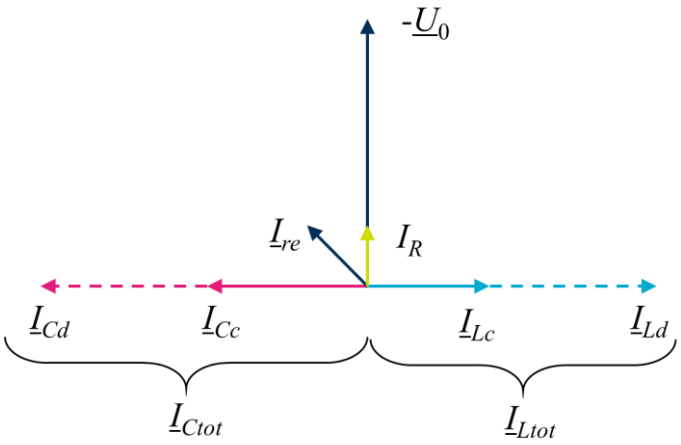

Figure 34. *Phasor diagram of distributed and centralized compensation currents.*

In Figure 34:

$\underline{I}_{Ld}$ is sum of inductive current of the distributed Petersen coils

$\underline{I}_{Lc}$ is inductive current of centralized Petersen coil

$\underline{I}_{Ltot} = \underline{I}_{Ld} + I_{Lc}$ total current of the compensation units

$\underline{I}_{Cd}$ capacitive fault current compensated by the distributed units

$\underline{I}_{Cc}$ capacitive fault current flowing to the substation, (current of the resonance point)

$\underline{I}_{Ctot} = \underline{I}_{Cc} + \underline{I}_{Cd}$ total capacitive fault current produced by the network

To summarize the interpretation, capacitive earth fault current can be interpreted as the total capacitive fault current produced by the network $\underline{I}_{Ctot}$, or as only the capacitive current flowing to the substation $\underline{I}_{Cc}$. The latter is also the current of the resonance point

measured by the centralized Petersen coil regulator. Consequently, the effect of these two alternative interpretations was also studied.

5.3 Plausible approaches

In this thesis three different approaches of estimating residual earth fault current were attempted. To assess the feasibility of the approaches, the following requirements were set for the estimation model:

1. The model must be applicable with the information available in the network information system,
2. changes in the switching state of the network must be easily accounted into the model,
3. model must be generalizable into networks with similar operating principles.

In the following section the plausible estimation approaches are presented.

5.3.1 Analytical solution

First, formulation of an analytical solution was attempted. In this case analytical solution refers to forming a set of equations that could be applied to calculate the resistive earth fault current production. The equations presented in Chapter 3 form a basis, from where it would be possible to calculate the current production by accounting the effect of the network zero sequence impedance. However, as the demand was for a more heuristic model that could be easily applied into different scenarios, the analytical solution soon proved to be impractical. Secondly, since the network zero sequence impedance is nonlinear with respect to cable length, the analytical solution would be laborious to use because the effect of the cable length should be calculated individually in every scenario. Besides, as demonstrated in Figure 20 the effect of an earth wire can remarkably affect the zero sequence impedance value, thus the zero sequence values should be calculated separately for all cable types and in addition account the effect of cable length.

Forming an analytical solution to estimate resistive current was an ambitious challenge and for a case-specific purpose it would be possible and even appropriate, but as the need was for a generalizable model the analytical solution approach was quickly discarded.

5.3.2 Computer aided analytical solution

The first criteria set for the estimation model was that it must be applicable with the information available in the network information system. In analytical solution the problem was that it is difficult to apply to multiple large networks. However, the networks are already documented in DSOs network information system and the information contains cable types, lengths and all the other needed parameters. So, if zero sequence impedance values could be calculated, the information could be utilized directly in the network information system.

Obtaining the zero sequence values would require solving the matrix equations (15-20) by hand and doing so for a large amount of cable types of different length would again be laborious and inconvenient, so the alternative approach was to use PSCAD transient simulation software's *solve line constants* feature that calculates the zero sequence impedance values. Required cable parameters are available in public data sheets so this type of calculation would be possible. Chapter 3 highlights the uncertainties related to cable zero sequence impedance so the values calculated by PSCAD would be as good as the initial data and the possibility of inaccuracies must be accounted, but this approach would easily give some first estimates of the zero sequence impedance. The impedance values would be then inserted into corresponding cables in network information system which would then be used to calculate the resistive current production. The original thought was to validate the results by comparing the calculated resistive current values from a certain substation to the live measurement provided by the Petersen coil regulator.

However, this approach soon faced an insurmountable challenge. The network information system used in Elenia was not able to take into account the cable zero sequence impedance values in radial network computation mode. Thus, in earth fault analysis, the system only calculated the capacitive current produced by the network, even though the zero sequence values were inserted to the corresponding cables. The meshed network operation mode on the other hand was able to account the zero sequence values but as it is intended for 110 kV network computation, the meshed network mode did not regard the compensation effect of the centralized Petersen coil. That is why resistive current calculation was not possible with the current version of Elenia's network information system. These insufficiencies were critical and hence, also the computer aided analytical solution was discarded.

5.3.3 Statistical examination

Neither of the analytical approaches fulfilled the requirements, so the last option was to apply statistical examination. Large amount of network data is available in the network information system and real-time resistive current measurements are provided by the Petersen coil regulators, so estimating resistive current with statistical methods would be possible.

One can argue why an additional estimation method is needed if the Petersen coil regulators already provide resistive earth fault current measurements. Firstly, the resistive current measurements are not available from all the substations and even if it is provided the measurement might be available only locally at the substation, which is a problem if the substation is in a remote location. Secondly, the measurement is from the present state of the network, so topology changes cannot be studied without real switching operations, which would be impractical. With the additional estimation model, resistive earth fault current, and analogously residual earth fault current, can be analysed in different network configurations as a part of protection design.

The objective in the statistical examination was to find parameters that would describe resistive earth fault current production sufficiently to form a model that would be accurate enough, while also fulfilling the requirements presented earlier. It was obvious that statistical examination would not provide perfectly accurate results, but after all, the need is for a practically oriented heuristic model, that will provide more accurate values than the SFS 6001 10% assumption. The results of the statistical examination are presented in the following chapter.

6. RESULTS OF STATISTICAL EXAMINATION

Calculation of the resistive earth fault current proved to be challenging and impractical in the extent that was needed for this thesis. If direct calculation was not possible the alternative solution was to search for variables with known values, that would behave in similar way with respect to network properties, as the resistive earth fault current. If strong enough correlation exists, the found variables could be used to estimate the resistive current production in the network. Again, the requirements set in Section 5.3 were applied so that the variables needed to be available in the network information system, comply with the switching state of the network and be generalizable.

6.1 Data acquisition

For the statistical examination, a network parameter dataset was composed. Only MV network was included in the dataset because 110 kV and 0.4 kV networks are galvanically isolated form the MV system, so they do not affect the earth fault behaviour of the MV system. The samples of the dataset were network areas fed by a 110/20 kV primary transformer, and the attributes of the dataset were the measurements of the regulator and network parameters from that primary transformer network area. Network parameters were obtained from the network information system.

As presented in Section 3.5 the centralized Petersen coil regulator provides real-time measurements from the network so if a substation is equipped with the regulator the network resistive earth fault current production can be measured in the present state. The regulator measurement corresponds to resistive current production during a solid earth fault. If there are multiple centralized Petersen coils allocated for one primary transformer, only one of them is adjusted, as rest of the coils have fixed position. This prevents disturbances in the adjustment procedure and hence, the resistive current measurement is always taken from the regulator of the adjustable coil. In addition to the resistive current, also measurements of the coil position and current of the resonance point were saved from the regulator.

6.1.1 The locations of the dataset samples

The foundation of the dataset were the resistive current measurements from the regulators. Therefore, the samples were only taken from locations were the measurement was available. The latest regulator models send the measurement

information straight to the SCADA control system but not all the devices do. Even though most of Elenia's substations are operated resonant earthed, some of the older regulators do not provide resistive current measurement at all. Some models do provide the measurement, but it is not sent to SCADA, so it must be collected manually from the substation. Therefore, the dataset does not contain Elenia's entire network but only the locations where resistive current measurement was available in SCADA, complemented with some manually collected measurements, comprising of 45 distinct measurements in total. This corresponds to approximately 30% of Elenia's entire network.

The geographical distribution of the samples is illustrated in Figure 35, where the points illustrate the locations of the substations. Some of the substations contain multiple primary transformers, but the networks fed by the transformers are galvanically isolated, so the measurements are treated separately. The measurements are located around the Elenia network area, even though most frequently around Pirkanmaa region, because the manual measurements were collected there.

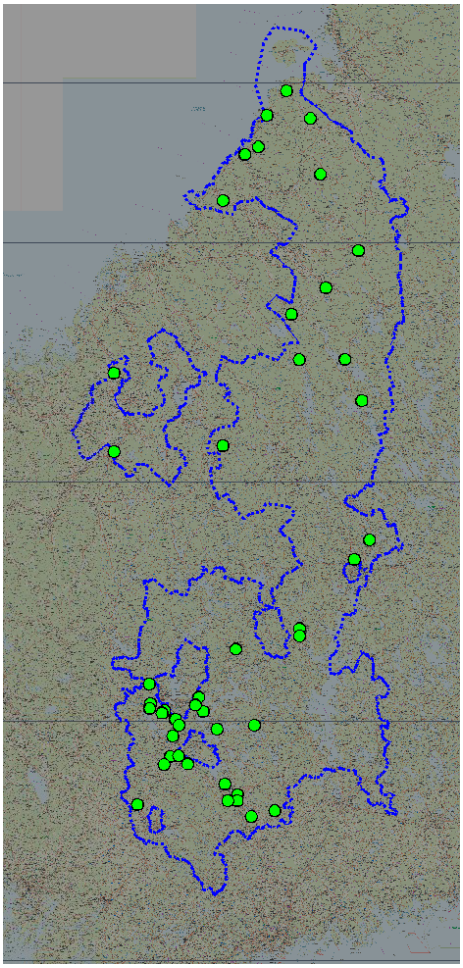

Figure 35. *Elenia network area and geographical distribution of the substations in the dataset.*

6.1.2 Network parameters

The dataset was composed in matrix form so that samples that consisted of the primary transformer areas corresponded rows and the network parameters from that location corresponded columns, as follows

	parameter 1	*parameter 2*	….	*parameter m*
PT1	value 11	value 21	….	value 1m
PT2	value 21	value 22	….	value 2m
⋮	⋮	⋮	⋮	⋮
PTn	value n1	value n2	….	value nm

where PT denotes primary transformer and the number of samples n=45.

Chapter 3 presents different factors that affect the resistive earth fault current production. When comprising the dataset these factors were to be considered so that the chosen parameters would describe the earth fault behaviour of the system and thus possibly correlate with the resistive earth fault current production. The chosen parameters are as follows, first is the symbol or shortened name of the parameter, that is used in following figures and in computation.

- I_R [A], resistive earth fault current during a solid earth fault. Measured by the Petersen coil regulator, parallel resistor current production reduced.
- I_{res} [A], current of the resonance point. Corresponds to inductive current of the centralized coil if compensation degree K = 1. Measured by the Petersen coil regulator.
- I_{pos} [A], centralized Petersen coil position, inductive current produced by the centralized coil. Measured by the regulator.
- *NumberOfFeeders*, number of feeders connected to the corresponding primary transformer.
- *TotalLineLength* [m], total line length, sum of line lengths (cable + OHL) connected to the primary transformer.
- *CableLength* [m], cable length, total length of cables connected to the primary transformer.
- *CablingDegree* [%], cabling degree of the corresponding network.
- ≥*95Cable* [m], length of cables with conductor diameter ≥95mm^2.
- >*120Cable* [m], length of cables with conductor diameter >120mm^2.
- *RatioOf>120* [%], ratio of cables with conductor diameter >120mm^2 of total cable length.
- <*95Cable* [m], length of cables with conductor diameter <95mm^2.

- *EWCable* [m], length of cables with earth wire.
- *RatioOfEWCable* [%], ratio of cables with earth wire.
- I_{Cc} [A], capacitive fault current flowing to the substation. Values calculated with network information system.
- I_{Cd} [A], capacitive fault current compensated by the distributed units. Values calculated with network information system.
- I_{Ctot} [A], total capacitive earth fault current produced by the network, calculated as $I_{Cc} + I_{Cd}$.
- *DegOfDistComp* [%], degree of distributed compensation, calculated as I_{Cd} / (I_{Cc} + I_{Cd})
- *LongestCableRoute* [m], longest uniform cable route from the primary transformer.

In Elenia's network, Petersen coil parallel resistor is always connected. Therefore, resistive earth fault current I_R measurements naturally contain the current production of the parallel resistor, but as the interest is the resistive current production of the network, and the current production of the resistor is known, the effect of the parallel resistor is reduced from the measurement value. The resistive losses of the compensation units are more difficult to estimate but as the values are expected to be minimal, they are not reduced from I_R. To summarize, in the dataset I_R contains resistive current produced by the network zero sequence impedances and compensation units.

An important parameter that is not included in the dataset is ground resistivity. In some locations ground resistivity values are accounted in network information system but the measured values did not cover all the areas where the cables were located. Also, the ground conditions change along the seasons as well as weather and even the ground properties along a single feeder can vary remarkably. Hence, reliable consideration of ground resistivity was not possible and was therefore left out from the dataset.

6.2 Correlation analysis

When all measurement values and values of the network parameter presented above were combined into the dataset, dependencies between resistive earth fault current and the parameters were studied by calculating Pearson's correlation coefficient for all parameters, to see which has the strongest correlation with respect to I_R. The strongest and weakest correlations were then visualized with scatter plots. The calculated correlation coefficients with respect to I_R are illustrated in Figure 36.

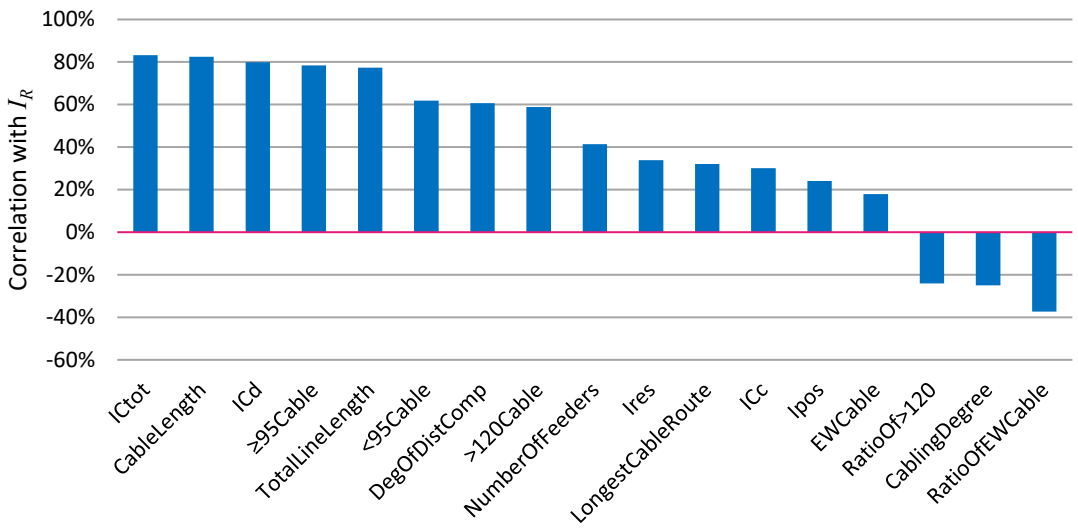

Figure 36. *Correlations of the network parameters with respect to I_R.*

Figure 36 gives an overview of the dependencies resistive earth fault current has with the other network parameters. The figure confirms the intuition, that total capacitive earth fault current I_{Ctot} has a strong positive correlation with I_R. Also, the cable length has nearly similar correlation. This is analogous to the total capacitive current, because cable capacitance remarkably affects the capacitive earth fault current production, therefore if cable length increases, so does capacitive earth fault current. So, in addition to correlation with I_R, I_{Ctot} and *CableLength* have strong mutual correlation. Also *≥95Cable* has strong correlation, but the values are close to equal with *CableLength*.

Pekkala (2010) and Malm et al. (2015) state that earth wires remarkably decrease cable network zero sequence impedance and therefore restrain resistive earth fault current production. The correlation is not strong, but this can be seen from the negative correlation of *RatioOfEWCable*. This implies that as the share of cable with earth wire increases the resistive current production decreases.

Pearson's correlation coefficients illustrated in the Figure 36 only represent linear dependency between the variables. Therefore, it is important to visualize the values to conform the dependency. Scatter plots are presented in the following sections.

6.2.1 Strong correlations

As illustrated by the correlations in Figure 36, I_R has a strong dependency with some of the parameters, I_{Ctot}, I_{Cd} and *DegOfDistComp* being the most promising ones. The scatter plots of resistive earth fault current with respect to I_{Ctot}, I_{Cd} and degree of distributed compensation are illustrated in Figure 37.

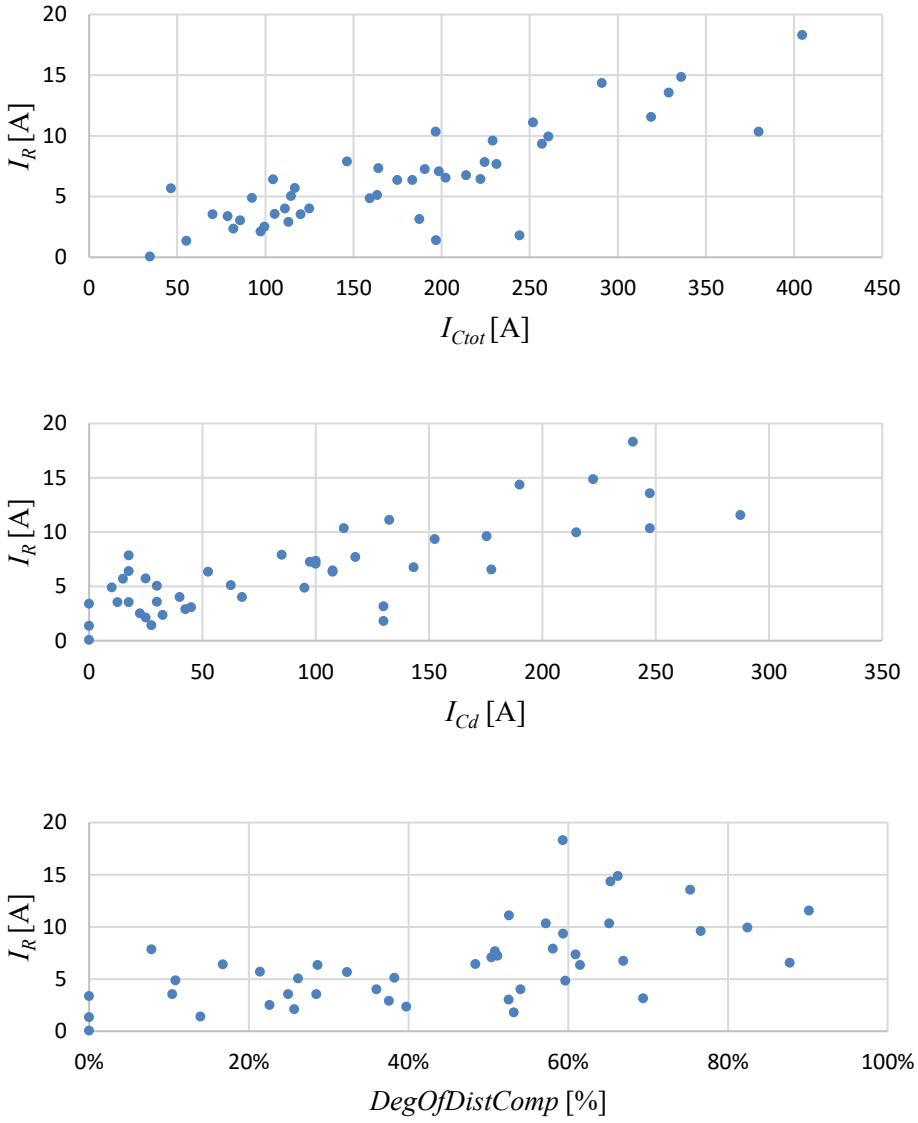

Figure 37. *Scatter plots of resistive earth fault current with respect to total capacitive current (uppermost), distributed compensation current (middle) and degree of distributed compensation (lowest).*

For I_{Ctot} and I_{Cd} the scatter plots clearly illustrate the correlation, as the trend in both graphs is close to linear. Thus, the total capacitive earth fault current and current of distributed compensation behave close to analogous with respect to resistive earth fault current. The degree of distributed compensation on the other hand, does have some dependency with I_R but it is not as strong as I_{Ctot} and I_{Cd}.

Interestingly, according Figure 37, as current of the distributed compensation increases, also resistive earth fault current increases, respectively. In addition, for all resistive current values above 10 A the degree of distributed compensation is over 50%. This seems to contradict the presented theory, because distributed compensation is expected to decrease the resistive current production. However, based on the dataset, it seems

that if distributed compensation is applied extensively, the quantity of resistive current produced by the network also increases. It is questionable if one can make such conclusions based entirely on correlations, but the plausible positive dependency between the distributed compensation and the resistive earth fault current production should be considered in designing of compensation strategy.

6.2.2 Weak correlations

Some unanticipated weak correlations appeared also. IR had, a bit surprisingly, very weak dependency on CablingDegree, ICc and LongestCableRoute, even though they were expected to represent IR moderately. Scatter plots are illustrated in Figure 38.

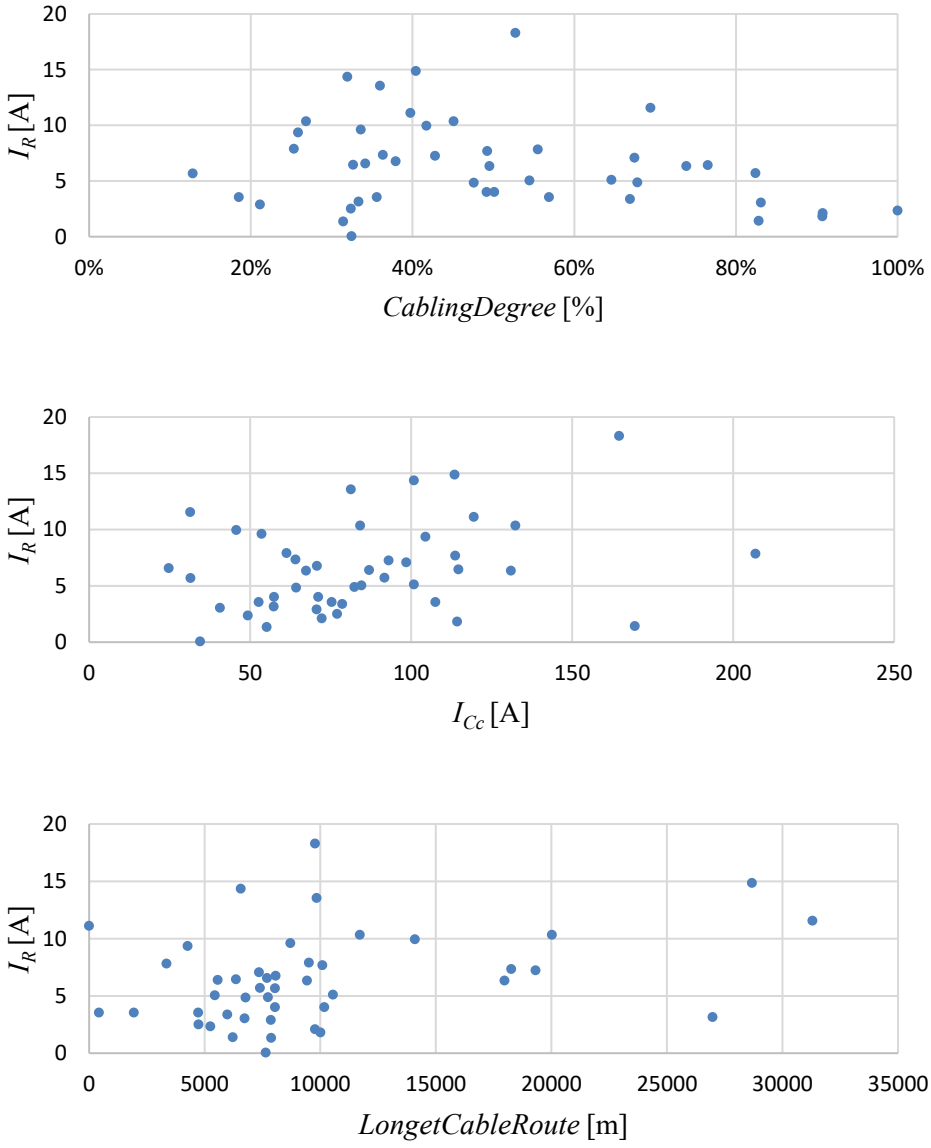

Figure 38. *Scatter plots of resistive earth fault current with respect to cabling degree (uppermost), capacitive fault current flowing to the substation I_{Cc} (middle) and longest uniform cable route (lowest).*

All the scatter plots in Figure 38Figure 38 have nonuniform formations, which verifies the weak dependency between resistive earth fault current production and the parameters. Cabling degree was expected to reflect resistive current production. Against the intuition, the correlation was not strong, being only -25%. This implies that it is not reasonable to estimate resistive current magnitude based entirely on cabling degree. One of the reasons explaining weak correlation is the fact that resistive current production is related to network capacitance and cable length, whereas cabling degree does not consider the cable length but only the ratio of cable and OHL. Therefore, cabling degree can be high, even if the total cable length is relatively short, which is the case in many urban networks.

Another surprisingly weak correlation is with capacitive fault current flowing to the substation, I_{Cc}. This is an important finding because as presented earlier, the alternative interpretation of SFS 6001 residual current estimation method is that I_{Cc} can be used to estimate the residual earth fault current of the network. Even though, residual current does not equal to resistive current, the weak correlation already implies that I_{Cc} does not behave similarly as I_R. This, in turn might distort the values of residual current if the SFS 6001 10% assumption is applied with I_{Cc}.

Longest uniform cable route was added to the dataset to see if one long cabled connection can dominate the resistive current production. The correlation is not strong, but it does not necessarily prove that single long cables could not be a remarkable source of resistive current. On the other hand, based on the correlations, length of the longest cabled connection does not either provide a reliable measure to estimate resistive current production.

6.3 Statistical methods used in the study

In the statistical examination some mathematical and statistical methods are applied, so the basics concepts are introduced in the following sections. The emphasis of this thesis is in electrical engineering therefore the mathematical aspects of the applied methods are treated only briefly. For in depth description of mathematical foundations see Pitkäranta (2015).

6.3.1 Mean Square Error

Mean square error (MSE) is a measure of error used in statistical analysis. MSE measures distance, or in other words error between datapoints. The errors are squared to remove negative values. MSE is defined as

$$\mathrm{MSE}=\frac{1}{n}\sum_{i=1}^{n}\left(Y_i-\hat{Y}_i\right)^2 \tag{31.1}$$

Where n is the number of samples, Y_i is the original observation and $\hat{Y}_i$ is the estimator. The smaller the MSE the smaller is the error between the original values and the estimator, so if MSE = 0 the datapoints are equal. In many applications MSE is used to measure the error of a regression line and the original dataset. By minimizing the MSE an optimal fit can be obtained. However, in this study MSE is used to measure the error of distinct vectors containing equal number of samples.

Because no regression is used $\hat{Y}_i$ is adjusted by adding a correction factor e to the MSE equation so that

$$\mathrm{MSE}=\frac{1}{n}\sum_{i=1}^{n}\left(Y_i-e\hat{Y}_i\right)^2 \tag{31.2}$$

Also, second estimator X with correction factor b can be added. Now there are two estimators with adjustable correction factors that are used to estimate the observations. For two estimators MSE function is defined as

$$\mathrm{MSE}=\frac{1}{n}\sum_{i=1}^{n}\left(Y_i-\left(e\hat{Y}_i+b\hat{X}_i\right)\right)^2 \tag{31.3}$$

By finding an optimal value for e (and b in case of two correction factors) the value of the MSE function can by minimized.

6.3.2 Optimization

In mathematics, optimization aims to find minimum (or maximum) value of a real-value function. A general formulation of an optimization problem is as follows. $f : X \rightarrow \mathbb{R}$ and a subset $\Omega \subset X$ find

$$\min f(x), \quad x \in \Omega \tag{32}$$

Where f is called objective function and Ω is the feasible set. The aim is to find a value $x^* \in \Omega$ that minimizes the objective function f. Then $f(x^*)$ is the optimal value and x^* is the optimal solution. Hämäläinen (2015)

Multiple mathematical methods are developed for optimization and the choice of an adequate method depends on the complexity of the problem. In this study there are no constraints, therefore $\Omega \in \mathbb{R}$. Objective function is the MSE function which is a second-degree function where the correction factors represent variables. If a second-degree

function is continuous and differentiable in $\mathbb{R}$ the minimum value of the function is obtained at the zero of the gradient. So that

$$\min f(x, y) \tag{33.1}$$

can be obtained with optimal solutions x^* and y^* that satisfy

$$\nabla f(x^*, y^*) = \frac{\partial}{\partial x} f(x^*, y^*) + \frac{\partial}{\partial y} f(x^*, y^*) = 0 \tag{33.2}$$

6.3.3 Clustering

Clustering refers to a process of partitioning a set of datapoints, or observations into arbitrary number of subsets. The subsets are called clusters and the observations are assigned to the clusters based on their properties so that observations in a certain cluster are similar to another but dissimilar to the observations in other clusters. Clustering is often applied in machine learning applications that operate with large amount of data so that clustering is not done by humans but by an algorithm. (Han et al. 2012)

The clustering algorithm applied in this study is called k-means. The algorithm partitions a dataset *D* of *n* elements into *k* clusters, so that $n \geq k$. First, the algorithm randomly chooses *k* datapoints from *D*, which then form the initial centre points, i.e. centroids of the clusters. The rest of the datapoints in *D* are then allocated to the clusters, so that the datapoint is allocated to the cluster where the distance from the data point to the centroid of the cluster is smallest. Now, the algorithm computes new centroids for each cluster and again datapoints are assigned to the cluster with nearest centroid. The iteration is repeated until a stopping criterion is satisfied. (Han et al. 2012) The iterations of k-means algorithm are illustrated in Figure 39.

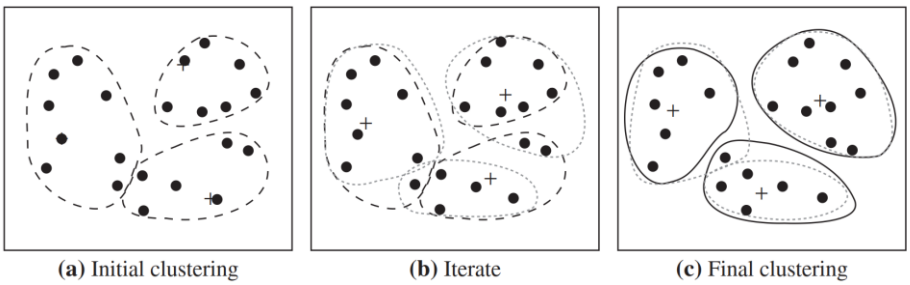

Figure 39. *The iterations of k-means algorithm, where centroids are marked with +. In (b) the centroids are recomputed and datapoints allocated to new clusters accordingly. (Han et al. 2012)*

Clustering is a broad topic with multiple applications in different fields. Considering the extent of the subject the presentation given above is very concise. For detailed description see (Han et al. 2012).

6.4 Estimating resistive earth fault current with statistical methods

In the statistical examination the goal was to find parameters that behave similarly as the resistive earth fault current, so that the found parameters could then be used to estimate the network resistive current production. The magnitude of the parameters is different than the magnitude of the resistive earth fault current, therefore the parameters are then to be adjusted with adequate correction factor so that the resulting value represents the corresponding resistive earth fault current value as correctly as possible.

MSE value is used as a measure to estimate the convenience of the parameters and correction factors. The smaller the MSE the better is the estimate. Also, graphical representation is used to verify the convenience of the estimate.

First, for all the parameters presented in Section 6.1.2 a separate optimal correction factor is calculated and then values are compared, which of the parameters best represents the resistive earth fault current, in other words results lowest MSE. Based on the correlations I_{Ctot} and I_{Cd} are promising candidates but the calculation is done to all the parameters to confirm the presumption. A combination of two variables with two correction factors is also tested. Furthermore, clustering is used to partition the values into three categories to see if individual correction factors for small, medium and large values will decrease the MSE.

6.4.1 Correction factor optimization

Resistive earth fault current is now the original observation in the MSE function and rest of the parameters, each in turn, functions as the estimator. If MSE is calculated for I_R and I_{Ctot}

$$\mathrm{MSE}=\frac{1}{n}\sum_{i=1}^{n}\left(I_R - eI_{Ctot}\right)^2 \tag{34}$$

Even though the values have strong correlation, without correction factor e the magnitude of the variables are remarkably apart as illustrated in Figure 40. There I_R and I_{Ctot} are ascendingly sorted according to I_R, so that vertically aligned datapoints correspond the same network.

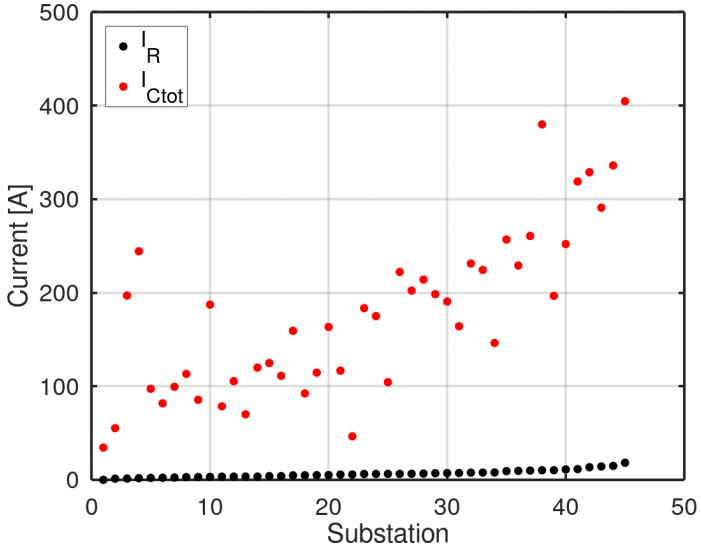

Figure 40. *I_R values with corresponding I_{Ctot} values without correction factor, sorted according to I_R.*

If correction factor is accounted as in equation (34) the MSE can be minimized according to the equations (33.1) and (33.2). Now, if there is only one variable the optimal value can be obtained

$$\nabla \mathrm{MSE}\left(e^*\right) = \frac{\partial}{\partial e}\mathrm{MSE}\left(e^*\right) = 0 \tag{35}$$

The MSE function of I_R and I_{Ctot} as a function of correction factor e is illustrated in Figure 41. The optimal solution is indicated in the plot and the optimal value of the correction factor that satisfies the equation (35) when rounded to three decimal precision is 0.036.

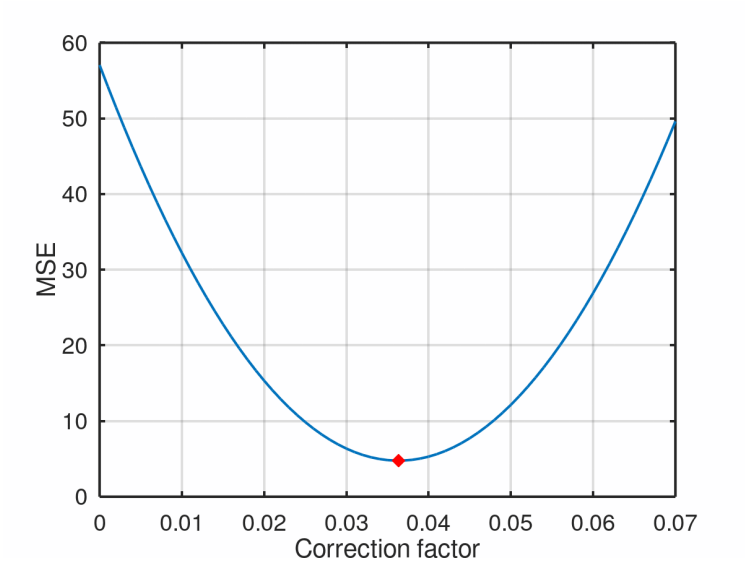

Figure 41. *MSE of I_R and I_{Ctot} with respect to correction factor. Optimal value is indicated with the red marker.*

The obtained correction factor minimizes the error between I_R and the corresponding parameter. For I_R and I_{Ctot} the correspondence after I_{Ctot} is reduced with the correction factor is illustrated in Figure 42.

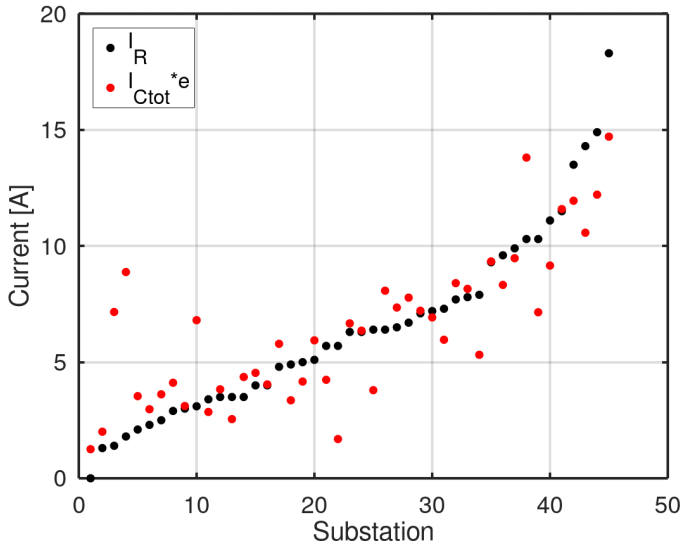

Figure 42. *I_R and I_{Ctot} multiplied with the optimal correction factor. Sorted according to I_R.*

I_{Ctot} multiplied with the correction factor now represents resistive earth fault current production moderately. If MSE is now calculated according to equation (34) with the optimized correction factor the result is 4.8, which can also be seen in Figure 41. The same procedure was then repeated for all the parameters.

6.4.2 Variable selection

To verify which parameters best represent resistive earth fault current the correction factor optimization presented in Section 6.4.1 was done to all of the parameters and then MSE was calculated with the resulting values. Results are presented in Table 4, where correction factor e is presented in three decimal precision.

Table 4. *MSE and optimal correction factor of the parameters calculated according to the equation (31.2).*

Parameter	*MSE*	*e*
I_{res}	15.8	0.065
I_{pos}	17.7	0.068
NumberOfFeeders	13.4	1.002
TotalLineLength	6.9	0.000
CableLength	5.0	0.000
CablingDegree	26.4	10.300
≥95Cable	6.0	0.000
>120Cable	11.1	0.000
RatioOf>120	25.3	9.378
<95Cable	21.9	0.000
EWCable	23.2	0.000
RatioOfEWCable	36.4	13.744
I_{Cc}	16.4	0.069
I_{Cd}	8.7	0.057
DegOfDistComp	10.8	13.519
LongestCableRoute	20.7	0.001
I_{Ctot}	4.8	0.036

The results are analogous to correlations in Figure 36, hence I_{Ctot} and *CableLength* give the smallest MSE values, *≥95Cable*, *TotalLineLength* and I_{Cd} also fairly good results. I_{Ctot} with optimal correction factor is illustrated in Figure 42. From the figure it is evident that even though I_{Ctot} gives the smallest MSE it does not perfectly align with the resistive earth fault current. Some of the values differ remarkably, and some minor deviation can also be noted.

Therefore, a two variables approach was tried to get a better fit. The expectation was that by applying two variables values with high deviation could be reduced, because now more factors that possibly cause the deviation are considered in the computation. Two distinct variables with correction factors were added to the MSE function according to equation (33.2). I_{Ctot} already gave the best results, so it was used as the first variable in every round and rest of the parameters served as the second variable, each in turn. The resulting MSE values are presented in Table 5.

Table 5. *MSE and optimal correction factor of the parameters, calculated according to the equation (31.3). I_{Ctot} is the second parameter with correction factor e.*

Parameter	*MSE*	e	b
I_{res}	4.7	0.039	-0.006234
I_{pos}	4.6	0.040	-0.009015
NumberOfFeeders	4.7	0.038	-0.062341
TotalLineLength	4.1	0.025	0.000013
CableLength	4.7	0.032	0.000013
CablingDegree	4.5	0.040	-1.655000
≥95Cable	4.4	0.069	-0.000104
>120Cable	4.3	0.049	-0.000066
RatioOf>120	4.6	0.039	-1.004400
<95Cable	4.5	0.034	0.000054
EWCable	4.2	0.043	-0.000076
RatioOfEWCable	4.6	0.038	-1.284200
I_{Cc}	4.6	0.040	-0.009124
I_{Cd}	4.6	0.031	0.009124
DegOfDistComp	4.7	0.034	1.079600
LongestCableRoute	4.7	0.038	-0.000031

The values for correction factor b are presented in higher precision to illustrate that the values converge to a smaller value than the values of the correction factor e that corresponds to I_{Ctot}. The percentage unit variables are an exception because the values are naturally on the range of [0,1] so the correction factors behave differently. However, the smaller values of b imply that I_{Ctot} dominates the computation and is thus a better representative of I_R. Secondly, the value of MSE does not significantly improve if second variable is added. The MSE values on the average are smaller, but none of them is significantly smaller than in case of just one variable.

With two variables, *TotalLineLength* together with I_{Ctot} provides the smallest MSE. However, this combination is not very meaningful because I_{Ctot} is analogous to cable length, that is naturally a part of *TotalLineLength,* which means that these two variables represent nearly the same thing. To better evaluate the two correction factors approach, *DegOfDistComp* was chosen as the second variable. MSE in Table 5 is not the lowest but the dependency of *DegOfDistComp* and I_R in Figure 37 is fairly strong, which justifies the choice of *DegOfDistComp.* The representation of I_R with I_{Ctot} and *DegOfDistComp* multiplied with the corresponding correction factors is illustrated in Figure 43.

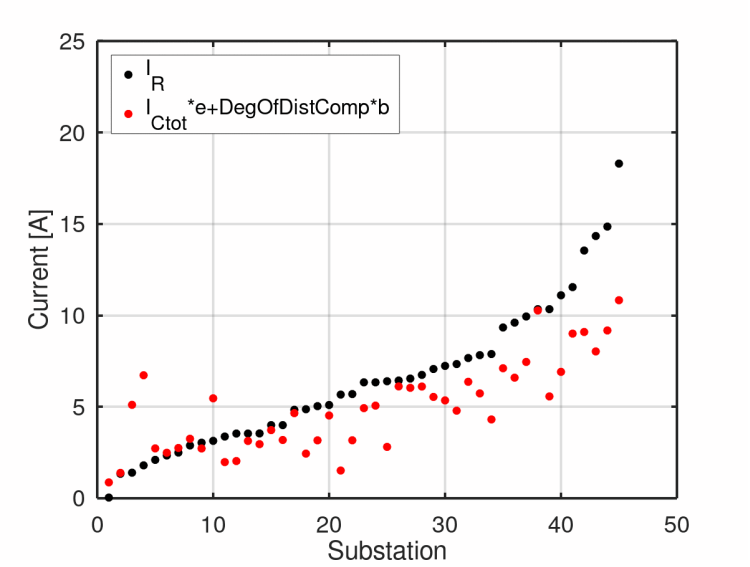

Figure 43. *I_R compared to I_{Ctot} and DegOfDistComp multiplied with optimal correction factors e and b.*

Applying two correction factors does not improve the representation of I_R remarkably. Even though MSE value is moderate the estimated values are as scattered as in Figure 42, which means that two variables approach does not help to reduce the high deviation as expected. In addition, the estimated values are systematically too low, which is undesirable for the model.

Therefore, based on the correlations and MSE, I_{Ctot} appears to be the best variable to represent resistive earth fault current produced by the network. Applying two variables does not bring any significant benefit and for convenience it is better to have only a single variable. Secondly, I_{Ctot} fulfills the requirements set in Section 5.3 as total capacitive earth fault current can be obtained from network information system, it changes if network is modified and is also generalizable.

6.4.3 Correction factors with k-means clustering

K-means clustering algorithm was applied to see if the representation could be improved by categorizing the networks into three separate clusters. Clustering was based on the properties of the data so that ideally networks with low resistive current production were one cluster, medium current production networks one and lastly the networks with high current production were one cluster. An optimal correction factor was then calculated separately for all three clusters.

The idea of clustering is illustrated in Figure 44 where the datapoints are clustered with k-means. In this example, clustering is done according to I_{Ctot} and Cable length so that

clusters are illustrated with the colors of the datapoints and centorids of each cluster are marked with the black star.

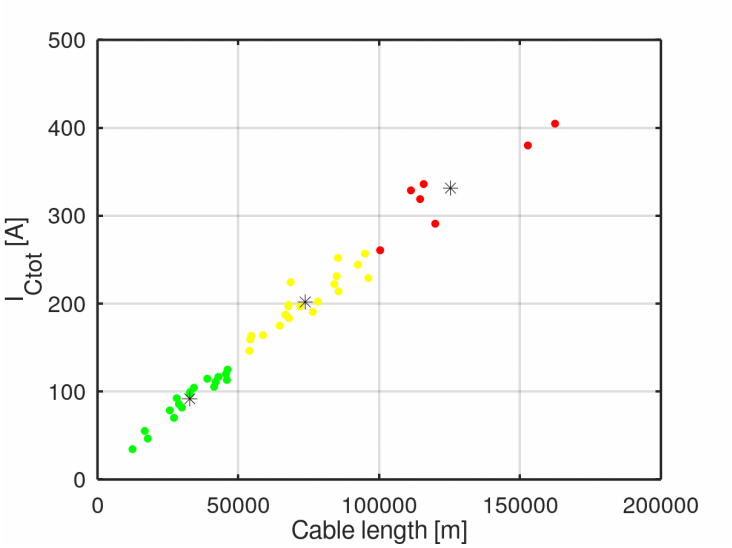

Figure 44. *Clustering of the dataset according to I_{Ctot} and Cable length.*

This type of clustering does not directly consider the resistive earth fault current production but if the applied variables behave in similar way as I_R the representation should be fairly good. If I_R is illustrated according to the clustering of Figure 44 the result looks as in Figure 45.

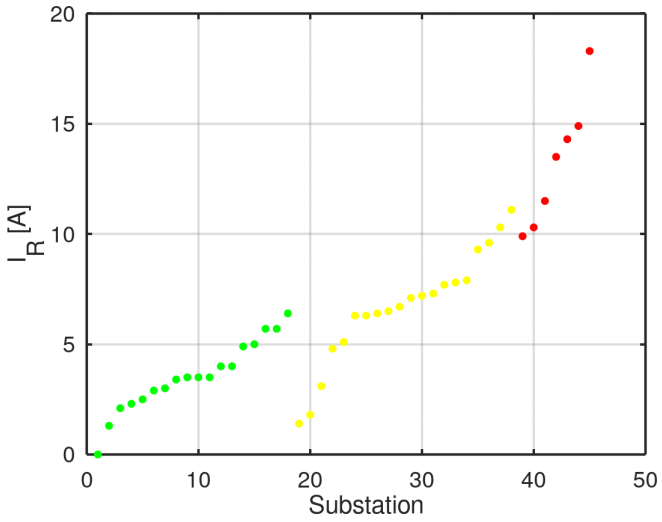

Figure 45. *I_R according to the clustering of Figure 44.*

The assumption is that in normal operation I_R is not known, therefore the value cannot be applied directly into clustering but now it is used to validate the clustering. Most of the I_R values are clustered correctly, only some of the yellow medium values should be allocated to the green cluster and one or two of the higher yellow datapoints should be in the red cluster. It is not the primary objective of this study, but the clustering also

indicates that networks can be classified into different categories of resistive earth fault current production without knowing the resistive current production but based on other parameters that behave similarly as the resistive earth fault current.

Now, an individual correction factor for each cluster can be computed. The procedure was again repeated with all the parameters to see which one gives best results. For clustering, two variables were used, therefore also the MSE and correction factor computation was done according to equation (31.3) but now the computation is done for each cluster separately. To limit the number of variations, I_{Ctot} served again as the second variable in all the cases. Therefore, I_{Ctot} is not included in the results as an individual parameter. The MSE values obtained with clustering are presented in Table 6.

Table 6. *MSE values with three distinct correction factors based on the clustering of the dataset.*

Parameter	*MSE*
I_{res}	4.14
I_{pos}	4.17
NumberOfFeeders	3.85
TotalLineLength	3.74
CableLength	4.27
CablingDegree	3.35
≥95Cable	3.97
>120Cable	3.88
RatioOf>120	4.05
<95Cable	3.67
EWCable	3.95
RatioOfEWCable	3.78
I_{Cc}	4.02
I_{Cd}	4.09
DegOfDistComp	4.07
LongestCableRoute	4.61

The MSE values are now slightly reduced. The best result is with I_{Ctot} and, a bit surprisingly, *CablingDegree* resulting MSE of 3.35. The correction factors of this combination are presented in 0, e again corresponding to I_{Ctot} and b *CablingDegree.*

Table 7. *Correction factors of I_{Ctot} and CablingDegree in each cluster.*

	Cluster 1	*Cluster 2*	*Cluster 3*
e	0.043165	0.045414	0.048203
b	-0.66069	-4.047	-6.8022

The correction factor e has rather stable and reasonable values, but values of b deviate remarkably which implies that the seemingly good fit indicated by low MSE value is only caused by lucky convergence of the MSE function. However, the representation of the obtained estimator compared to I_R is illustrated in Figure 46.

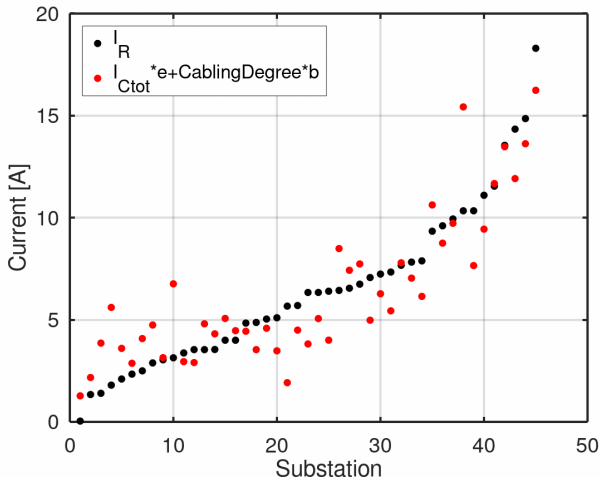

Figure 46. *I_R and the estimator composed of I_{Ctot} and CablingDegree multiplied with the three correction factors obtained with clustering.*

The MSE value with clustering is in fact lower but visually the difference of Figure 46 compared to Figure 42 is imperceptible. The values still deviate and especially the small values are systematically too high. Similar examination was done for all the combinations of the parameters but because they did not produce any better results, for convenience only I_{Ctot} and *CablingDegree* are presented. Consequently, because clustering complicates the process of computing correction factors remarkably and the gained benefit is negligible, clustering is not wort the effort in this application.

6.4.4 Resistive current approximation with total capacitive current

In the previous sections different methods of estimating the resistive earth fault current were studied. Out of the gathered dataset the total capacitive earth fault current produced by the network I_{Ctot} best represented the network resistive earth fault current production, therefore it was further studied. In addition, I_{Ctot} is similar electrical parameter as I_R so it is feasible from electrical engineering perspective also.

By optimizing the correction factor of the MSE function an optimal fit can be obtained. This means that some values are higher and some lower than the ones that are being estimated, but the mean is close to equal. This is illustrated in Figure 47 where regression line of I_{Ctot} is included in the figure.

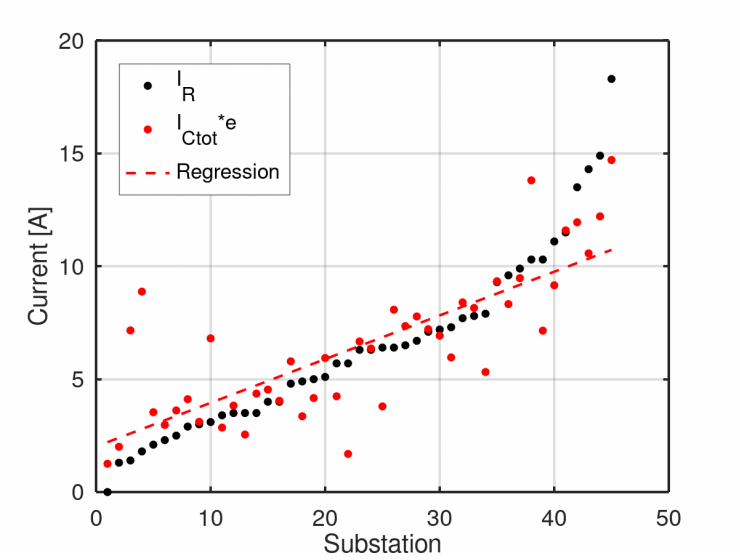

Figure 47. *I_R and the regression of I_{Ctot} multiplied with optimal correction factor.*

The regression in Figure 47 appears to follow the values of I_R considerably well but after all, one of the key factors of this thesis is safety. It is not enough to have optimal mean if some of the estimated current values are too low, because if real values are higher than the estimated ones, safety might be compromised in the worst case. Mathematically optimal solution is therefore not the most feasible from safety perspective. Another problem related to optimization is that the values used in dataset are inexact but the optimization by computing the zero of the gradient is done as they would be exact.

Naturally there is some inaccuracy in the measurements, but it must be considered in the precision of the presented results. Hence, to have enough marginal of certainty and to account the inaccuracy of the initial data, value of the correction factor must be rounded. According to the rules the optimal value of 0.036 should be rounded to 0.04 but to gain the needed certainty 0.05 is used. With the correction factor of 0.05 representation of I_{Ctot} is illustrated in Figure 48.

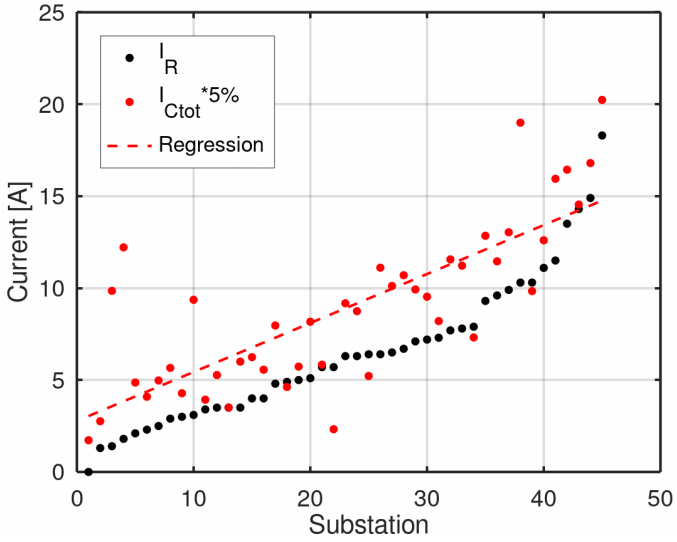

Figure 48. *I_R and regression of I_{Ctot} multiplied with 5%.*

Now, most of the estimated values are slightly higher than the measured I_R values, but the margin is to the right direction in terms of safety. Some values estimated according to 5%I_{Ctot} are in fact lower than the measured I_R values but the trend of the regression line follows I_R values being on the safe side, so the 5% correction factor applied to I_{Ctot} can be viewed as adequate estimate of I_R. Assessment of the values that are lower than I_R is provided in the following section.

6.5 Evaluation of the results

Based on the results of the previous section resistive earth fault current produced by the network can be estimated to be 5% I_{Ctot}. With this method the resistive component of the residual earth fault current I_{re} can be approximated if resistive current produced by the parallel resistor I_{Rp} is added to the 5% I_{Ctot} to get the total resistive current. Therefore, residual earth fault current estimation method can be defined

$$I_{re}^{*} = \sqrt{\left(\left|\underline{I}_C\right| - \left|\underline{I}_L\right|\right)^2 + \left(5\% I_{Ctot} + I_{Rp}\right)^2} \tag{36}$$

Where $|\underline{I}_C|$-$|\underline{I}_L|$ denotes the capacitive detuning of the centralized Petersen coil that is always 5 A in Elenia's network. To validate the results of equation (36) values were compared with the measured values in the dataset. The measured residual earth fault current is defined

$$I_{re} = \sqrt{\left(I_{res} - I_{pos}\right)^2 + \left(I_R + I_{Rp}\right)^2} \tag{37}$$

Where I_{res}-I_{pos} is the actual detuning measured from the centralized Petersen coil regulator. The results of equations (36) and (37) are illustrated in Figure 49, where the developed method is denoted with the red dots.

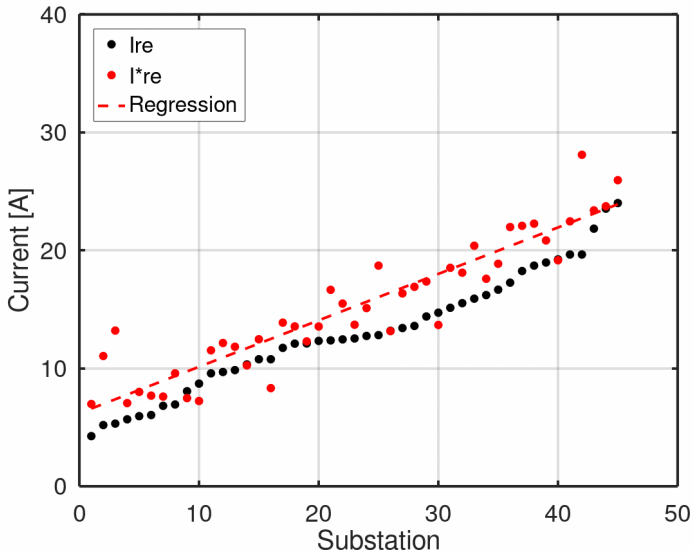

Figure 49. *Comparison of measured I_{re} (black) and I^*_{re} (red) estimated with the developed method.*

The values are finely aligned and the regression of I^*_{re} increases equally with the trend of measured I_{re}. Most of I^*_{re} values are a little higher than I_{re} which is a benefit for the model because approximations always contain certain level of uncertainty, but now the marginal is almost systematically on the safe side. This is desirable from the safety point-of-view because now the given estimation is rather safe, as the values represent the measured residual current values well, being still slightly on the safe side. This ensures that if the model is applied, touch voltage examinations are conducted with values that do not compromise safety.

Yet, few of the I^*_{re} values in Figure 49 are lower than the measured I_{re} values. For the too low values, one common denominator was found. In all these networks, the magnitude of resistive earth fault current is high compared to the total capacitive earth fault current. This is illustrated in Figure 50, where the samples that produce only moderately lower I^*_{re} values are marked with orange and samples that produce notably low I^*_{re} values, are marked with red.

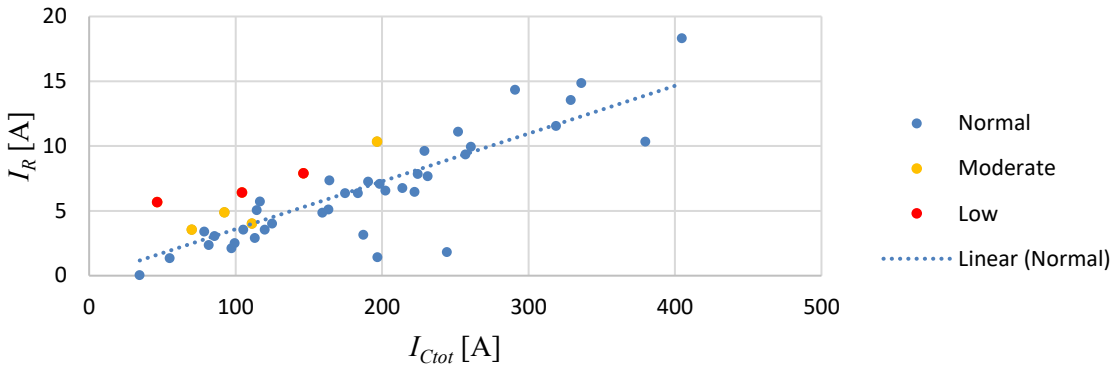

Figure 50. *Scatter plot of I_{Ctot} and I_R, where I^*_{re} values of Figure 49 that are lower than I_{re} are illustrated in orange and red.*

The samples that produce too low I^*_{re} values are located above the dotted linearization line. This means that the ratio of I_R and I_{Ctot} is higher than the average of the dataset. This is not the primary cause of the error, but in this study no explaining factors were identified. However, only one of the I^*_{re} values in Figure 49 is significantly lower than I_{re}, which indicates that the model is after all adequate.

In this study the reference model was the estimation method specified in the SFS 6001: 2018 standard. Due to interpretational difficulties there are two alternative ways to apply the 10% estimation as presented in Section 5.2. The two alternatives were tested to see if the developed model of equation (36) is more accurate than the 10% assumption specified by the standard. First, the interpretation where *network capacitive current* is assumed to be the current flowing to the substation I_{Cc} was tested and the results are presented in Figure 51.

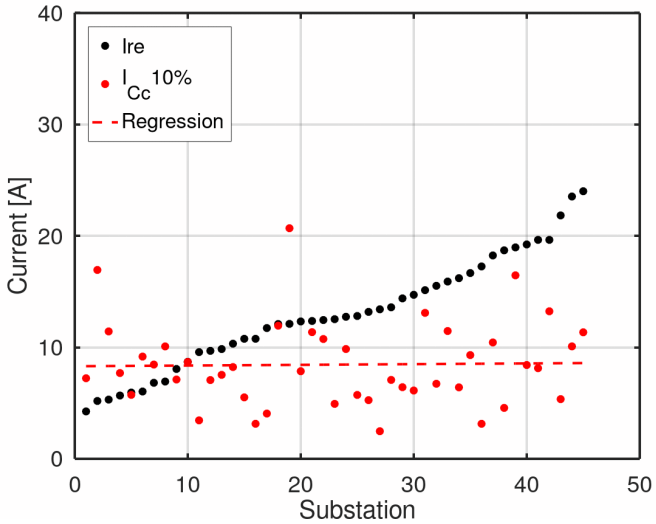

Figure 51. *Measured I_{re} (black) and the SFS 6001 10% estimation applied to I_{Cc} (red).*

Figure 51 clearly illustrates that if the 10% assumption is applied to I_{Cc} the values are systematically incorrect. For the smallest measured values, the estimations are too high and for the high-end values estimations are significantly too low. The difference can be close to 10 A, which is already considerable magnitude of inaccuracy when considering touch voltage examinations. Consequently, 10% I_{Cc} is not an adequate method to estimate residual earth fault current.

The second interpretation was that *network capacitive current* denotes the total capacitive earth fault current produced by the network I_{Ctot}, so capacitive current compensated by the distributed units is also regarded. 10% I_{Ctot} with measured I_{re} is illustrated in Figure 52.

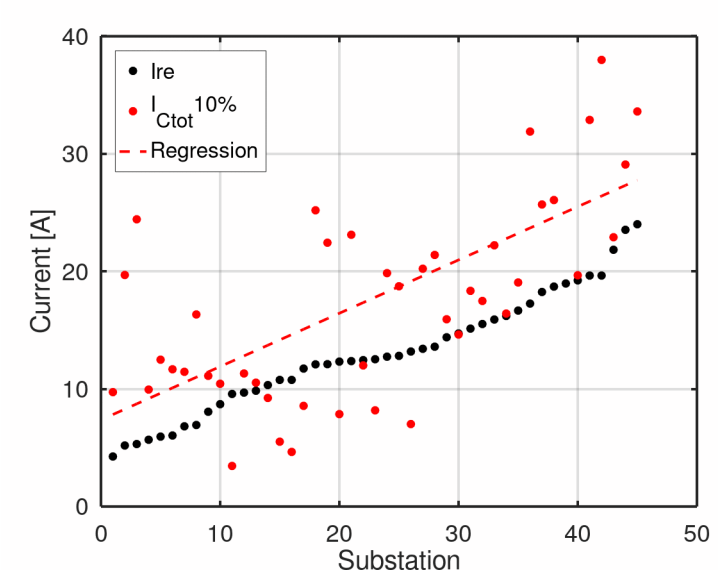

Figure 52. *Measured I_{re} (black) and the SFS 6001 10% estimation applied to I_{Ctot} (red).*

In Figure 52 the regression of 10%I_{Ctot} follows I_{re} moderately but the values are widely scattered. Thus, the results obtained with the 10%I_{Ctot} are not perfectly reliable as there can be major deviation in the results. From safety perspective, the good thing is that the estimated values are mostly on the safe side. On the other hand, as there can be major inaccuracies the situation may seem worse than it actually is, which might support unnecessary investments. Yet, some of the values are too low, which can be dangerous especially because there is no pattern from which to recognize the possibly falsely too low values.

The scaling of the y-axis of the Figures 49-51 is intentionally equal. This emphasizes the deviation that is present in both estimations provided by the SFS 6001 10% assumption. Comparably, in Figure 49 the developed method proves to accurately estimate the

measured residual earth fault current values yet being on the safe side. Therefore, equation (36) is an adequate method to estimate residual earth fault current.

6.5.1 Reliability assessment

No field tests were conducted in this study; therefore, the obtained results should be treated cautiously. The model developed in the study is a heuristic approach and it is not to be taken as perfectly precise solution. After all, the basis of the statistical examination was to develop a model that is more accurate than the one presented by the standard, but it was not expected to be perfectly precise as there are always inaccuracies related to measurements. According to the results the model proved to provide more accurate results than the method presented by the standard. Therefore, the developed model can be considered adequate.

The foundation of the study is the I_R measurement of the centralized Petersen coil regulator. The measurements were taken from multiple substations and the computations were based on the measurements. Therefore, the accuracy of the regulator measurements is utmost important.

The accuracy of the measurements was validated as a part of this thesis. During the commissioning of a new compensation device, primary earth fault tests are always conducted. Artificial earth fault with adjustable fault resistance is created into distribution transformer cabinet near the substation bus bar. Test arrangement of one primary earth fault test is illustrated in Figure 53, where the fault is connected to the cable connector and the fault resistor is in front of the picture.

Figure 53. *Primary earth fault test arrangements.*

The actual values of voltages and currents were analyzed with the measurements from the protection relays at the substation. As a part of the examination, the solid earth fault was tested. Then the resistor was disconnected, and the conductor was connected directly to earth. The resistive earth fault current measurement of the regulator and resistive earth fault current measurement of the protection relay are compared in Table 8 and the measurement values are also illustrated in Figure 54 where the blue phasor is I_0 and red phasor is U_0.

Table 8. *Resistive earth fault current measurements from the Petersen coil regulator and protection relays.*

Regulator measurement (rms)	Protection relay measurement (rms)
25.4 A	24.9 A

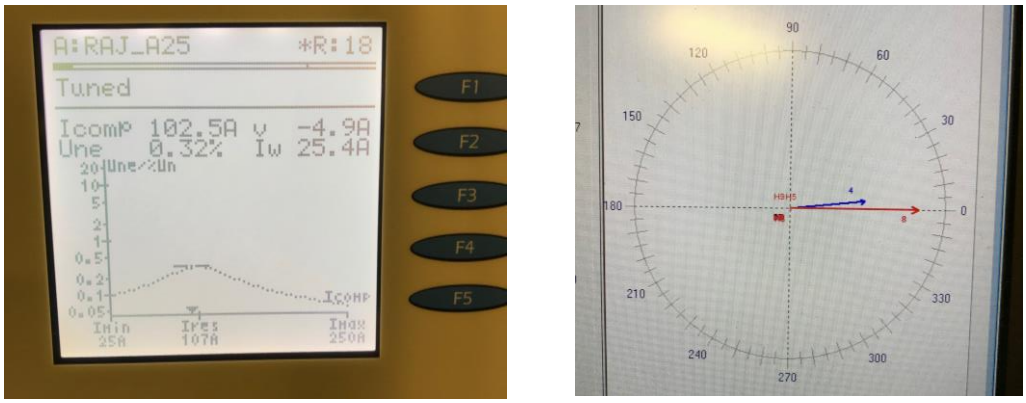

Figure 54. *Pictures of the measurements form the regulator and the protection relay.*

The values in the earth fault examination proved to be close to equal with the regulator measurement. According Forsblom (2019) the manufacturer of one regulator type used in Elenia, has conducted similar tests to study the accuracy of the resistive earth fault current measurement. The manufacturers results were in accordance with the results above. Therefore, in this work, regulator measurements are assumed to be accurate, which the results from the earth fault tests, and from the manufacturer, seem to support. However, based on only these test results, measurement accuracy cannot be fully guaranteed. That is why, as part of the future work, more specific validation of the accuracy of the regulator measurement should be conducted.

6.5.2 Generalization of the results

The results presented in this thesis are strongly related to the earth fault behaviour of the system. Many of the features that affect the earth fault behaviour of the system, such as neutral earthing method, network topology and compensation strategy are DSO specific. This a result of operational history, location of the network and customer base, as they all heavily affect the way the network is designed and operated. The initial expectation is that in rural areas long cable feeders will become more common and contribute to increase of resistive earth fault current. However, in many locations this is not the case and therefore, the increase of resistive earth fault current might not cause problems or at least the residual current estimation methods specified by the standard might be satisfactory.

Secondly, even in similar rural area networks as Elenia, compensation principles might be different which can have significant effect to the results. Consequently, the presented results are not directly generalizable, but the application to different networks should be investigated case-by-case. Even if network structure is similar the compensation principles presented in Section 2.3.3 should be alike, before applying these results.

6.6 Discussion

Some factors were brought up during the study that seemed to contain certain incoherences. Losses of distributed compensation and cable network reduction factor are not directly involved in the estimation methods presented in Section 6.5. However, both effect on the implementation of the results and as there are some confusing factors related to both, some discussion is provided in the following sections.

6.6.1 Distributed compensation

The conclusion in theoretical examinations has been that with properly dimensioned distributed compensation cable network resistive earth fault current production can be decreased, as presented in Sections 2.3.2 and 3.2. However, the correlation of distributed compensation current and degree of distributed compensation with respect to I_R in Figure 36 is rather strong, which indicates that with high implementation of distributed compensation, there seems to be large resistive earth fault current.

Originally the hypothesis was that as OHLs are renewed with cable and the increasing capacitance increases capacitive earth fault current in the network, the resistive earth fault current increases respectively. Now, as distributed compensation is introduced, the amount of resistive earth fault current is already high, due to high capacitive earth fault

current, so even though, the distributed compensation decreases the resistive earth fault current the remaining magnitude of resistive current is rather high due to the high capacitive current.

Yet, in the study conducted by Reikko et al. (2019) the disconnection of 70 A (5x15 A units) distributed compensation resulted in decrease of resistive earth fault current by 5 A! So, the compensation units themselves seemed to produce so much resistive current that it exceeded the amount produced by the network by 5 A. This seems to contradict the presented theory, that expects distributed compensation to decrease resistive earth fault current. It is worth noticing that the compensation units used in Reikko et al. (2019) are YN-connected three-phase reactors with earthed neutral, so the configuration of the units might have an influence on the resistive current production.

One possible source of the resistive earth fault current is losses of the units. Losses of a centralized coil used in Elenia's network are illustrated in Figure 22. To estimate the losses, the resistive current production according to Figure 22 was applied in the studied model but as only the losses of the centralized units were accounted, no significant results were obtained.

During this study there was no information available on the losses of the distributed units, but presumably the distributed units also produce some amount of resistive losses, which could explain the positive correlation of resistive earth fault current and distributed compensation current in Figure 36 and Figure 37. Therefore, the question is as follows. If the number of distributed units connected to the interconnected network increases significantly, can the sum of losses of the units increase to a level where the resistive current production of the units themselves increase the magnitude of the residual earth fault current?

6.6.2 Cable network reduction factor and touch voltages

In this study the interest in residual earth fault current is related to its application in touch voltage examinations. In Elenia, touch voltage examinations are conducted so that the complete residual earth fault current is assumed to flow to the fault point, which is the case in OHL network, where usually are no earthing conductors. In case of cable network, if reduction factor is applied, current flowing to the fault is be remarkably reduced. Similarly, the presence of the global earthing system also ensures that no dangerous touch or step voltages occur. Therefore, even though cabling of the network increases earth fault currents, it also improves the situation, if the fault is in cabled section of the network. Consequently, the situation might not be as severe as the results of the

developed method indicate, but if the effect of the reduction factor is unknown the examinations should be conducted by the safe way.

An interesting result related to cable network reduction factor is obtained in the study by Antoine et al. (2019). In their simulation a suction effect caused by Lenz law, caused all the earth fault current to return in the screen of the cable, thus there was no current flow in the ground, that would cause touch voltages. The simulation was conducted in efficiently grounded neutral system, so it cannot be directly applied to resonant earthed neutral system, but it is a fascinating result that certainly is worth studying more, because if similar phenomena happens in resonant earthed networks, it would remarkably improve the safety of the network.

7. CONCLUSIONS

The aim of this study was to identify the sources of the medium voltage network resistive earth fault current and based on the findings, develop a model to estimate the residual earth fault current. Calculation of the resistive earth fault current contains multiple uncertainties; therefore, an estimation method is needed to have an approximation of the magnitude of the resistive current component. This result is then used to calculate the residual earth fault current at the fault location. Long cabled MV feeders produce resistive earth fault current, so that it might increase the absolute value of the residual earth fault current and consequently increase touch voltages. Therefore, this residual earth fault current estimation method that takes the resistive current component into account more accurately, is needed to have a better understanding of the touch voltages in the network. Now, the parts of the network where touch voltage limits are possibly exceeded can be identified and corrective safety actions can allocate correctly.

Forming an analytical method to calculate the resistive earth fault current proved to be inconvenient and because the present version of Elenia's network information system was not able to consider the cable network zero sequence series impedance, the remaining option was to perform a statistical examination. The goal was to find parameters that correlate with resistive earth fault current, so that the found parameters could be used to estimate resistive earth fault current production in the network.

In the variable search, many of the parameters had strong correlation with the resistive earth fault current, yet most of the parameters with strong correlation were associated with network capacitance. Of these parameters, total capacitive earth fault current represented the effect of network capacitance well and was electrically the most meaningful parameter. Thus, it was chosen as the estimator parameter. The estimation results with I_{Ctot} were reasonably good, but the problem was that some of the estimated values had high deviation. The assumption was that perhaps there are some other explaining factors that could be accounted in the analysis if multiple parameters were used. Or alternatively, if the values are clustered in different categories so that a distinct correction factors can be assigned for each cluster, maybe the deviation can be reduced. However, the more complicated methods did not improve the accuracy notably, but only increased the level of difficulty. The simple solution of estimating resistive earth fault current with I_{Ctot} provided satisfactory results, therefore it was chosen.

The choice of adequate correction factor was based on optimizing the MSE of measured I_R values and I_{Ctot} values, but some margin of certainty had to be added. With 5% correction factor, most of the estimated values were higher than the measured reference values, so that also the trend of both the actual measurements and the estimations was close to equal.

When resistive earth fault current produced by the network was estimated to be 5%I_{Ctot} and the results were further applied to calculation of the residual current, the obtained values aligned well with the measured values. This indicates that the developed model provides results that are close to the actual residual earth fault current values in the network. Yet again, few of the estimated values were lower than the measured values. One can argue that the correction factor of I_{Ctot} should be increased to ensure that all the estimates are certainly safe. However, this would increase the error on the other side, which might lead to the model giving too high results, which could lead to incorrectly allocated investments. To conclude, the accuracy of the model is appropriate, but future development is needed before the model can be fully applied, because safety must always be ensured.

The estimation method specified in SFS 6001: 2018 acted as a reference. Two alternative interpretations can be made from the method specified in the standard, whether the distributedly compensated capacitive earth fault current should be included in the *capacitive fault current produced by the network,* or not. These interpretations are not specified in the standard but were brought up during the assignment of this thesis.

In the standard, the network capacitive earth fault current is used to estimate the residual earth fault current directly, whereas in the developed model it is used to estimate the resistive earth fault current, which is then used in calculation of the residual current. The difference is remarkable. If there was a minor deviation in the results of the developed model, when the estimation method presented in the standard was applied to Elenia's network, the results were systematically inaccurate. If the distributedly compensated capacitive current was included in the estimation, the resulting values were mostly too high, having a remarkably high deviation. On the other hand, if the distributedly compensated capacitive current was excluded, the resulting values were too low. Consequently, the method developed in this study proved to provide more accurate results than the method specified in the standard.

As stated earlier, the results are not necessarily generalizable, because they are heavily reliant on the properties of the distribution system. Thus, in networks with different configurations, the results might be different. Especially compensation principles have a

major impact, since the implementation of distributed compensation affects considerably to the generation resistive earth fault current.

For future work, sources of resistive earth fault current should be further examined. For example, the effect of ground resistivity was omitted in this study, but presumably it has an influence on the network zero sequence impedance. Such a study would help to identify the cause of deviation in the developed model and thereby improve the safety and the accuracy of the touch voltage examinations.

Secondly, resistive losses of the compensation devices, and the corresponding resistive earth fault current generation, should be investigated in detail. The resistive current production of the distributed compensation units was not validated in this study, but the correlations indicate that there is a connection between distributed compensation and resistive current production. If in fact the compensation units themselves produce resistive current, as the number of installed units increase, the sum of resistive current produced by the losses can cancel the resistive current reduction effect noted in the theoretical examinations. The compensation capacity is needed to control the capacitive earth fault current, but if in turn the resistive current increases because of the compensation units, corrective actions might be needed.

REFERENCES

ABB 2018. *615 Series Technical Manual.* Online. [Cited 19.9.2019] Available at: https://library.e.abb.com/public/70602692769a4ffa87ca027e6fb1af1d/RE_615_tech_756887_ENn.pdf

ABB ltd, 2004. *Transformer Handbook.* 2nd ed. Zurich: ABB ltd.

ABB Oy, 2000. *Teknisiä tietoja ja taulukoita.* 10th ed. Vaasa: Suomalaiset ABB-yhtiöt. In Finnish.

A-EBERLE GmbH 2017, *Operating Instructions for The Petersen-Coil Regulator.* Online. [Cited 19.9.2019.] Available at: https://www.a-eberle.de/sites/default/files/media/ba_REG-DPA_en_2017_04.pdf

ANTOINE, Q., HENNUY, B., FINOTTO, W. and VALMACCO, D. 2019 Return paths of earth fault current in medium voltage grids with underground shielded cables. *CIRED International Conference on Electricity Distribution*, pp. 1081.

BASTMAN, J. 2018 *Sähköverkkojen mallintaminen ja analyysi.* Study materials for course DEE-24000 Power System Modelling and Analysis. Tampere University of Technology. Department of Electrical Energy Engineering. In Finnish.

CARSON, J.R., 1926. Wave propagation in overhead wires with ground return. *The Bell System Technical Journal,* **5**(4), pp. 539-554.

DA SILVA, F.F. and BAK, C. L. 2013. *Electromagnetic Transients in Power Cables*. London: Springer.

Electricity Market Act 588/2013

ELOVAARA, J. and HAARLA, L., 2011. *Sähköverkot 1: järjestelmätekniikka ja sähköverkon laskenta.* Helsinki: Otatieto. In Finnish.

FICKERT, L., MALLITS, T. and RESCH, M., 2018. Earth fault current distribution and proof method of global earthing systems, May 2018, IEEE, pp. 1-4.

FORSBLOM, M., 2019. Sales Manager, Multirel Oy. E-mail 29.10.2019.

GULDBRAND, A. and SAMUELSSON, O., 2007. Central or Local Compensation of Earth-Fault Currents in Non-Effectively Earthed Distribution Systems, Jul 2007, *IEEE Power Tech*, pp. 1129-1134.

GULDBRAND, A., 2006 *Nollföljdsimpedans och strömfördelning vid kabel med markåterledning.* Elforsk report 06:66, Stockholm, Sweden. In Swedish.

GULDBRAND, A., 2009. *Earth faults in extensive cable networks.* Licentiate Thesis, Department of measurement technology and industrial electrical engineering, Lund University.

HÄMÄLÄINEN, T., 2015. *Optimization Methods.* Study materials for course MAT-60456 Optimization Methods 2019. Tampere University.

HAN, J., KAMBER, M., and PEI, J. 2012. *Data Mining: Concepts and Techniques,* 3rd ed. Elsevier.

IEC/TS 60479-1: 2005. *Effects of current on human beings and livestock – Part 1: General aspects.* Edition 4.0.

IEEE 81 – 2012. *Guide for Measuring Earth Resistivity, Ground Impedance, and Earth Surface Potentials of a Grounding System.* 2012. IEEE Standards Association.

ISOMÄKI, R., 2010. *Sammutetun keskijänniteverkon kompensointilaitteiston lisävastuksen ohjaus.* Bachelor of Science Thesis, Vaasa University of Applied Sciences. In Finnish.

JAAKKOLA, J. and KAUHANIEMI, K., 2013. Factors affecting the earth fault current in large-scale rural medium voltage cable network, *CIRED International Conference on Electricity Distribution*, pp. 1081.

LAHTI, K., 2017 *Sähköturvallisuus ja -asennukset*, study materials for course DEE-23020 Electrical safety and installations. Tampere University of Technology. Department of Electrical Energy Engineering. In Finnish.

LAKERVI, E. and HOLMES, E.J., 1995. *Electricity distribution network design.* 2nd ed. London: Peter Peregrinus.

LAKERVI, E. and PARTANEN, J., 2008. *Sähkönjakelutekniikka.* Helsinki: Otatieto Helsinki University Press. In Finnish.

MÄKINEN, A. 2016 *Selvitys keskijänniteverkon maadoitusjärjestelmistä.* Report, Department of Electrical Engineering, Tampere University of Technology. In Finnish.

MALM, M., PETTERSON, A., SLOTH, J., HEMMINGSSON, M. and KARLSSON, D. 2015. *Kablars nollföljdsimpedans. Beräkning och mätning av 36 kilovotskablar.* Energiforsk report 2015:101. In Swedish.

MÖRSKY, J., 1993. *Relesuojaustekniikka.* 2nd ed. Espoo: Otatieto. In Finnish.

NIKANDER, A. and JARVENTAUSTA, P., 2005. Safety aspects and novel technical solutions for earth fault management in MV electricity distribution networks, 2005, IEE, pp. 207-211.

NIKANDER, A. and MÄKINEN A., 2017 *Laajan kaapeloidun keskijänniteverkon maasulkuilmiöiden vaikutukset -suojaushaasteet, yliaallot, vaarajännitteet.* Report, Laboratory of Electrical Energy Engineering, Tampere University of Technology. In Finnish.

PEKKALA, H., 2010. *Challenges in Extensive Cabling of the Rural Area Networks and Protection in Mixed Networks*. Master of Science Thesis, Department of Electrical Energy Engineering, Tampere University of Technology.

PITKÄRANTA, J., 2015. *Calculus Fennicus.* Helsinki: Avoimet oppimateriaalit. In Finnish

REIKKO, J., KESKINEN, A. and RISTIMÄKI, R., 2019. Touch voltages and earth fault currents in a rural large-scale underground cable network with connected earthing systems. *CIRED International Conference on Electricity Distribution,* pp. 1386.

SAARIJÄRVI, E., TAMMI, P. and LEHTONEN, M., 2014. *Low voltage network touch voltages caused by medium voltage network earth faults.* Test report, Aalto University School of Electrical Engineering, Department of Electrical Engineering and Automation. In Finnish

SFS 6001: 2018. *High voltage electrical installations*. 15.06.2018. Finnish Standards Association (SFS). In Finnish

SUURONEN, M., 2006. *Maadoituksen mittaustapojen soveltuvuuden arviointi.* Bachelor of Science Thesis, Tampere University of Applied Sciences. In Finnish.

TIAINEN, E., 2017. *D1-2017. Käsikirja rakennusten sähköasennuksista.* Helsinki: Sähköinfo Oy. In Finnish.

VEHMASVAARA, S., 2013. *Compensation strategies in cabled rural networks*. Master of Science Thesis, Faculty of Computing and Electrical Engineering, Tampere University of Technology.

WAHLROOS, A. and ALTONEN, J., 2014. Application of Novel Multi-frequency Neutral Admittance Method into Earth-Fault Protection in Compensated MV-networks, 2014, IET, pp. 5.1.3.